Journal of Vertebrate Paleontology 29(4):1046–1086, December 2009


ARTICLE

# THE POSTCRANIAL OSTEOLOGY OF *RAPETOSAURUS KRAUSEI* (SAUROPODA: TITANOSAURIA) FROM THE LATE CRETACEOUS OF MADAGASCAR

KRISTINA CURRY ROGERS
Biology and Geology Departments, Macalester College, 1600 Grand Avenue, St. Paul, MN 55105, U. S. A., rogersk@macalester.edu

ABSTRACT—*Rapetosaurus krausei* is a titanosaur sauropod from the Upper Cretaceous Maevarano Formation of northwestern Madagascar and is among the most complete titanosaurs ever discovered. To date, over 15 localities in a 10 km$^2$ field area have yielded hundreds of titanosaur bones, including associated and articulated specimens of *Rapetosaurus*. A juvenile skeleton is of particular significance because it was found directly associated with a well-preserved partial skull. The juvenile postcranial skeleton only lacks only the axis, atlas, representative elements from the proximal caudal series, carpals, and tarsals. The *Rapetosaurus* axial column consists of at least 17 cervical, 10 dorsal, six sacral, and 17 caudal vertebrae. Appendicular skeletal anatomy documents unique aspects of the titanosaur skeleton, and the association of large osteoderms with other, adult specimens confirms the lithostrotian status of *Rapetosaurus*. These new skeletal data have proven significant for phylogenetic resolution within Titanosauria, particularly because *Rapetosaurus* can be coded for 83% of over 400 characters for titanosaurs.

## INTRODUCTION

Since 1877, over 40 species of titanosaurs have been recovered from Late Jurassic–Late Cretaceous rocks from around the world. The group is easily recognized and represents over 30% of sauropod species (Upchurch et al., 2004; Curry Rogers, 2005), but key aspects of their phylogeny have only recently been scrutinized and resolved. Titanosaur bones were among the first fossils described from the Upper Cretaceous Maevarano Formation of Madagascar, and they provided some of the first hints at the unique anatomy of titanosaurs (e.g., osteoderms) as well as the persistence of sauropods in Cretaceous faunas (Depéret, 1896a,b; Thévenin, 1907; Lavocat, 1955).

*Rapetosaurus krausei* is one of two titanosaurs currently recognized from the Maevarano Formation of northwestern Madagascar and includes associated, well-preserved cranial and postcranial remains at a variety of ontogenetic stages. As such, *Rapetosaurus* is pivotal to ongoing revisions of titanosaur anatomy and morphology. Along with an associated, isolated holotypic adult skull (Curry Rogers and Forster, 2001, 2004; Curry Rogers, 2005), hundreds of isolated bones as well as articulated and associated postcranial specimens have been recovered over the course of nine field seasons (Curry Rogers and Forster, 2001; Curry Rogers, 2005). Included amongst numerous specimens from Quarry MAD 93-18 in the Anembalemba Member of the Maevarano Formation (Rogers et al., 2000; Rogers 2005) is an exceptionally preserved juvenile postcranial skeleton, found in association with a juvenile skull referable to *Rapetosaurus* (Curry Rogers and Forster, 2001, 2004). Elements from every region of the skeleton are represented, including the most delicate vertebral structures, forelimbs, hind limbs, and even distal caudal vertebrae (Fig. 1). Here I provide a brief history of Malagasy titanosaurs, a detailed description of *Rapetosaurus* postcranial anatomy on the basis of this juvenile skeleton, and comparisons of *Rapetosaurus* postcranial anatomy with that of other titanosaurs.

**Institutional Abbreviations**—**BMNH**, British Museum of Natural History, London, United Kingdom; **FMNH PR**, Field Museum of Natural History, Chicago, USA; **HMN**, Humboldt Museum für Naturkunde, Berlin, Germany; **IANIGLA-PV**, Instituto Argentino de Nivología, Glaciología y Ciencas Ambientales, Colección Paleovertebrados, Mendoza, Argentina; **ISI**, Indian Statistical Institute, Kolkata, India; **MACN**, Museo Argentino de Ciencias Naturales, Buenos Aires, Argentina; **MCNA**, Museo de Ciencias Naturales de Álava, Álava, Spain; **MCS**, Museo de Cinco Saltos, Río Negro Province, Argentina; **MD-E**, Musée des Dinosaures, Espéraza, France; **MLP**, Museo La Plata, La Plata, Argentina; **MN**, Museu Nacional, Rio de Janeiro, Brazil; **MPCA**, Museo Provincial "Carlos Ameghino," Cipolletti, Argentina; **MRS-Pv**, Laboratory of Rincón de los Sauces Museum, Rincón de los Sauces, Argentina; **MUCP**, Museo de la Universidad Nacional del Comahue, Neuquén, Argentina; **MUGEO**, Museu Geológico Valdemar Lefèvre, São Paulo, Brazil; **OMNH**, Oklahoma Museum of Natural History, Norman, USA; **PMU**, Palaeontological Museum of Uppsala University, Uppsala, Sweden; **PVL**, Fundación Miguel Lillo, Universidad Nacional de Tucumán, San Miguel de Tucumán, Argentina; MCF-**PVPH**, Museo Carmen Funes, Plaza Huincúl, Argentina; **PW**, Sahatsakhan Dinosaur Research Centre, Thailand; **SMM**, Science Museum of Minnesota; **SMU**, Southern Methodist University, Dallas, USA; **TMM**, Texas Memorial Museum, University of Texas, Austin, USA; **UA**, Université d'Antananarivo, Antananarivo, Madagascar; **UB**, Universitatea Bucuresti, Bucharest, Romania; **UCB**, Université Claude Bernard, Lyon, France; **UNPSJB-PV**, Museo de la Universidad Nacional de la Patagonia "San Juan de Bosco," Comodoro Rivadavia, Argentina; **USNM**, National Museum of Natural History, Washington, D.C., USA; **ZPAL**, Instytut of Paleobiologii, Polish Academy of Sciences, Warsaw, Poland.

## HISTORICAL PERSPECTIVE

In 1896 Charles Depéret reported the discovery of a sauropod dinosaur in Madagascar (Depéret 1896a, 1896b:fig 1). Two procoelous caudal centra (UCB 92829, UCB 92305, Fig. 2A, B) and an osteoderm (UCB 92827, Fig. 2D) were recovered at a single locality (site 1 in Depéret 1896b:fig 1; Fig. 3A), and a partial humeral diaphysis (UCB 92831, Fig. 2C) came from a separate

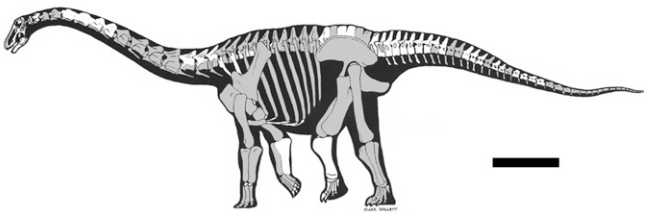

FIGURE 1. Skeletal reconstruction of *Rapetosaurus krausei*, based on a referred juvenile skeleton (FMNH PR 2209) recovered from MAD 93-18. Gray tone indicates bones that were recovered. Scale bar equals 1 m.

locality (site 3 in Depéret 1896b:fig 1; Fig. 3A), both on the northeastern bank of the Betsiboka River in Upper Cretaceous sediments. Depéret assigned all four elements to a new species he called *Titanosaurus madagascariensis*.

Later collecting in Madagascar from the same general localities resulted in additional appendicular elements, and anterior and mid-caudal vertebrae that Thévenin (1907) attributed to *T. madagascariensis*. He did not figure or describe the limb elements, but provided brief descriptions and images for four caudal vertebrae (Thévenin, 1907:133–134:pl. I, fig. 13–16). Huene (1929), though confirming the titanosaur identity of these elements (on the basis of procoely and anteriorly positioned neural arches), singled out the smaller vertebra in the Depéret sample (UCB 92305) and an undescribed caudal vertebra figured in the Thévenin report (1907:pl. I, fig. 16) as "cf. *Laplatasaurus madagascariensis*." With the exception of a referral of material from India by Huene and Matley (1933), other titanosaur material collected in Madagascar (Lavocat, 1955; Besairie, 1972; Russell et al., 1976; Ravoavy, 1991) was referred to *Titanosaurus madagascariensis*.

Beginning in 1993, the Mahajanga Basin Project renewed collecting efforts in the Maevarano Formation (Fig. 3B, C). To date, hundreds of new sauropod fossils have been recovered including associated and articulated remains. These new finds highlight the presence of two distinct titanosaur taxa in the Maevarano Formation, which can be readily distinguished on the basis of caudal vertebral and forelimb morphology (Ravoavy, 1991;

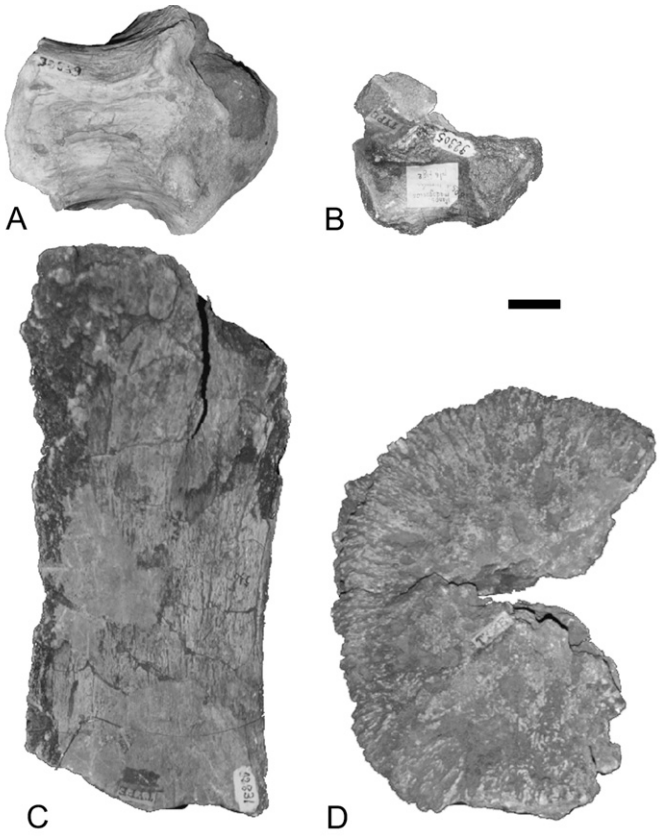


FIGURE 2. Syntype elements of *'Titanosaurus madagascariensis'* (Depéret, 1896a). **A**, proximal caudal centrum (UCB 92829) in ventral view; **B**, mid-caudal centrum (UCB 92305) in left lateral view; **C**, partial humeral diaphysis (UCB 92831) in anterior view; **D**, osteoderm (UCB 92827) in external view. **A** and **B** are now referred to *Rapetosaurus krausei* and Malagasy Taxon B (Curry Rogers, 2001), respectively; **C** and **D** cannot yet be referred to either taxon with certainty. Scale bar equals 3 cm.

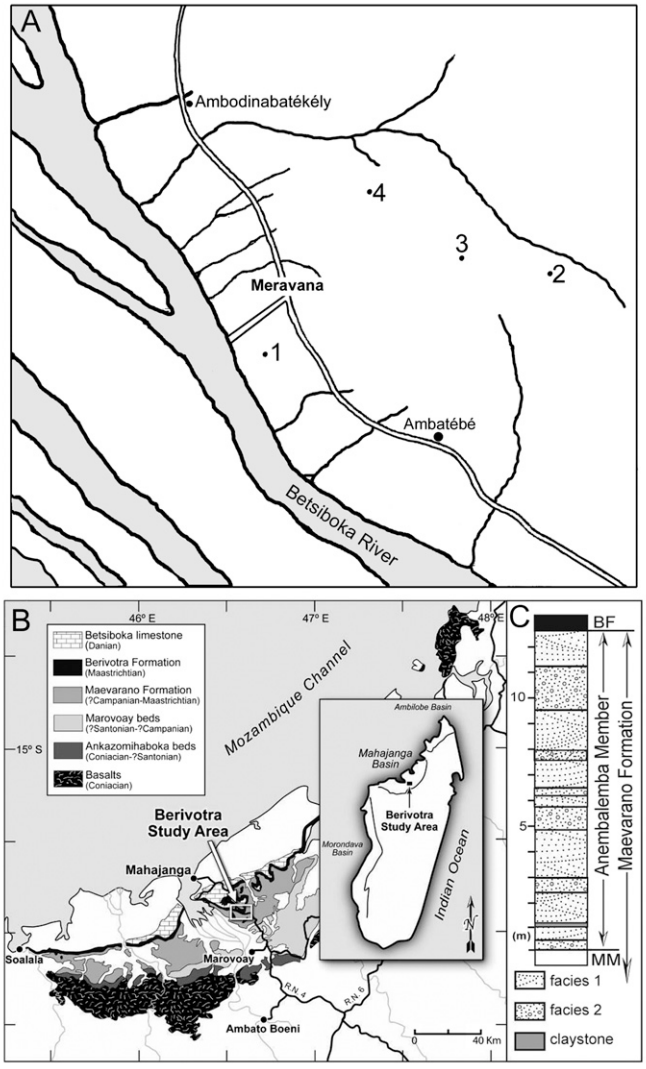


FIGURE 3. Fossil vertebrate localities from the Late Cretaceous of the Mahajanga Basin of northwestern Madagascar. **A**, map modified from Depéret (1896a) showing four localities recorded by collectors. Note that "Mevarana" was misspelled as "Meravana" on Depéret's map, and that current spelling is Maevarana. **B**, map modified from Rogers (2005) showing exposures of Upper Cretaceous and Tertiary strata (Berivotra study area is highlighted). **C**, Schematic profile of the Anembalemba Member, modified from Rogers (2005). The Anembalema Member in the Berivotra area is underlain by the Masorobe member of the Maevarano Formation (**MM**) and overlain by the marine Berivotra Formation (**BF**).

Curry Rogers, 2001, 2005; Curry Rogers and Forster, 2001). Both caudal morphologies are included in the *Titanosaurus madagascariensis* syntype (UCB 92829, 92305), and call into question the validity of the species. UCB 92829 is weathered and without diagnostic characters, but most closely resembles caudal vertebrae of *Rapetosaurus* (Curry Rogers and Forster, 2001, 2004). UCB 92305 exhibits a distinctive, dorsoventrally compressed morphology that characterizes caudal vertebrae of 'Malagasy Taxon B.' Recent revision of the genus *Titanosaurus* (Wilson and Upchurch, 2003) recognized only five diagnostic species, invalidated the type species *T. indicus*, and consequently abandoned the genus as well as its coordinated rank-taxa (Titanosaurinae, Titanosauridae, Titanosauroidea). Referral of any Malagasy titanosaur material to *Laplatasaurus*, as suggested by Huene (1929) awaits description of 'Malagasy Taxon B' and redescription of the original material. Two Malagasy titanosaur taxa can be easily distinguished on the basis of a number of cranial and postcranial autapomorphies (Curry Rogers and Imker, 2007) and indicate that the syntype material of *T. madagascariensis* may include elements from both Malagasy taxa (Curry Rogers and Forster, 2001, 2004; Curry Rogers and Imker, 2007).

## SYSTEMATIC PALEONTOLOGY

DINOSAURIA Owen, 1842
SAURISCHIA Seeley, 1888
SAUROPODA Marsh, 1878
TITANOSAURIA Bonaparte and Coria, 1993
*RAPETOSAURUS KRAUSEI* Curry Rogers and Forster, 2001
Figs. 5–47

**Holotype**—UA 8698, partial adult skull including right maxilla with eight associated teeth, left maxilla, right lacrimal, left jugal, right and left nasals, right quadrate, right and left pterygoids, partial basioccipital, right paroccipital process; left dentary with 11 teeth, right and left angulars, right surangular, and five additional associated teeth.

**Referred Specimens**—FMNH PR 2209, see Curry Rogers and Forster, 2001, 2004 for additional referred material.

**Revised Diagnosis**—Autapomorphies of *Rapetosaurus*: antorbital fenestra large, extending anteriorly over tooth row; preantorbital fenestra positioned posterior to antorbital fenestra; anteriorly located, elongate subnarial foramen; narrow, posterodorsally elongate maxillary jugal process; frontal with median dome; quadrate with V-shaped quadratojugal articulation; supraoccipital with two anteriorly directed median parietal processes; pterygoid anterior process dorsoventrally expanded; basipterygoid articulation of pterygoid extremely shallow; basipterygoid processes divergent only at distal ends; 11 alveoli extending for two-thirds the length of the dentary; 43 precaudal vertebrae (17 cervical, 10 dorsal, 6 sacral vertebrae); elongated cervical vertebrae with "butterfly"-shaped neurocentral articulations; cervical centra with midline ventral keel; prespinal lamina in anterior cervical vertebrae; mid-cervical vertebrae with deep prespinal and postspinal fossae, lacking prespinal or postspinal laminae; dorsal vertebrae with high neural spine, ~40% vertebral height; dorsal vertebrae with intrapostzygopophyseal lamina bearing ventral extension and weblike pre- and postspinal laminae; sacral centra with pneumatic fossae; sacral neural spines comprise half of total sacral vertebral height; mid-caudal neural spines taller than centrum, transversely expanded, anteroposteriorly reduced; mid-posterior caudal vertebrae with well-developed pre- and postspinal lamina in shallow fossae; coracoid with oblique lateral ridge; humeral head level with proximal deltopectoral crest; straight distal humeral diaphysis; shelf-like iliac peduncle of ischium and pubis; femur strongly constricted at mid-diaphysis, gracile. Differing from *Andesaurus* in: opisthocoelous posterior dorsal centra; absence of hyposphene-hypantrum articulations in dorsal vertebrae; dorsal vertebrae with undivided prespinal lamina; procoelous caudal vertebrae; elongate posterior caudal neural spines; V-shaped haemal canal; shelf-like iliac peduncle of pubis; anterior margin of pubis unexpanded. Differing from *Malawisaurus* in: cervical vertebrae with transversely compressed neural spine; cervicals with deep, narrow prespinal and postspinal fossae; dorsal neural spines triangular; chevrons with V-shaped haemal canal; low olecranon process of ulna; rounded iliac peduncle of ischium; Differing from *Isisaurus* in: elongated cervical centra; cervical neural arches with extensive, well-defined fossae; postspinal lamina of dorsal vertebrae extends to distal end of neural spine; presence of spinodiapophyseal lamina in dorsal vertebrae; pre- and postspinal laminae extend to distal neural spine in anterior caudal vertebrae; scapular blade uniform in width; acute angle of scapular blade-body intersection; ischial blade uniform in breadth. Differing from *Alamosaurus* in: cervical centra with divided pneumatic fossa; rounded coracoid without sharp borders; proximal end of ulna, not expanded; metacarpal V broad distally. Differing from *Opisthocoelicaudia* in: prespinal and postspinal laminae extending full length of dorsal neural spine; presence of a spinoprezygapophyseal lamina in dorsal vertebrae; sacral centra with round ventral margins; procoleous caudal vertebrae; acute angle of scapular blade-body intersection; coracoid foramen located on scapular suture; humeral head level with proximal deltopectoral crest. Differing from *Saltasaurus* in: basal tubera extend away from basipterygoid processes; cervical vertebral condyles and cotyles equal dimensions; dorsal neural spine, distal end triangular; dorsal vertebra, ventral extension of prespinal fossa roofs neural canal; dorsal vertebrae with undivided centroparapophyseal lamina; caudal vertebra not dorsoventrally compressed; rounded coracoid lacking infraglenoid lip; straight distal humeral diaphysis; gracile radius; metacarpal IV, subrectangular distal end; femur with mid-diaphyseal constriction; tibia with anterolaterally-directed cnemial crest.

**Age and Distribution**—All specimens of *Rapetosaurus krausei* were recovered from localities in the Anembalemba Member of the Maevarano Formation (Maastrichtian, Late Cretaceous), Mahajanga Basin, near the village of Berivotra in northwestern Madagascar. For an overview of the stratigraphy and sedimentology of the area see Rogers et al. (2000) and Rogers (2005). The postcranial skeleton described here was recovered in association with a juvenile skull from a single horizon in locality MAD 93-18. To date, MAD 93-18 documents at least three bone-bearing horizons emplaced during episodic debris-flows, all containing well-preserved material of *Rapetosaurus* (Fig. 4A–D). Though the bonebeds are typically time-averaged (Rogers, 2005), it is notable that in the case of FMNH PR 2209 there is no duplication of skeletal elements, and all of the material can be ascribed to a single individual (Fig. 4C, E).

## DESCRIPTION

The following description is primarily based on the associated juvenile *Rapetosaurus* skeleton (FMNH PR 2209) recovered from locality MAD 93-18 that includes an associated, disarticulated skull (FMNH PR 2184–2192, 2194, 2196–2197). The referral of these elements to *Rapetosaurus* is based upon cranial autapomorphies shared by the holotype adult skull from locality MAD 96-02 and the juvenile skull from MAD 93-18 (Curry Rogers and Forster, 2001, 2004). Osteological descriptions are organized as follows: vertebrae, ribs, chevrons, pectoral girdle, forelimb, pelvic girdle, hind limb. With regard to the vertebrae, each major anatomical subdivision (cervical, dorsal, sacral, and caudal vertebrae) is described sequentially. The landmark-based terminology for vertebral laminae developed by Wilson (1999) is utilized in the discussion of vertebral anatomy and in Figures 5–30. Abbreviations for vertebral laminae are listed with their first occurrence in the text. Because the described juvenile

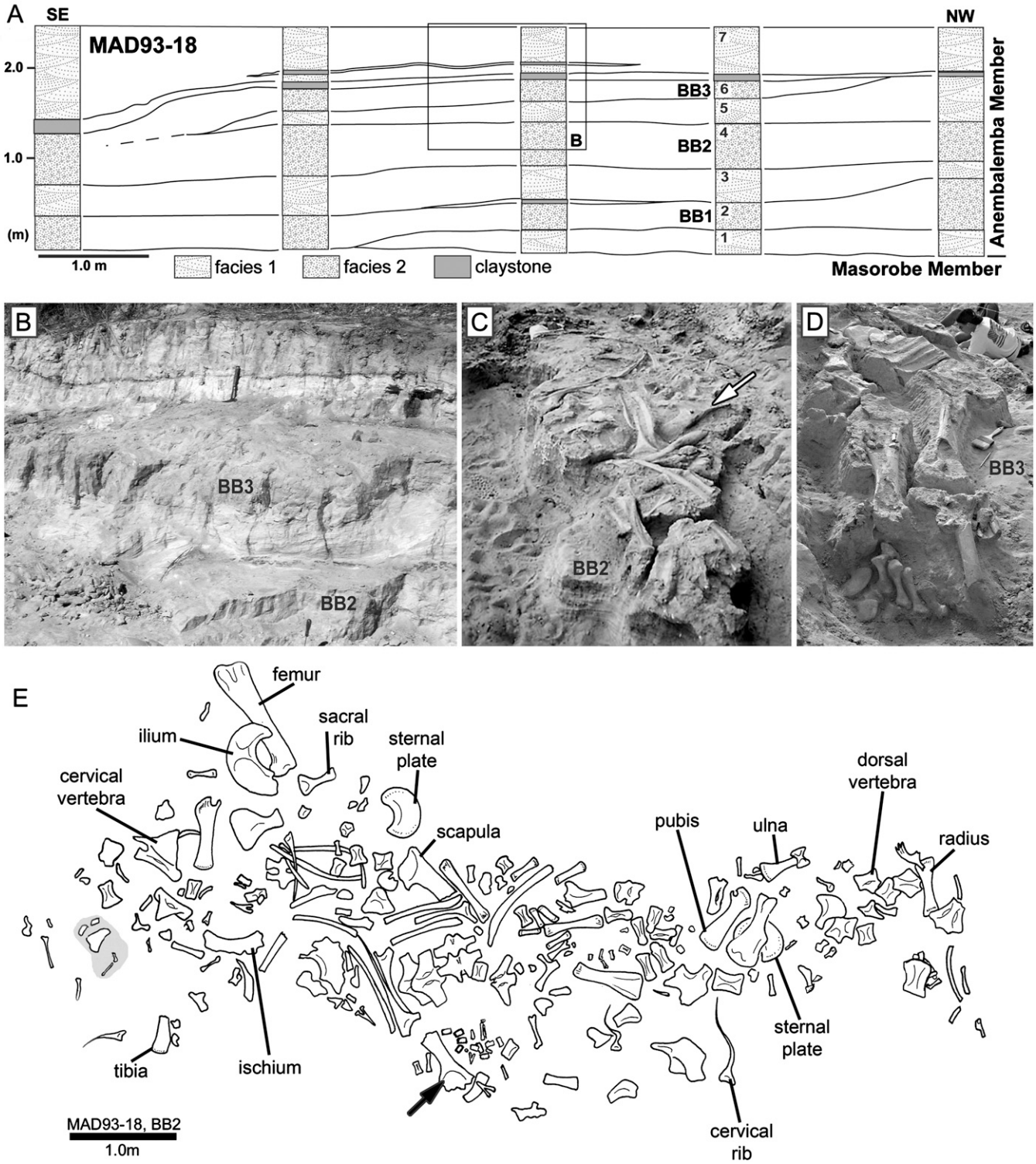


FIGURE 4. Locality MAD 93-18, Upper Cretaceous Maevarano Formation, Mahajanga Basin Madagascar. **A**, schematic cross-section through the multiple bone-bearing horizons of quarry MAD93-18 (BB1, BB2, BB3) that each yielded bones of *Rapetosaurus*, modified from Rogers (2005). **B**, BB2 and BB3 bonebeds of MAD 93-18. BB1 is not visible in this view, but it is positioned below BB2 and yielded bones of an adult *Rapetosaurus*. **C**, associated *Rapetosaurus* skull and skeleton (FMNH PR 2209) described in the text, photographed in situ at BB2. Cervical vertebrae, ribs, and radius are in the foreground, scapulae, metacarpals, and femur in the distance. White arrow points to scapula highlighted in **E**. **D**, subadult *Rapetosaurus* skeleton photographed in situ at BB3. Ribs are articulated in distance, and the forelimb and hind limb (including left foot) are also closely associated. **E**, Map of FMNH PR 2209 from BB2. Black arrow marks right scapula described in text and highlighted in **C**. Several specimens are labeled; not all associated bones are visible in map view. Contact author for a more detailed site map with field numbers and identifications.

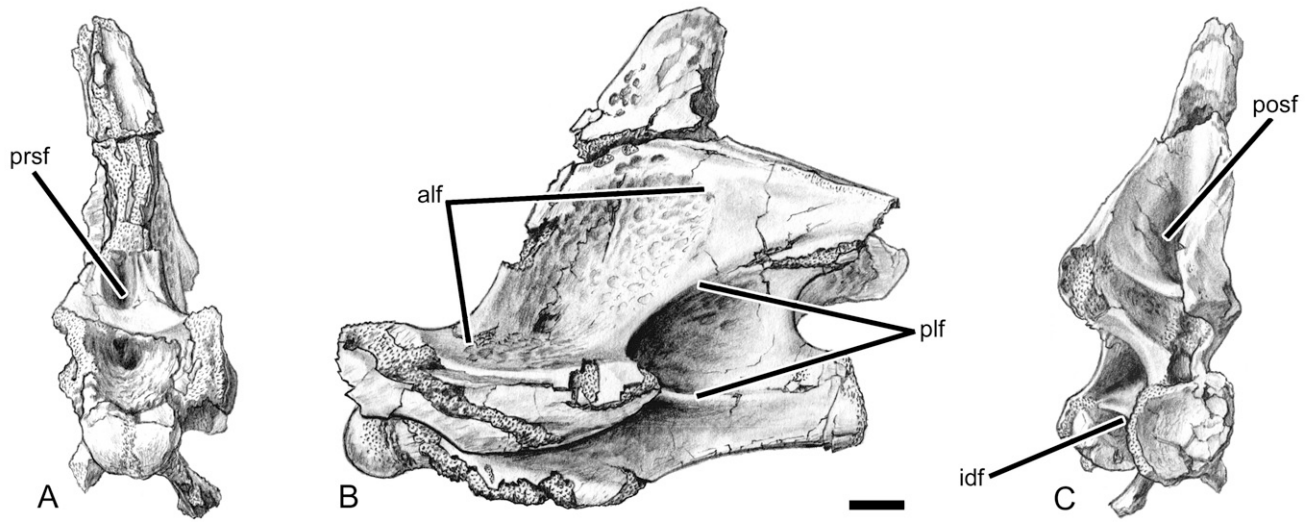


FIGURE 5. Eleventh cervical vertebra (FMNH PR 2209) of *Rapetosaurus krausei* illustrating standard cervical vertebral fossae and general characteristics of cervical centra in **A**, anterior view; **B**, left lateral view; **C**, posterior view. **Abbreviations**: **alf**, anterolateral fossa; **idf**, **infradiapophyseal fossa**; **plf**, posterolateral fossa; **posf**, postspinal fossa; **prsf**, prespinal fossa. Scale bar equals 3 cm.

skeleton has only one catalogue number (FMNH PR 2209), field numbers for each described specimen that are traceable in the paleontology database and collection at the Field Museum of Natural History (FMNH) are available from the author. The atlas (SMM P2007.3.1) is not a part of this juvenile skeleton, but is described here for completeness. It was recovered from MAD 96-01, and is referred to *Rapetosaurus* due to its association with other *Rapetosaurus* postcranial elements at that locality.

Descriptions of a series of vertebrae or of a region of the appendicular skeleton are followed by a summary set of comparisons with other titanosaurs. To date, nine analyses specifically addressing the interrelationships of Titanosauria have employed different numbers and types of characters, and all but one included ten or fewer terminal taxa of the possible 41 titanosaur species. In spite of the poorly resolved relationships of Titanosauria as a group, a few well-known taxa are consistently utilized and provide some general resolution on the topology of titanosaur interrelationships. *Andesaurus* and *Malawisaurus* are generally considered as basal titanosaurs (although Curry Rogers 2005 placed *Malawisaurus* as the sister taxon to more derived titanosaurs). *Saltasaurus* is the only taxon included in all analyses, and is always resolved as the most derived titanosaur. When included, *Neuquensaurus* is always the sister-taxon of *Saltasaurus*, and *Alamosaurus* and *Opisthocoelicaudia* are recovered as outgroups to this group of derived South American titanosaurs. *Isisaurus* is typically nested between *Malawisaurus* and more derived forms (Wilson, 2006). More than 30 titanosaur species still need to be accommodated by phylogenetic analysis, leaving some ambiguity with regard to character distribution among titanosaur terminal taxa. For these reasons, comparisons below are specifically limited to these seven well-documented titanosaur taxa, with additional comparisons only when particularly informative.

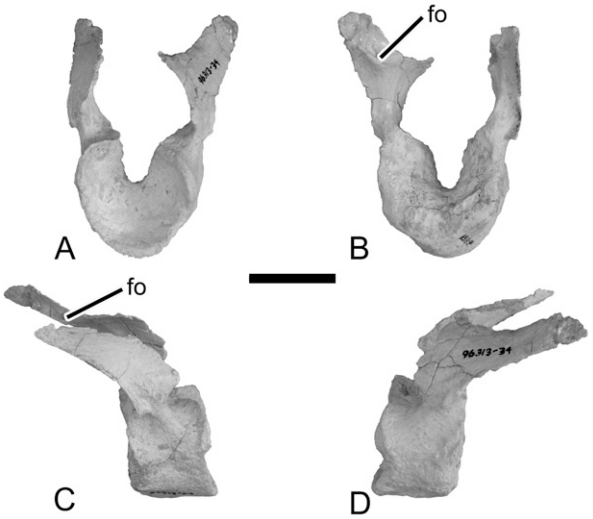


FIGURE 6. Atlas (SMM P2007.3.1) of *Rapetosaurus krausei* in **A**, anterior view; **B**, poserior view; **C**, right lateral view; **D**, left lateral view. **Abbreviation**: **fo**, foramen. Scale bar equals 3 cm.

## Cervical vertebrae

Elements from a total of 15 cervical vertebrae were recovered from quarry MAD 93-18 (Figs. 5–13). The atlas and axis were not preserved, but the 15 preserved cervicals form a natural series, and result in a total of 17 cervical vertebrae for *Rapetosaurus*. The sample includes six unfused cervical centra with respective unfused neural arches that can be rearticulated along well-preserved sutures. Three additional fused mid-cervical vertebrae result in a total of nine cervical vertebrae that are relatively complete. Six isolated centra can be placed in series based on size, articulation with preceding and subsequent centra, and position and morphology of parapophyses. When neural arches and centra articulate, they are described together below, with measurements recorded in Table 1. Cervical vertebrae from FMNH PR 2209 are described sequentially beginning with cervical vertebra three, following the description of a *Rapetosaurus* atlas from a separate locality.

Cervical centra are opisthocoelous and gradually elongate toward the middle part of the series, then broaden and abruptly shorten to a more robust morphology at the cervicodorsal transition. Centra are typically somphospondylous (= camellate). All centra are characterized by anteroposteriorly extensive, shallow, lateral pneumatic fossae (Fig. 5). These fossae are smooth and house pneumatic foramina demarcated by sharp borders. The prespinal fossa contains a median prespinal lamina (prsl) in the

anteriormost cervical vertebrae, but deepens in more posterior cervical centra and may preclude the presence of a prsl (Fig. 5A). Laminae and the same set of well-developed fossae are present throughout the cervical series, but the arrangement of these fossae varies slightly from anterior to posterior cervical vertebrae. All cervical centra have "butterfly" or "hourglass"-shaped neurocentral articulations, such that the neural canal is constricted either at its midpoint (anterior cervical vertebrae) or more anteriorly (posterior cervical vertebrae), and wider at anterior and posterior extremes (Figs. 7, 11, 13). The neural arches of anterior cervical vertebrae are relatively low. They gradually increase in height through mid-series and become broader and lower by the cervicodorsal transition. Transversely oriented aliform diapophyses are more pronounced in the posterior cervical neural arches.

**Atlas**—The atlas (SMM P2007.3.1, Fig. 6) was not found in association with FMNH PR 2209 at MAD 93-18, but was recovered from MAD 96-01, another locality in the Anembalemba Member that included remains of the theropod *Majungasaurus crenatissimus*, as well as fragmentary *Rapetosaurus* axial elements. The atlas is complete, gracile, and has a crescentic intercentrum with a deep, vertical excavation on the dorsal surface in anterior view. The bases of the neurapophyses gently flare laterally before expanding into short 'wings'. Posteriorly, these short, anteromedially directed flanges grade into long, posterodorsally tapering processes. A small foramen punctuates the distalmost medial surface of the flange (Fig. 6B, C). The occipital facet of the intercentrum is subrectangular in lateral view, though the anteroventral margin of the intercentrum is slightly expanded anteriorly, extending a few millimeters beyond the anterodorsal margin of the intercentrum. The axis of *Rapetosaurus* has not yet been recovered from the Maevarano Formation.

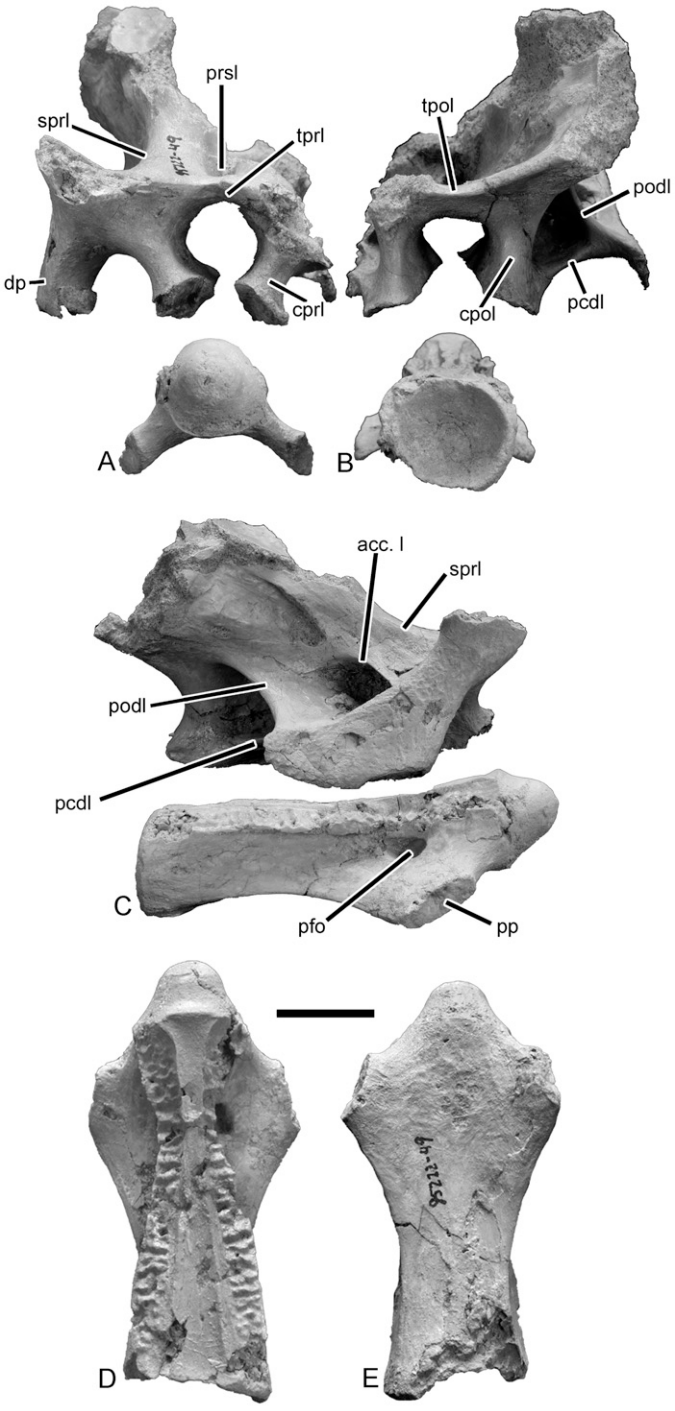


FIGURE 7. Third cervical vertebra (FMNH PR 2209) of *Rapetosaurus krausei* in **A**, anterior view; **B**, posterior view; **C**, right lateral view; **D**, centrum in dorsal view; **E**, centrum in ventral view. **Abbreviations**: **acc. l.**, accessory lamina found only in third cervical vertebra; **cpol**, centropostzygapophyseal lamina; **cprl**, centroprezygapophyseal lamina; **dp**, diapophysis; **pcdl**, posterior centrodiapophyseal lamina; **pfo**, pneumatic foramen; **podl**, postzygodiapophyseal lamina; **pp**, parapophysis; **prsl**, prespinal lamina; **sprl**, spinoprezygapophyseal lamina; **tpol**, intrapostzygapophyseal lamina; **tprl**, intraprezygapophyseal lamina. Scale bar equals 3 cm.

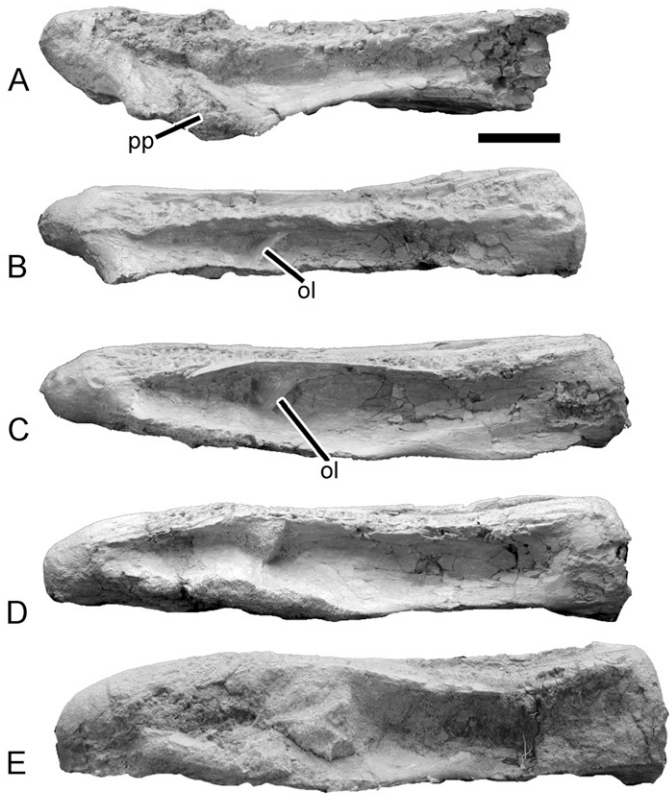


FIGURE 8. Fourth to eighth cervical centra (FMNH PR 2209) of *Rapetosaurus krausei* in left lateral view. **A**, fourth cervical centrum; **B**, fifth cervical centrum; **C**, sixth cervical centrum; **D**, seventh cervical centrum; **E**, eighth cervical centrum. **Abbreviations**: **ol**, oblique lamina; **pp**, parapophysis. Scale bar equals 3 cm.

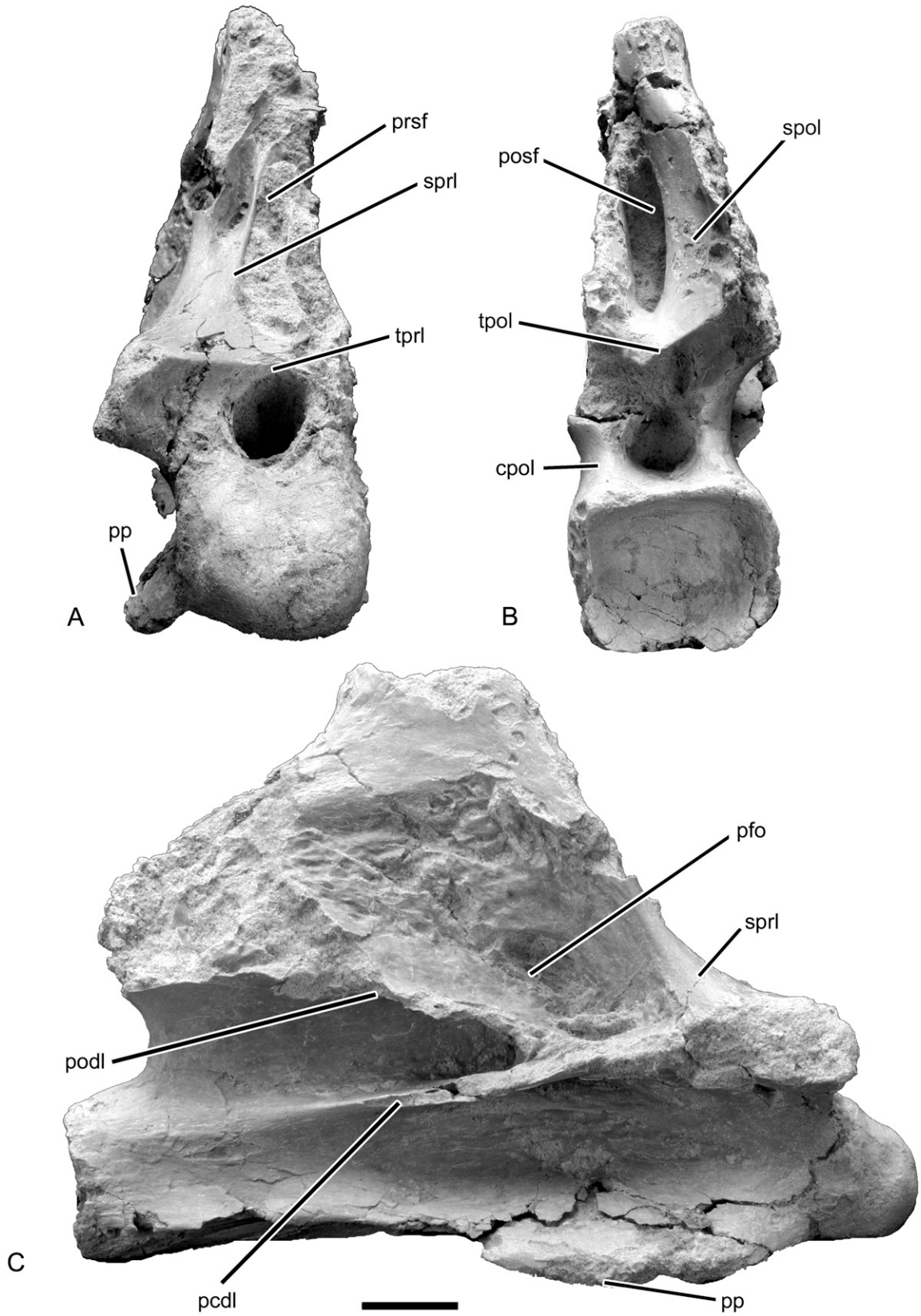


FIGURE 9. Ninth cervical vertebra (FMNH PR 2209) of *Rapetosaurus krausei* in **A**, anterior view; **B**, posterior view; **C**, right lateral view. **Abbreviations**: **cpol**, centropostzygapophyseal lamina; **pcdl**, posterior centrodiapophyseal lamina; **pfo**, pneumatic foramen; **podl**, postzygodiapophyseal lamina; **posf**, postspinal fossa; **pp**, parapophysis; **prsf**, prespinal fossa; **spol**, spinopostzygapophysesal lamina; **sprl**, spinoprezygapophyseal lamina; **tpol**, intrapostzygapophyseal lamina; **tprl**, intraprezygapophyseal lamina. Scale bar equals 3 cm.

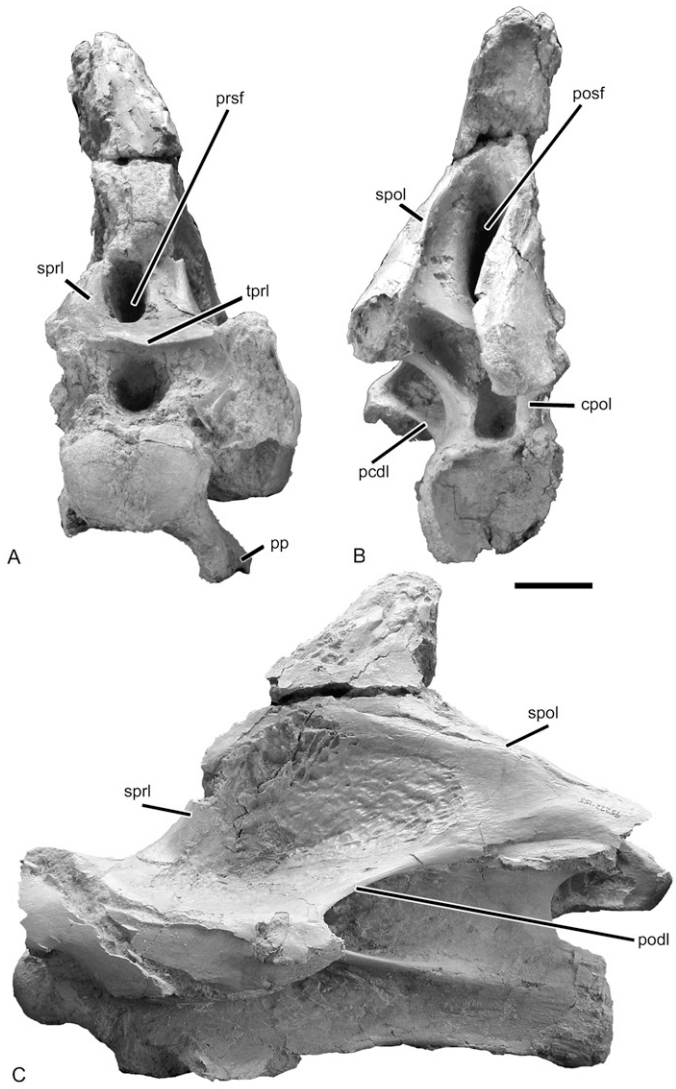


FIGURE 10. Eleventh cervical vertebra (FMNH PR 2209) of *Rapetosaurus krausei* in **A**, anterior view; **B**, posterior view; **C**, left lateral view. **Abbreviations**: **cpol**, centropostzygapophyseal lamina; **pcdl**, posterior centrodiapophyseal lamina; **podl**, postzygodiapophyseal lamina; **posf**, postspinal fossa; **pp**, parapophysis; **prsf**, prespinal fossa; **spol**, spinopostzygapophysesal lamina; **sprl**, spinoprezygapophyseal lamina; **tprl**, intraprezygapophyseal lamina. Scale bar equals 3 cm.

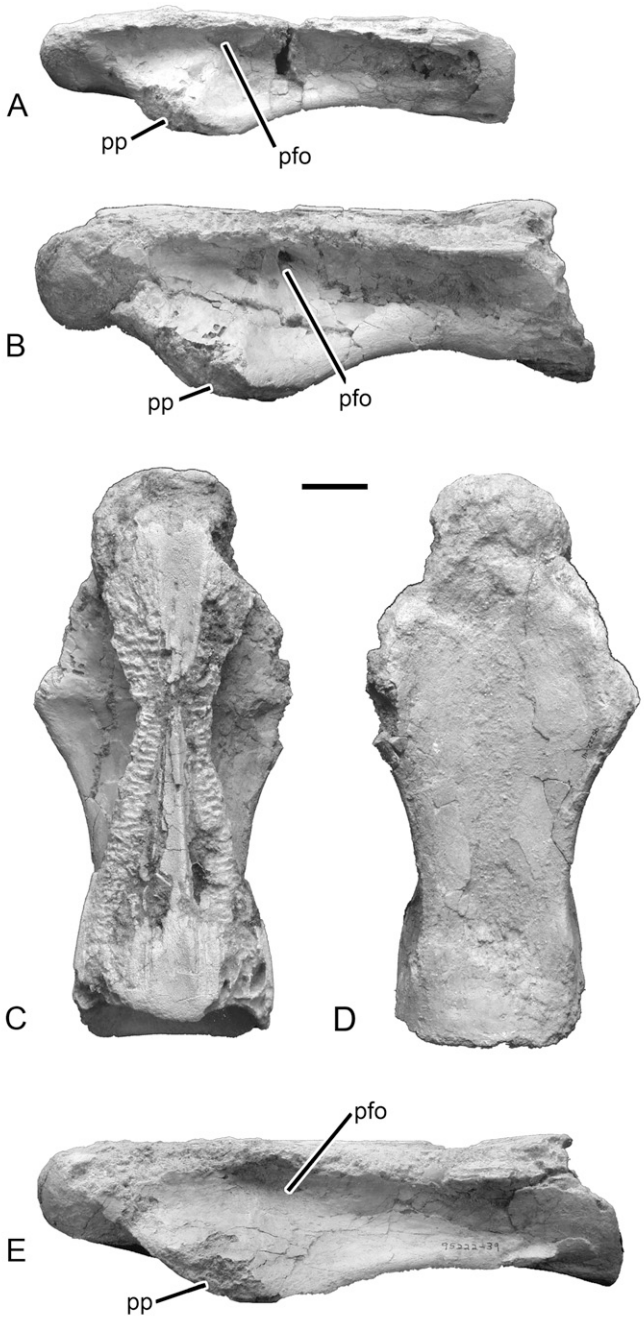


FIGURE 11. Thirteenth to fifteenth cervical centra (FMNH PR 2209) of *Rapetosaurus krausei*. **A**, thirteenth cervical centrum in left lateral view; **B**, fourteenth cervical centrum in left lateral view; **C**, fourteenth cervical centrum in dorsal view; **D**, fourteenth cervical centrum in ventral view; **E**, fifteenth cervical centrum in left lateral view. **Abbreviations**: **pfo**, pneumatic foramen; **pp**, parapophysis. Scale bar equals 3 cm.

**Cervical vertebrae 3 and 4**—Cervical vertebrae 3 (Fig. 7) and 4 (Fig. 8) include disarticulated centra and their closely associated neural arches. The centrum of the third cervical vertebra is slightly elongated (Elongation Index, the centrum length divided by the width of the posterior centrum face (EI, Upchurch, 1998) = 3.3) with an elevated condyle relative to the cotyle. The posteroventral third of cervical vertebra 3 is slightly keeled at the midline. The lateral surface of the centrum is dominated by shallow, elongate, and poorly defined pneumatic fossae. At the anterior edge of the pneumatic fossa, a deep foramen penetrates the body of the centrum and exposes an internal view of the somphospondylous bone texture that characterizes *Rapetosaurus* cervical, dorsal, sacral, and anterior caudal vertebrae. The parapophyses are triangular in cross-section and face anteroventrally, with articular facets positioned directly ventral to the anterior border of the pneumatic fossa. Articular facets that are widely separated anteriorly and posteriorly characterize the neurocentral junction. These facets approach one another in the middle of the centrum, and thus sharply constrict the centrum's contribution to the ventral margin of the neural canal. This constriction persists, with some slight variation, throughout the cervical series.

Five pneumatic fossae bounded by distinct laminae characterize both the cervical 3 and cervical 4 neural arches and are

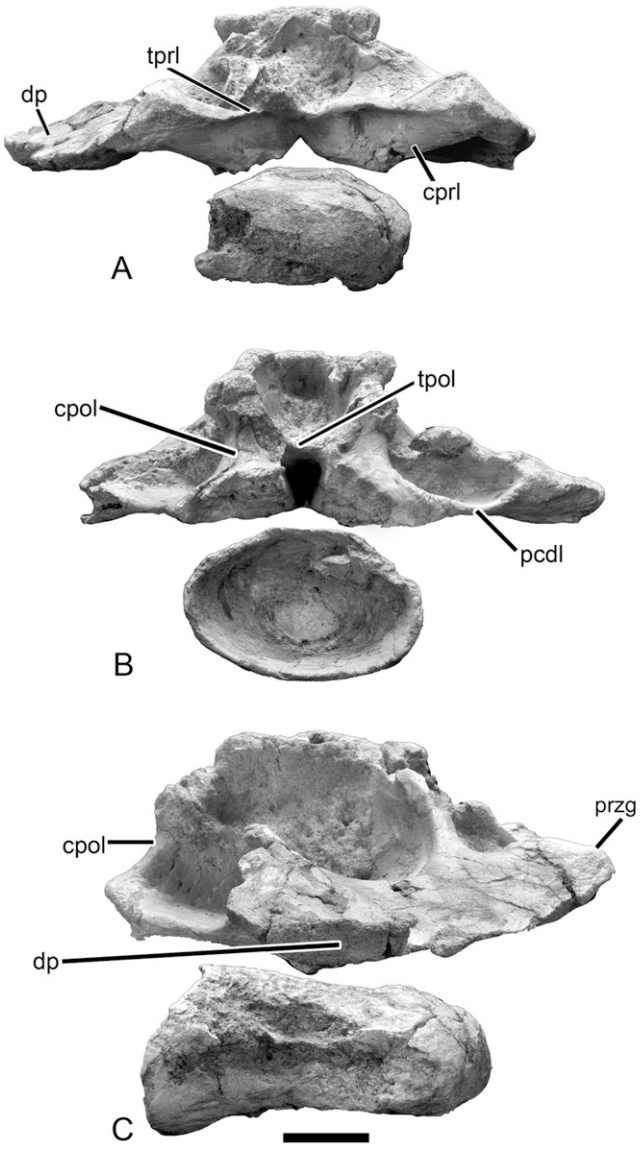


FIGURE 12. Sixteenth cervical vertebra (FMNH PR 2209) of *Rapetosaurus krausei* in **A**, anterior view; **B**, posterior view; **C**, right lateral view. **Abbreviations**: **cpol**, centropostzygapophyseal lamina; **cprl**, centroprezygapophyseal lamina; **dp**, diapophysis; **pcdl**, posterior centrodiapophyseal lamina; **przg**, prezygapophysis; **tpol**, intrapostzygapophyseal lamina; **tprl**, intraprezygapopohyseal lamina. Scale bar equals 3 cm.

elaborated in more posterior cervical vertebrae (Figs. 5, 7). These fossae persist and retain their boundaries throughout the cervical series: (1) an anterolateral fossa; (2) a posterolateral fossa; (3) an infradiapophyseal fossa; (4) a prespinal fossa; and (5) a postspinal fossa. The anterolateral fossa is bounded dorsally by the spinoprezygopophyseal lamina (sprl), the dorsal surface of the diapophysis, and the postzygodiapophyseal lamina (podl). In cervical vertebrae 3 and 4 this fossa is divided into a deep, ventral section by the presence of a sharply defined ridge ("accessory lamina," Fig. 7C), and a dorsally positioned subdivision that lacks well-defined ventral or posterior boundaries. The posterolateral fossa is bounded dorsally by the podl, ventrally by the posterior centrodiapophyseal lamina (pcdl), and posteriorly by the infrapostzygapophseal lamina (ipol), and is consistently larger than the anterolateral fossa. The infradiapophyseal fossa is bounded dorsally by the diapophysis, ventrally by the neurocentral junction, and merges with the diapophysis posteriorly. The prespinal fossa occurs at the base of the neural spine and is bounded ventrally by the intraprezygapophyseal lamina (tprl), and by the left and right spinoprezygapophyseal laminae (sprl), whereas the postspinal fossa is bounded ventrally by the intrapostzygapophyseal lamina (tpol), and on either side by the spinopostzygapophyseal lamina (spol). The pre- and postspinal fossae are elaborated throughout the mid-cervical series (e.g., in cervical vertebrae 9 and 11). A posl is not preserved in the third cervical vertebra, but in the third and fourth cervical vertebrae the prespinal fossa contains a short, midline prespinal lamina (prsl, Fig. 7A).

Pre- and postzygapophyseal facets are also not preserved in cervical vertebra 3, but in cervical vertebra 4, the preserved prezygapophysis is transversely elongate, faces dorsomedially, and lies even with the anterior extent of the centrum. Distally, the neural spine is incompletely preserved, but it is undivided in cervical vertebrae 3 and 4.

**Cervical vertebrae 5–8**—The fifth cervical vertebra includes a centrum and weathered neural arch fragment that can be rearticulated along the neurocentral suture. Cervical vertebrae 6–8 are represented only by centra. In each, the cotyle and condyle occur at the same level (Fig. 8). Elongate but shallow pneumatic fossae occur on the lateral surfaces of each centrum, with pneumatic foramina perforating their anterodorsal corners. Pneumatic fossae extend further posteriorly in these centra than in more proximal vertebrae, encompassing at least two-thirds of the total length of the centrum. A low, oblique ridge of bone extends from the posterodorsal to the anteroventral corner of the pneumatic fossa, dividing it into two subequal halves. Parapophyses arise slightly anterolateral to the pneumatic fossa. The keel is absent from the posteroventral surfaces of the centra. Neural arch facets maintain their constricted middle portions, and attain a wide divergence so that their rugose surfaces are visible in a wide 'V' on the anterolateral and posterolateral surfaces of the centra. At midcentrum a sharp ridge results from the constriction of these facets and overhangs the pneumatic fossa. Cervical vertebrae 5–8 bear a thin area of longitudinally striated bone interposed between the smooth neural canal and the neural arch facets. The striated bone is separated from the neural canal by a high, thin, bony ridge.

**Cervical vertebrae 9–12**—Cervical vertebrae 9 (Fig. 9), 11 (Fig. 10), and 12 are the only cervical vertebrae in which the neural arch and centrum are fully fused. Cervical vertebra 10 includes a poorly preserved neural arch and centrum, which articulate within the series outlined here, but are too poorly preserved to illustrate. In cervical vertebrae 9, 11, and 12, the centrum bears an elongate shallow pneumatic fossa with two anterior pneumatic foramina surrounded by sharp, lip-like boundaries. The pneumatic fossa extends for over two-thirds of the full length of the centrum, from the level of the parapophysis and diapophysis to the postzygapophyses. The parapophysis arises from the centrum's anterior half, and projects strongly ventrolaterally.

The neural arches of cervical vertebrae 9–12 are unique in several respects, particularly with regard to the neural spine. The anterolateral fossa is shallow and broad, whereas the posterolateral fossa is deeper than in more anterior cervical vertebrae. In these vertebrae the anterolateral fossa is bounded by the sprl, podl, prdl, and, to some extent, the spol. The sharply defined spdl of cervical vertebrae 3 and 4 is absent in cervical vertebrae 9–12. Two large, ovoid pneumatic foramina mark the lateral surface of the anterolateral fossa, and are surrounded by smooth, crenulated bone (Figs. 9C, 10C). Such structures have been observed in other dinosaurs and are viewed as possible osteological correlates of lung diverticula (e.g., Janensch, 1947; O'Connor, 2004, 2006). The infradiapophyseal fossa is also very deep, smoothly excavated, and smooth.

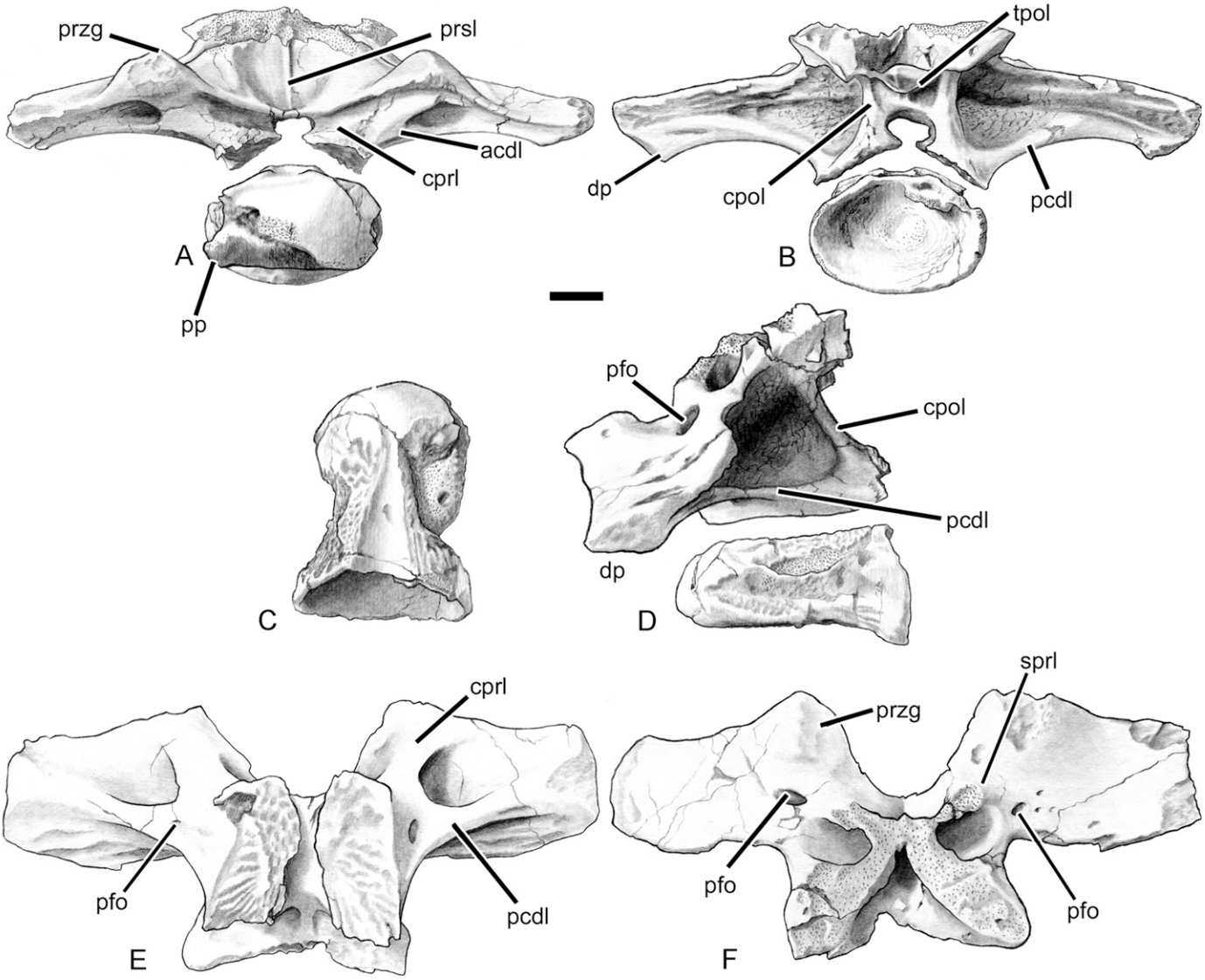


FIGURE 13. Seventeeth cervical vertebra (FMNH PR 2209) of *Rapetosaurus krausei* in **A**, anterior view; **B**, posterior view; **C**, centrum in dorsal view; **D**, left lateral view; **E**, neural arch in ventral view; **F**, neural arch in dorsal view. **Abbreviations**: **acdl**, anterior centrodiapophyseal lamina; **cpol**, centropostzygapophyseal lamina; **cprl**, centroprezygapophyseal lamina; **dp**, diapophysis; **pcdl**, posterior centrodiapophyseal lamina; **pfo**, pneumatic foramen; **pp**, parapophysis; **prsl**, prespinal lamina; **przg**, prezygapophysis; **sprl**, spinoprezygapophyseal lamina; **tpol**, intrapostzygapophyseal lamina. Scale bar equals 3 cm.

One of the most striking features of the *Rapetosaurus* presacral series is evident in this series of cervical vertebrae: the pre- and postspinal fossae are deep in the proximal regions of the neural spine (Figs. 9A, B; 10A, B). In anterior view, the sprl are widely separated by a deep prespinal fossa that extends for approximately three-fifths of the height of the neural spine. The shape of the prespinal fossa varies, ranging in breadth and dorsal extent in this series of mid-cervical vertebrae. Prsl are not visible in cervical vertebrae 9–12, and may be precluded by the depth of the prespinal fossa. The prezygapophyses are widely separated by the tprl and face dorsomedially. In posterior view, there is a wide, tear-shaped space between the postzygapophyses (the postspinal fossa), bounded ventrally by the tpol and laterally by the bilateral spol. As in anterior view, the postspinal fossa separates the spol proximally. These laminae merge more distally to form a single, posterodorsally directed neural spine. There is no posl dorsal to the fossa, or within it. The deep pre- and postspinal fossae at the base of the neural spine may have been present in more anterior cervical vertebrae, for which neural arches were not preserved.

**Cervical vertebrae 13–15**—These three cervical centra differ from more anterior cervical vertebrae of *Rapetosaurus* (Fig. 11). They are more robust with neural arch pedicle facets that are no longer bounded laterally and medially by striated bone and narrow ridges. The neural arch facets retain their midpoint constriction and continue to broadly overhang the centrum dorsal to the pneumatic fossa. Fan-like anterior and posterior extensions of these facets broadly drape the articular faces of the centrum. Pneumatic fossae are restricted to the middle portions of centra, in contrast to the wide antero-posterior extent of pneumatic fossae in most other cervical vertebrae. The parapophyses remain well below and posterior to the anterior articular surface, arising at a level even with the anterior border of the pneumatic fossa. In these posterior cervical centra, parapophyses are far more robust and project anteroventrally.

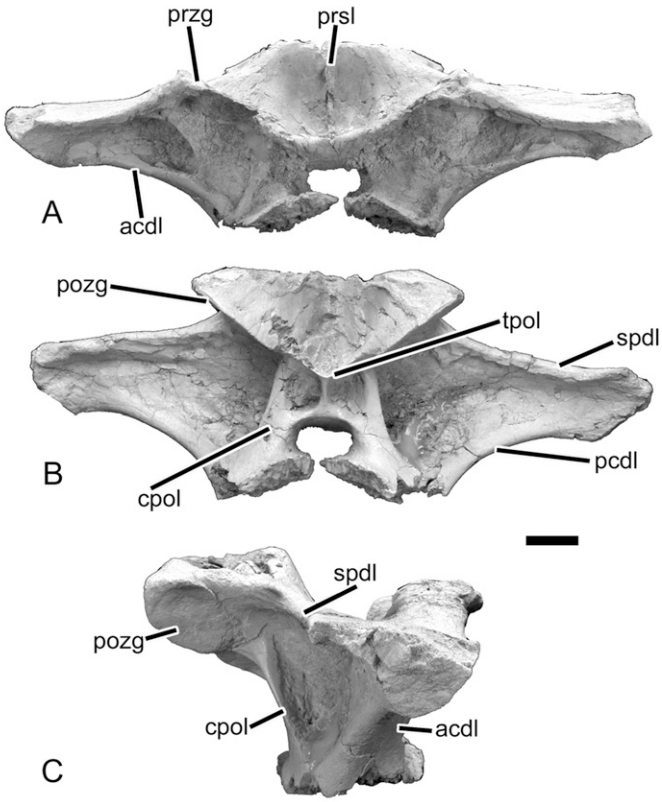


FIGURE 14. First dorsal neural arch (FMNH PR 2209) of *Rapetosaurus krausei* in **A**, anterior view; **B**, posterior view; **C**, right lateral view. **Abbreviations**: **acdl**, anterior centrodiapophyseal lamina; **cpol**, centropostzygapophyseal lamina; **pcdl**, posterior centrodiapophyseal lamina; **prsl**, prespinal lamina; **pozg**, postzygapophysis; **przg**, prezygapophysis; **spdl**, spinodiapophyseal lamina; **tpol**, intrapostzygapophyseal lamina. Scale bar equals 3 cm.

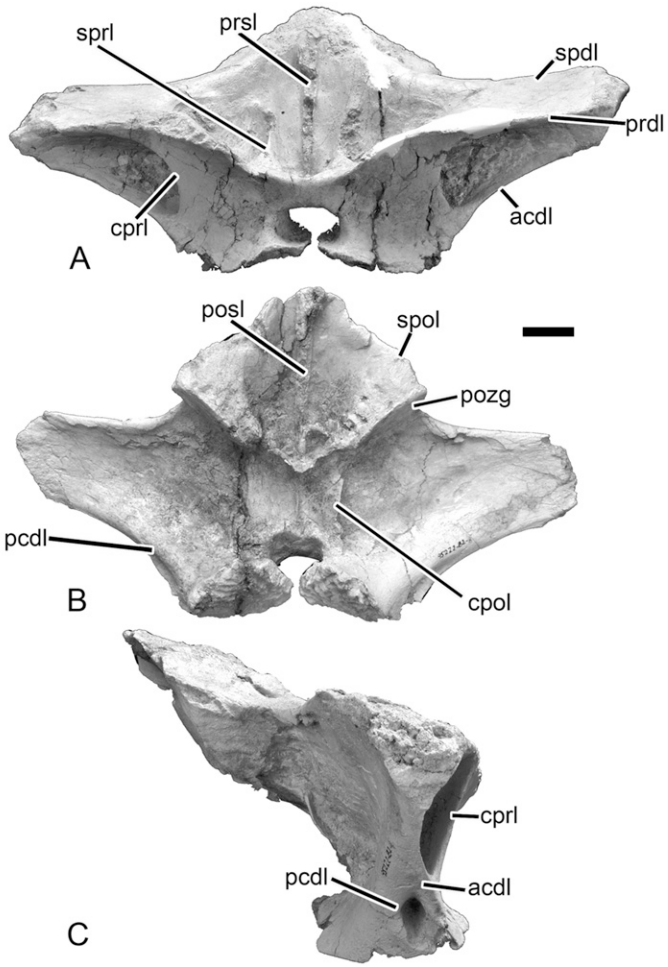


FIGURE 15. Second dorsal neural arch (FMNH PR 2209) of *Rapetosaurus krausei* in **A**, anterior view; **B**, posterior view; **C**, right lateral view. **Abbreviations**: **acdl**, anterior centrodiapophyseal lamina; **cpol**, centropostzygapophyseal lamina; **cprl**, centroprezygapophyseal lamina; **pcdl**, posterior centrodiapophyseal lamina; **posl**, postspinal lamina; **pozg**, postzygapophysis; **prdl**, prezygodiapophyseal lamina; **prsl**, prespinal lamina; **spdl**, spinodiapophyseal lamina; **spol**, spinopostzygapophysesal lamina; **sprl**, spinoprezygapophyseal lamina. Scale bar equals 3 cm.

**Cervical vertebrae 16–17**—These two vertebrae typify the "cervicodorsal transition", but a few key morphological features indicate that they should be considered a part of the cervical series. In particular, the anterolateral and posterolateral fossae are deep and retain their laminar boundaries, and the neurocentral junction is characteristically butterfly-shaped. Cervical vertebra 16 (Fig. 12) consists of a weathered, poorly preserved, isolated centrum that articulates with a well-preserved neural arch. The centrum is markedly shorter anteroposteriorly than the preceding cervical vertebrae, exhibits shallow and poorly demarcated lateral pneumatic fossae, and slightly flared neural arch facets. The accompanying neural arch is well preserved and distinctive, with wide, aliform, laterally directed diapophyses. The spinal fossae occupy identical placement and laminar boundaries as those of more anterior cervical vertebrae, but are greatly modified in overall shape and size. The prezygapophyses extend past the anterior margin of the centrum, and their broad facets face dorsally. They are separated by an elongate, dorsoventrally narrow tprl, which forms the dorsal boundary of the neural canal and the ventral boundary of the prespinal fossa. This fossa is expanded relative to its homologue in more anterior cervical vertebrae, but maintains bilateral sprl boundaries. The medial cprl forms the lateral boundary of the neural canal, and is separated from the lateral cprl by a deep fossa (Fig. 12A).

The anterior centrodiapophyseal lamina (acdl) is broad, forming a large bony strut for the anterior wing of the neural arch that bears the prezygapophyses. Ventrally, the infradiapophyseal pneumatic fossa is wide and nearly divided into anterior and posterior halves by an unnamed lateral wing of the acdl. In posterior view, the postspinal fossa is expanded into a broad, U-shaped excavation that lies between the left and right spol and the tpol. The centropostzygapophyseal lamina (cpol) is undivided and forms the lateral boundary of the posterior neural canal. The neural spine is incompletely preserved, but does not exhibit the deep proximal excavation observed in cervical vertebrae 9–12. There is no sign of a prsl or posl in cervical vertebra 16.

Cervical vertebra 17 is comprised of a centrum and neural arch that were found in close association with the anterior dorsal vertebrae. They rearticulate precisely along the neurocentral junction (Figs. 4E, 13) and embody the combination of characters that are expected in the cervicodorsal transition. The centrum is strongly opisthocoelous, but is shorter and more robust than that of cervical vertebra 16. Although butterfly-shaped neural arch facets constrict the neural canal most anteriorly, it remains wider than in cervical vertebrae 3–16 posteriorly (Fig. 13C, E). The pneumatic fossa is deep, well defined, and undivided. It is much shorter than those of the anterior cervical vertebrae and occupies only the middle portion of the centrum.

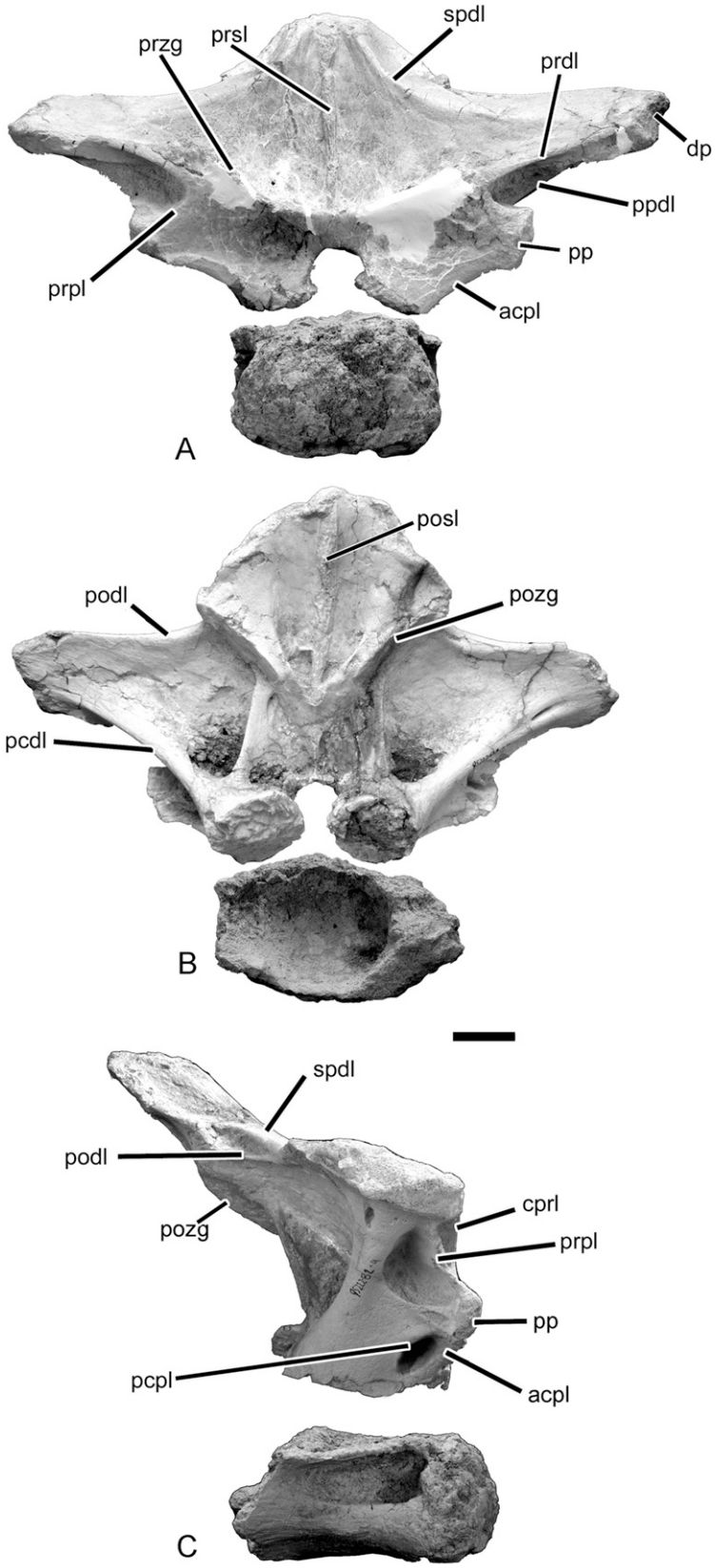


FIGURE 16. Third dorsal vertebra (FMNH PR 2209) of *Rapetosaurus krausei* in **A**, anterior view; **B**, posterior view; **C**, right lateral view. **Abbreviations**: **acpl**, anterior centroparapophyseal lamina; **cprl**, centroprezygapophyseal lamina; **dp**, diapophysis; **pcdl**, posterior centrodiapophyseal lamina; **podl**, postzygodiapophyseal lamina; **posl**, postspinal lamina; **pozg**, postzygapophysis; **pp**, parapophysis; **ppdl**, paradiapophyseal lamina; **prdl**, prezygodiapophyseal lamina; **prpl**, prezygoparapophyseal lamina; **prsl**, prespinal lamina; **przg**, prezygapophysis; **spdl**, spinodiapophyseal lamina. Scale bar equals 3 cm.

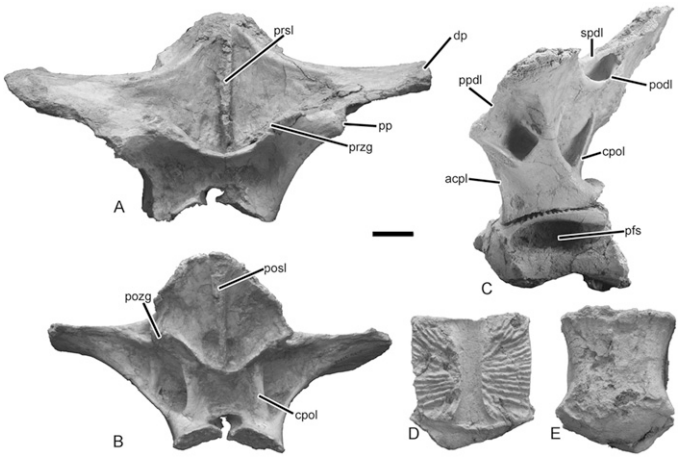


FIGURE 17. Fourth dorsal vertebra (FMNH PR 2209) of *Rapetosaurus krausei*. **A**, neural arch in anterior view; **B**, neural arch in posterior view; **C**, articulated centrum and neural arch in left lateral view; **D**, centrum in dorsal view, anterior towards top; **E**, centrum in ventral view, anterior toward bottom. **Abbreviations**: **acpl**, anterior centroparapophyseal lamina; **cpol**, centropostzygapophyseal lamina; **dp**, diapophysis; **pfs**, pnematic fossa; **podl**, postzygodiapophyseal lamina; **posl**, postspinal lamina; **pozg**, postzygapophysis; **pp**, parapophysis; **ppdl**, paradiapophyseal lamina; **prsl**, prespinal lamina; **przg**, prezygapophysis; **spdl**, spinodiapophyseal lamina. Scale bar equals 3 cm.

In lateral view, the parapophysis is flush with the centrum and no longer projects strongly laterally. It is subrectangular and is positioned just anterior to and level with the pneumatic fossa.

The aliform diapophyses of the neural arch are broad transversely and flattened dorsoventrally. A broad, shallow fossa divides the acdl and pcdl on the ventral surface of the diapophysis. The base of the neural arch is perforated by irregularly positioned pneumatic foramina. The anteroposteriorly and transversely expanded diapophysis also houses a pneumatic foramen on its dorsal surface (Fig. 13D, F). The elliptical prezygapophyseal facets are angled dorsolaterally. The medial cprl forms portions of the lateral walls of the neural canal, as well as the ventral wall of a median fossa. This median fossa is bounded dorsally by the tprl, and is not found in cervical vertebrae 3–16. The lateral cprl forms the dorsomedial border of an anteriorly directed fossa (bordered dorsally by the diapophysis and ventromedially by the acdl). Instead of a discrete, deeply excavated prespinal fossa devoid of prsl (as in cervical vertebrae 8–16), cervical vertebra 17 exhibits a well-developed prsl that occupies a large broadly excavated subtriangular region along the anterior neural spine. The prsl extends for at least half of the neural spine, and is broken at its distalmost end. The postzygapophyses are broad and subcircular. They are connected medially by an elongate, narrow tpol, dorsally by a flange-like spol, and ventrally by robust cpol. The deep, narrow postspinal fossa is absent, and is replaced by a cavernous excavation on the posterior surface of the neural spine and a sharp, median posl. The posl is only traceable for the proximal one-third of the neural spine.

A fossa occurs ventral to the tprl where the cprl is divided. An additional ventral excavation of the neural arch occurs on the underside of the diapophysis and is bounded dorsally by the prezygodiapophyseal lamina (prdl) and ventrally by the acdl. On the posterior side of the vertebra, strong median laminae are developed between infrapostzygaopophyseal laminae to result in bilateral, paramedian, shallow and triangular coels.

**Cervical Vertebrae, Comparisons**—*Rapetosaurus* cervical vertebral centra exhibit elongation indices range from 3.3 to 4.3, similar to that known for most titanosaurs including *Malawi-*

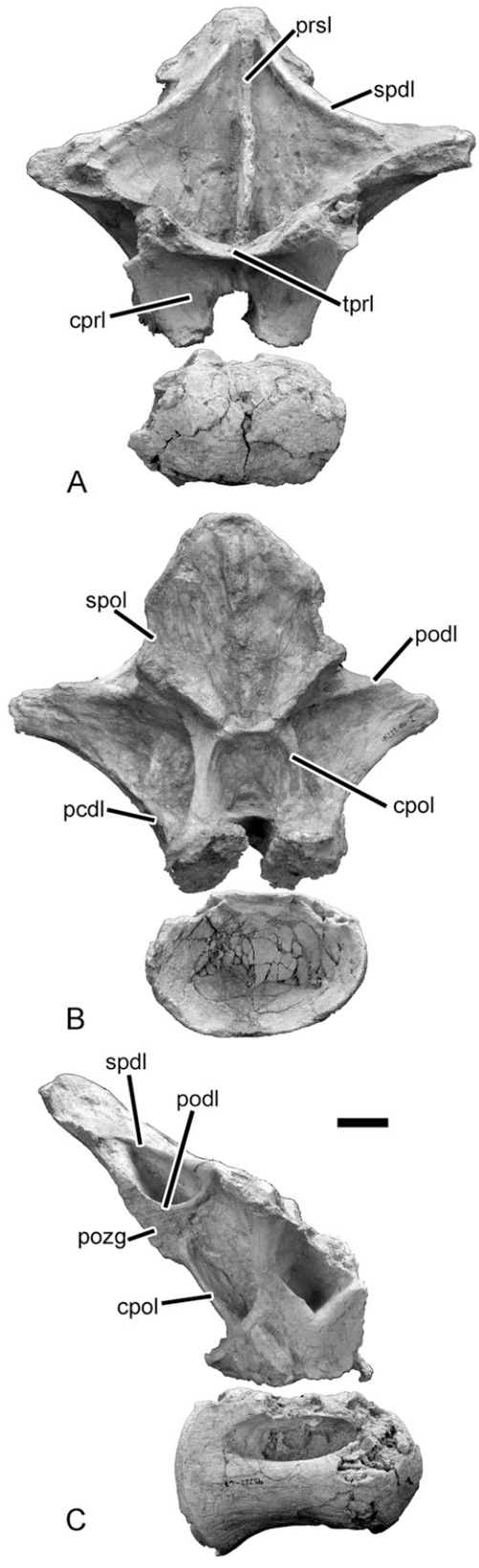


FIGURE 18. Fifth dorsal vertebra (FMNH PR 2209) of *Rapetosaurus krausei* in **A**, anterior view; **B**, posterior view; **C**, right lateral view. **Abbreviations**: **cpol**, centropostzygapophyseal lamina; **cprl**, centroprezygapophyseal lamina; **pcdl**, posterior centrodiapophyseal lamina; **podl**, postzygodiapophyseal lamina; **pozg**, postzygapophysis; **prsl**, prespinal lamina; **spdl**, spinodiapophyseal lamina; **spol**, spinopostzygapophyseal lamina; **tprl**, intraprezygapophyseal lamina Scale bar equals 3 cm.

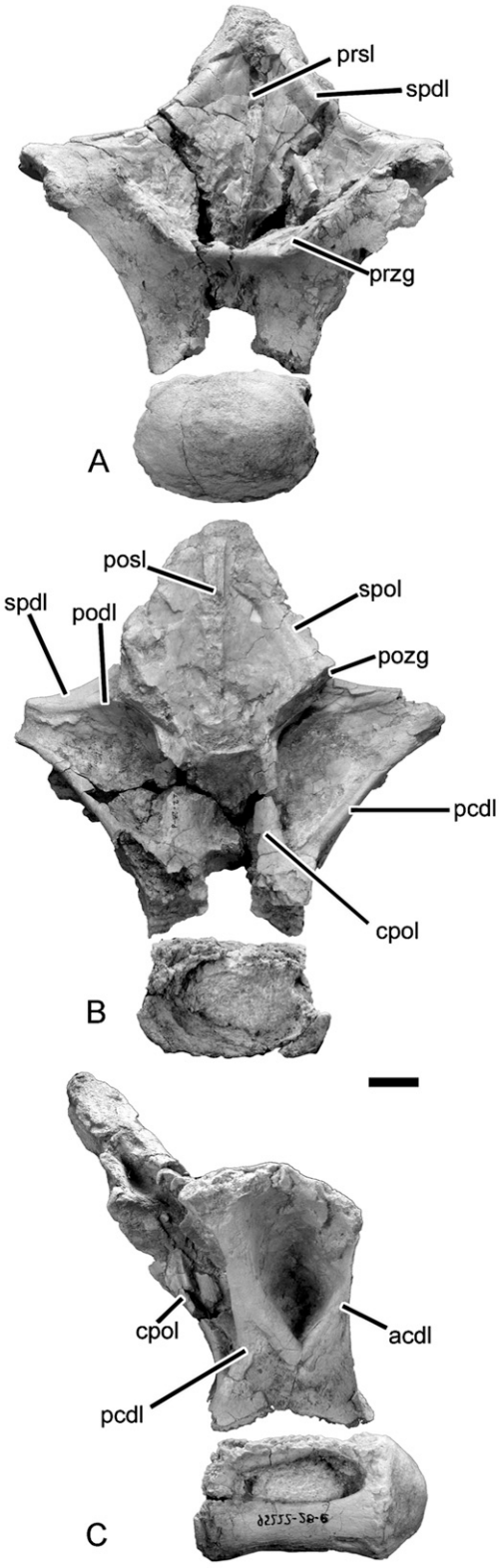


FIGURE 19. Sixth dorsal vertebra (FMNH PR 2209) of *Rapetosaurus krausei* in **A**, anterior view; **B**, posterior view; **C**, right lateral view. **Abbreviations**: **acdl**, anterior centrodiapophyseeal lamina; **cpol**, centropostzygapophyseal lamina; **pcdl**, posterior centrodiapophyseal lamina; **podl**, postzygodiapophyseal lamina; **posl**, postspinal lamina; **pozg**, postzygapophysis; **prsl**, prespinal lamina; **przg**, prezygapophysis; **spdl**, spinodiapophyseal lamina; **spol**, spinopostzygapophyseal lamina. Scale bar equals 3 cm.

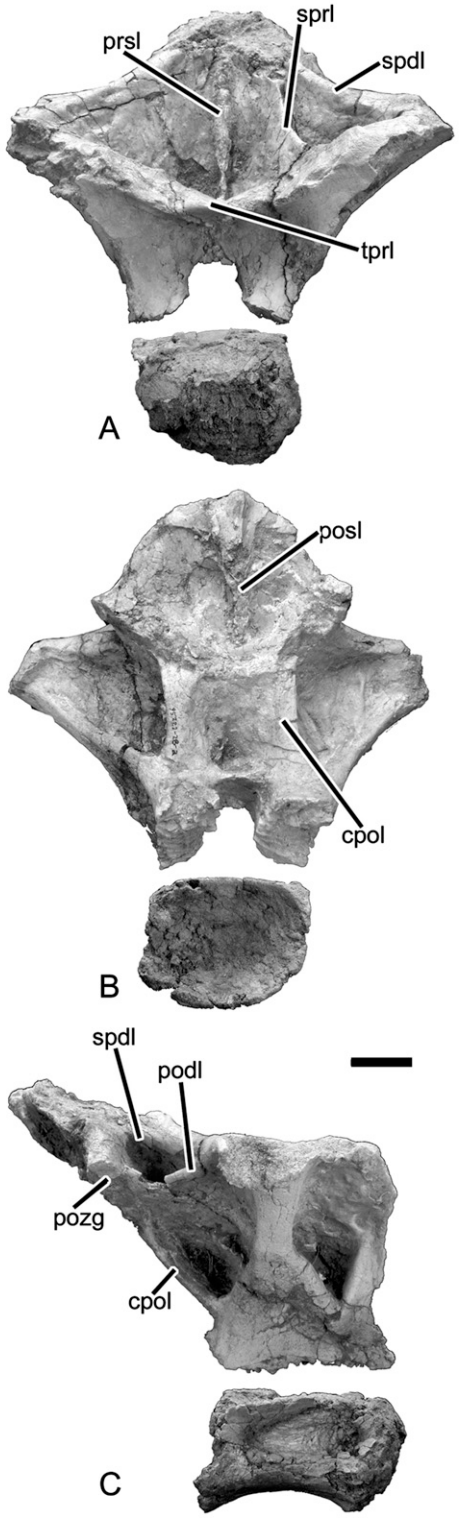


FIGURE 20. Seventh dorsal vertebra (FMNH PR 2209) of *Rapetosaurus krausei* in **A**, anterior view; **B**, posterior view; **C**, right lateral view. **Abbreviations**: **cpol**, centropostzygapophyseal lamina; **podl**, postzygodiapophyseal lamina; **posl**, postspinal lamina; **pozg**, postzygapophysis; **prsl**, prespinal lamina; **spdl**, spinodiapophyseal lamina; **sprl**, spinoprezygopophyseal lamina; **tprl**, intraprezygapophyseal lamina. Scale bar equals 3 cm.

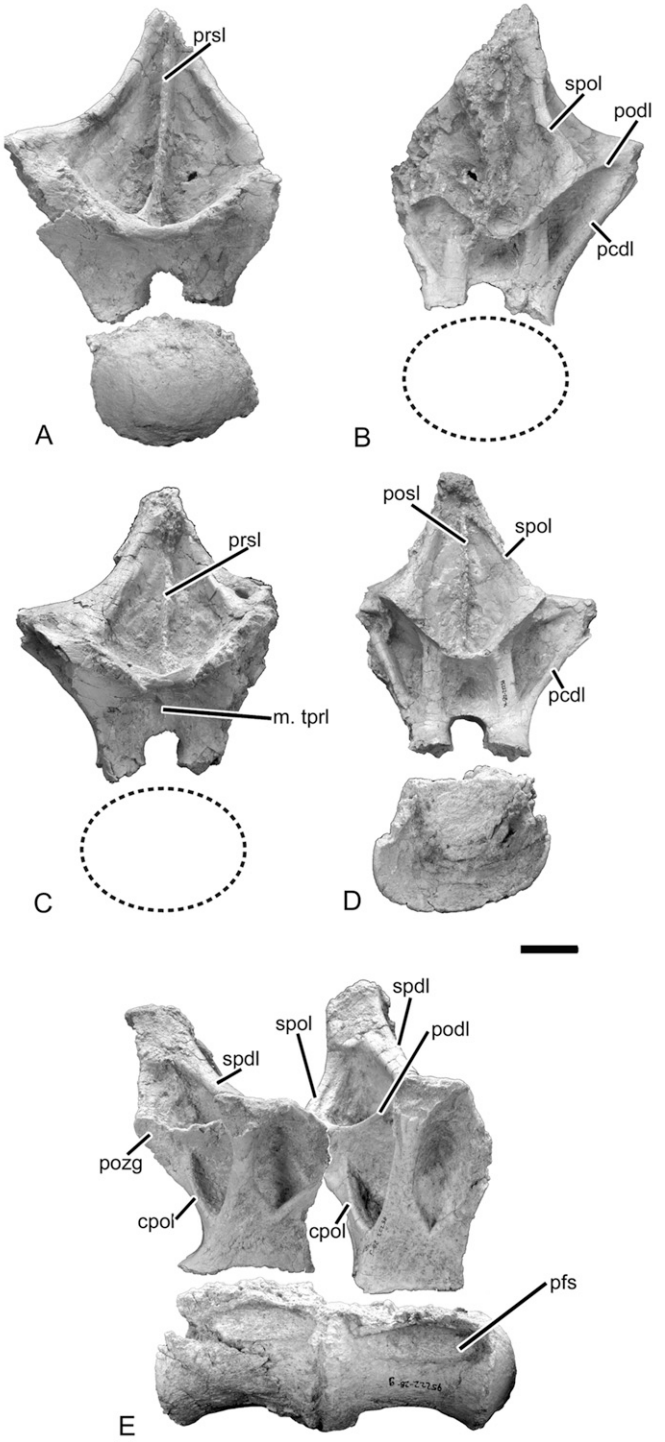


FIGURE 21. Eighth and ninth dorsal vertebrae (FMNH PR 2209) of *Rapetosaurus krausei*. **A**, eighth dorsal vertebra in anterior view; **B**, ninth dorsal neural arch in posterior view; **C**, eighth dorsal neural arch in anterior view; **D**, ninth dorsal vertebra in posterior view; **E**, eighth and ninth dorsal vertebrae in right lateral view. **Abbreviations**: **cpol**, centropostzygapophyseal lamina; **m. tprl**, midline extension of intraprezygapophyseal lamina; **pcdl**, posterior centrodiapophyseal lamina; **pfs**, pneumatic fossa; **podl**, postzygodiapophyseal lamina; **posl**, postspinal lamina; **pozg**, postzygapophysis; **prsl**, prespinal lamina; **spdl**, spinodiapophyseal lamina; **spol**, spinopostzygapophyseal lamina. Scale bar equals 3 cm.

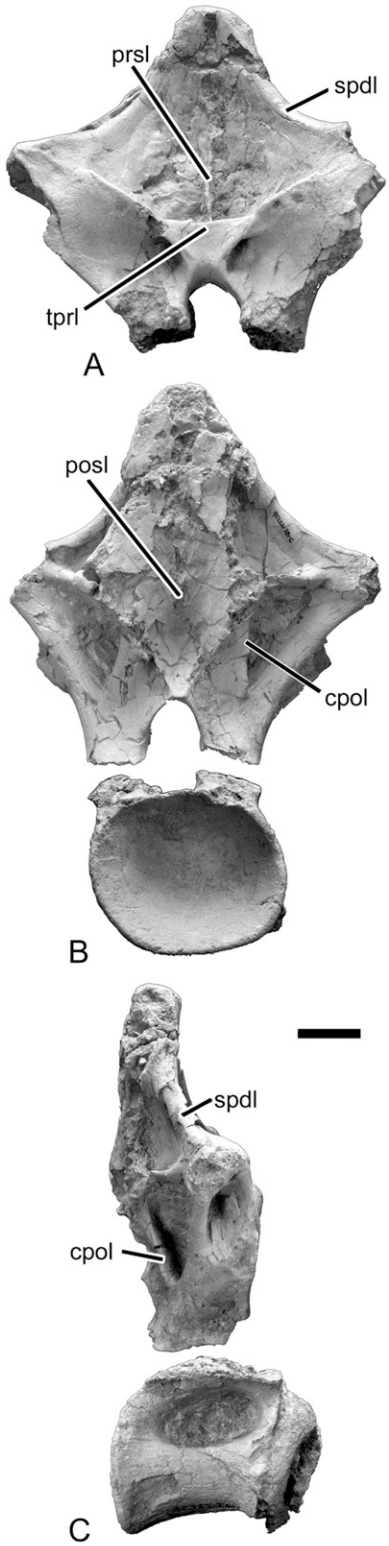


FIGURE 22. Tenth dorsal vertebra (FMNH PR 2209) of *Rapetosaurus krausei*. **A**, neural arch in anterior view; **B**, articulated vertebra in posterior view; **C**, vertebra in right lateral view. **Abbreviations**: **cpol**, centropostzygapophyseal lamina; **posl**, postspinal lamina; **prsl**, prespinal lamina; **spdl**, spinodiapophyseal lamina; **tprl**, intraprezygapophyseal lamina. Scale bar equals 3 cm.

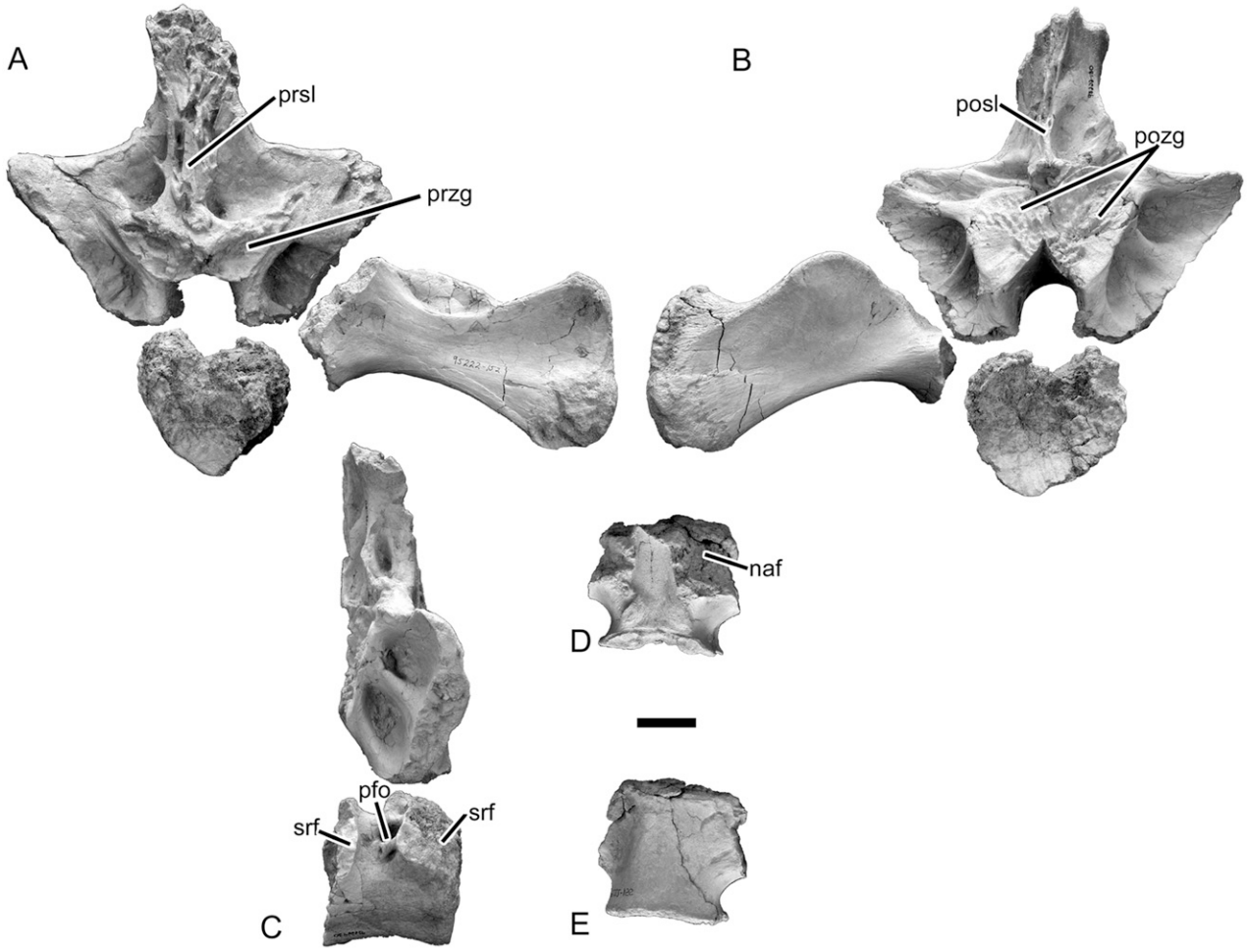


FIGURE 23. Second sacral vertebra (FMNH PR 2209) of *Rapetosaurus krausei*. **A**, articulated centrum, neural arch, and left sacral rib in anterior view; **B**, articulated centrum, neural arch, and left sacral rib in posterior view; **C**, articulated vertebra in right lateral view; **D**, centrum in dorsal view, anterior towards top; **E**, centrum in ventral view, anterior towards top. **Abbreviations**: **naf**, neural arch facet; **pfo**, pneumatic foramen; **posl**, postspinal lamina; **pozg**, postzygapophysis; **prsl**, prespinal lamina; **przg**, prezygapophysis; **srf**, sacral rib facet. Scale bar equals 3 cm.

*saurus dixeyi* (SMU Mal-280, Gomani, 2005), *Alamosaurus sanjuanensis* (TMM 43621-1, Lehman and Coulson, 2002), *Saltasaurus loricatus* (PVL 4017-3, 6, 139, Powell, 1992), *Phuwiangosaurus sirindhornae* (PW 1-1, Martin et al., 1994), and *Rinconsaurus caudamirus* (MRS-pv 2-4, Calvo and González Riga, 2003). It differs from the relatively short cervical centra of *Isisaurus colberti* (ISI R335, Jain and Bandyopadhyay, 1997) and *Mendozasaurus neguyelap* (IANIGLA-PV 076-1-4, González Riga, 2005), in which EI $\leq$ 2.5, and from the exceptionally elongated cervical centra of *Erketu ellisoni* (EI $\geq$ 5.0, IGM 100/1803, Ksepka and Norell, 2006). A ventral keel is present along the ventral midline of all *Rapetosaurus* cervical centra; it is most strongly developed in posterior cervical vertebrae. The ventral keel has a restricted distribution among other titanosaurs. It is absent in the anterior cervical vertebrae for all other titanosaurs with preserved cervical centra (e.g., *Neuquensaurus australis* (MLP CS1406, Huene, 1929; Powell, 1986, 2003), but is present on the posteroventral surfaces of posterior cervical centra in *Isisaurus, Saltasaurus, Magyarosaurus dacus* (BMNH R 4898, pers. observ.), and *Lirainosaurus astibiae* (MCNA 7445, Sanz et al., 1999). Development of pneumatic fossae differs dramatically among titanosaur centra. *Malawisaurus, Isisaurus, Rapetosaurus*, and *Saltasaurus* are unique among derived titanosaurs in the presence of elongate, shallow lateral pneumatic fossae that are divided by a thin, oblique lamina. In these taxa, the pneumatic fossae contain one or more well-defined pneumatic foramina. Other derived titanosaurs such as *Alamosaurus* and *Neuquensaurus* bear poorly developed, undivided pneumatic fossae. Unlike most titanosaurs, the parapophysis in *Rapetosaurus, Saltasaurus, Phuwiangosaurus*, and *Rocasaurus* arises just posterior to the anterior articular surface of the centrum rather than at mid-centrum.

The neurocentral junction in *Rapetosaurus* cervical vertebrae is unique among titanosaurs. In all cervical vertebrae it is constricted, butterfly-shaped in dorsal view, and extends the full length of the centrum. Only *Alamosaurus* approaches this morphology, with a very slight medial constriction of the sutural surfaces of the neural arch pedicles. In other titanosaurs, the neurocentral junction is straight and does not extend the full length of the centrum. *Rapetosaurus* and *Saltasaurus* share the presence of prezygapophyses that do not extend beyond the anterior border of the centrum, and postzygapophyses that extend well beyond the posterior border of the centrum.

The neural spine of *Rapetosaurus* is single, anteroposteriorly expanded, transversely compressed, at least two times higher than the centrum, and exhibits distinctive pre- and postspinal fossae. *Malawisaurus* shares the development of shallow pre- and postspinal fossae, but only in the mid-cervical neural spines.

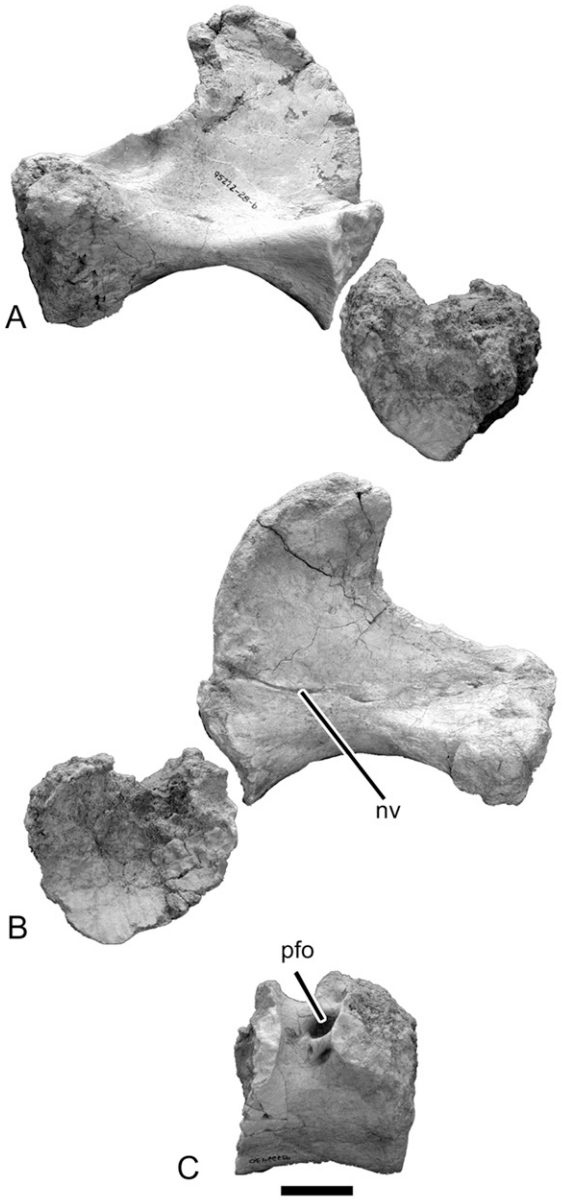


FIGURE 24. Fourth sacral centrum and right sacral rib (FMNH PR 2209) of *Rapetosaurus krausei*. **A**, anterior view; **B**, posterior view; **C**, right lateral view. **Abbreviations**: **nv**, neurovascular groove; **pfo**, pneumatic foramen. Scale bar equals 3 cm.

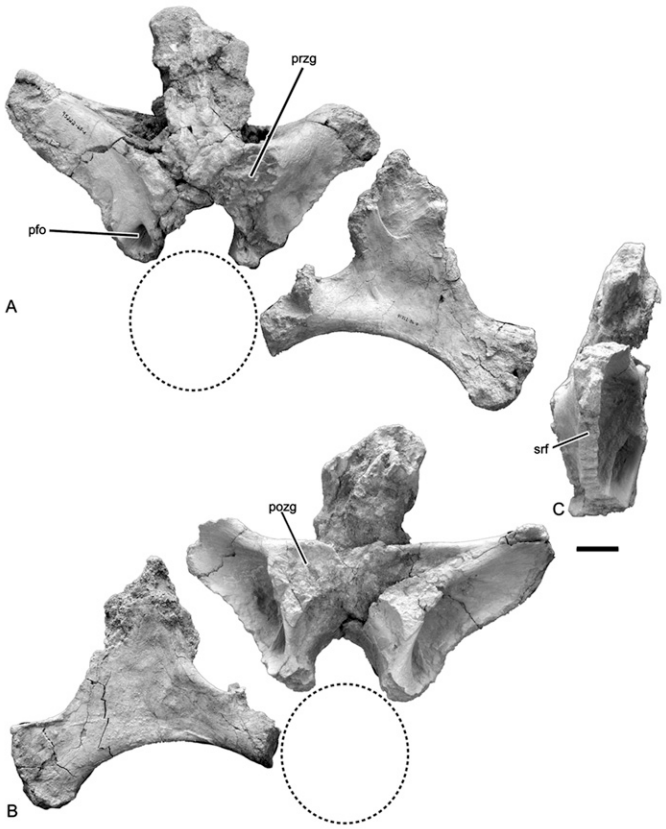


FIGURE 25. Fifth sacral neural arch and left sacral rib (FMNH PR 2209) of *Rapetosaurus krausei*. **A**, anterior view; **B**, posterior view; **C**, neural arch in left lateral view. **Abbreviations**: **pfo**, pneumatic foramen; **pozg**, postzygapophysis; **przg**, prezygapophysis; **srf**, sacral rib facet. Scale bar equals 3 cm.

Other derived titanosaurs vary in the development and position of these fossae. *Alamosaurus* exhibits a deep, round postspinal fossa. *Neuquensaurus* and *Saltasaurus* share the presence of a shallow postspinal fossa. In most other titanosaurs, pre- and postspinal fossae are absent (e.g., *Ligabuesaurus leanzi*, MCF-PVPH-233/2, Bonaparte et al., 2006; *Mendozasaurus*). *Rapetosaurus* cervical neural spines exhibit strongly developed lateral fossae bounded by discrete laminae. Other derived titanosaurs, including *Saltasaurus* and *Isisaurus* exhibit less discretely bound fossae. *Rapetosaurus* and *Saltsaurus* share the presence of a divided cprl as well as aliform diapophyses that are extremely expanded transversely. Powell (2003:pl. 21.2b) figured a lamina dividing an anterolateral fossa in an anterior cervical vertebra of *Saltasaurus* similar to the division observed in the third cervical vertebra of *Rapetosaurus*. *Rapetosaurus* is unique among titanosaurs in exhibiting a prsl in the anteriormost cervical vertebrae.

## Dorsal Vertebrae

Elements from ten dorsal vertebrae were recovered from MAD 93-18, including eight disarticulated neural arches and centra that can be rearticulated along neurocentral facets (Figs. 14–22). Centra for dorsal vertebrae 1 and 2 are not preserved. Significantly, in spite of some slight deformation, vertebrae can generally be rearticulated with one another in series, thus imparting confidence to the positions outlined below. Throughout the series, centra are strongly opisthocoelous and are marked by deep, undivided lateral pneumatic fossae. The centra maintain a relatively constant length through the sixth dorsal vertebra, then shorten along the series toward the sacrum. The constricted neurocentral junction that is characteristic of cervical vertebrae is absent in the dorsal series. Instead, neural arch facets are generally anteroposteriorly straight and extensive. Neural spines are low and angled posteriorly, with transversely oriented, aliform diapophyses in the anteriormost dorsal vertebrae. By the mid-dorsal region, the distal neural spine exhibits broad, triangular processes that flare laterally. The neural spine gradually attains a more vertical orientation, such that by the posteriormost dorsal vertebrae, it does not project posteriorly beyond the neural arch facets. Pre- and postspinal laminae are prominent throughout the series, as are other strongly developed

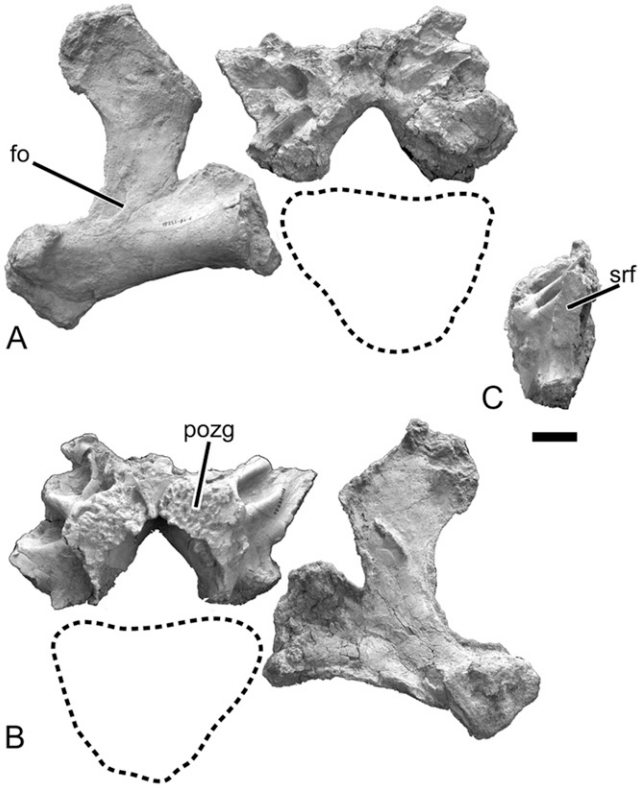


FIGURE 26. Sixth sacral neural arch and right sacral rib (FMNH PR 2209) of *Rapetosaurus krausei*. **A**, anterior view; **B**, posterior view; **C**, neural arch in left lateral view. **Abbreviations**: **fo**, foramen; **pozg**, postzygapophysis; **srf**, sacral rib facet. Scale bar equals 3 cm.

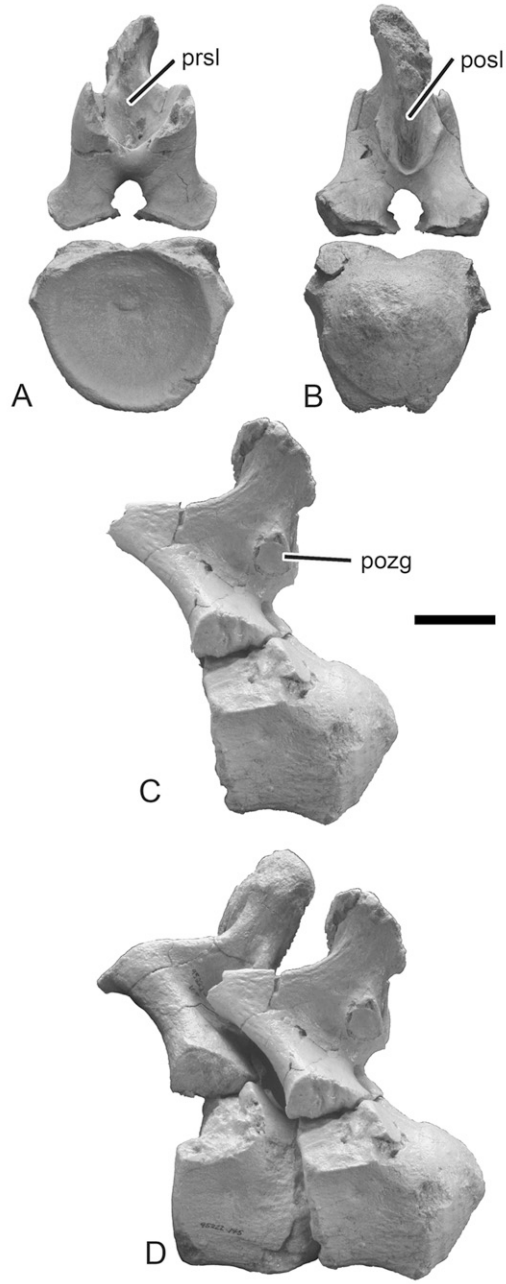


FIGURE 27. Proximal caudal vertebrae (FMNH PR 2209) of *Rapetosaurus krausei* in **A**, anterior view; **B**, posterior view; **C, D**, left lateral view. **Abbreviations**: **posl**, postspinal lamina; **prsl**, prespinal lamina; **pozg**, postzygapophysis. Scale bar equals 3 cm.

lateral neural arch laminae and fossae. By dorsal 6 or 7, the parapophysis and diapophysis merge. Dorsal vertebrae with similar morphologies are described together below.

**Dorsal vertebrae 1 and 2**—Only the neural arches are preserved for the first two dorsal vertebrae. In contrast to the constricted morphology of the neural arch facets in the cervical vertebrae, in dorsal neural arches 1 (Fig. 14) and 2 (Fig. 15) they are subcircular and broad. The parapophysis is restricted to the centrum in dorsal vertebrae 1 and 2. The transverse processes in the first dorsal vertebra resemble those of the cervicodorsal transitional vertebrae but are dorsally convex and curved rather than dorsoventrally flat. In the second and subsequent dorsal vertebrae, the diapophyses extend from the neural arch via steeply angled, ventrally concave, straight, transverse processes. In dorsal vertebra 2, the spdl extends posterodorsally, and meets the triangular distal neural spine at a low angle. The distal neural spine of the second dorsal vertebra is broader transversely than anteroposteriorly, and extends beyond the posterior extent of the neural arch facets in lateral view.

The prezygapophyses of dorsal vertebra 1 are broad, subcircular, and face dorsomedially. They are positioned at a level just above that of the diapophyses, such that the prdl extends lateroventrally in anterior view. The postzygapophyses are subcircular and lateroventrally-directed. In the second dorsal vertebra, the prezygapophyses lie below the diapophyses and are compressed anteroposteriorly with transversely elongate oval articular surfaces. The postzygapophyses of the second dorsal vertebra are anteroposteriorly compressed and are steeply angled.

The prespinal fossa of dorsal neural spines 1–2 is broad, U-shaped, and concave. The fossa is ventrally bounded by the tpol and laterally bounded by short, gracile right and left sprl. On the midline, an elongate, planar prsl arises just dorsal to the tprl and extends for the proximal four-fifths of the neural spine. Distally on neural spine 2, the prsl fans out transversely into a broad planar process (Fig. 15A). The tpol forms the ventral boundary of the broad, concave postspinal fossa. This fossa is deepest just above the tpol on the midline. A sharp, narrow posl

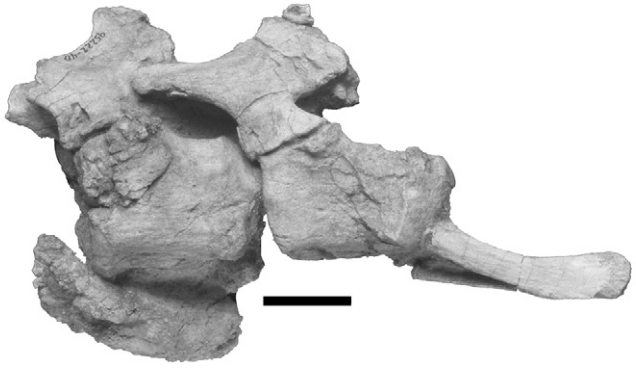

FIGURE 28. Articulated mid-caudal vertebrae and chevrons (FMNH PR 2209) of *Rapetosaurus krausei* in left lateral view. Scale bar equals 3 cm.

extends dorsally to the apex of the neural spine. The sharp tpol also forms the dorsal boundary of an elongate excavation between it and the neural canal. The gracile and elongate cpol forms the lateral boundary of this excavation. At the depressed midline of this excavation lies a strongly developed vertical extension of the tpol that extends from the horizontally oriented tpol to the neural canal. This vertical extension of the tpol persists through the middle of the dorsal series.

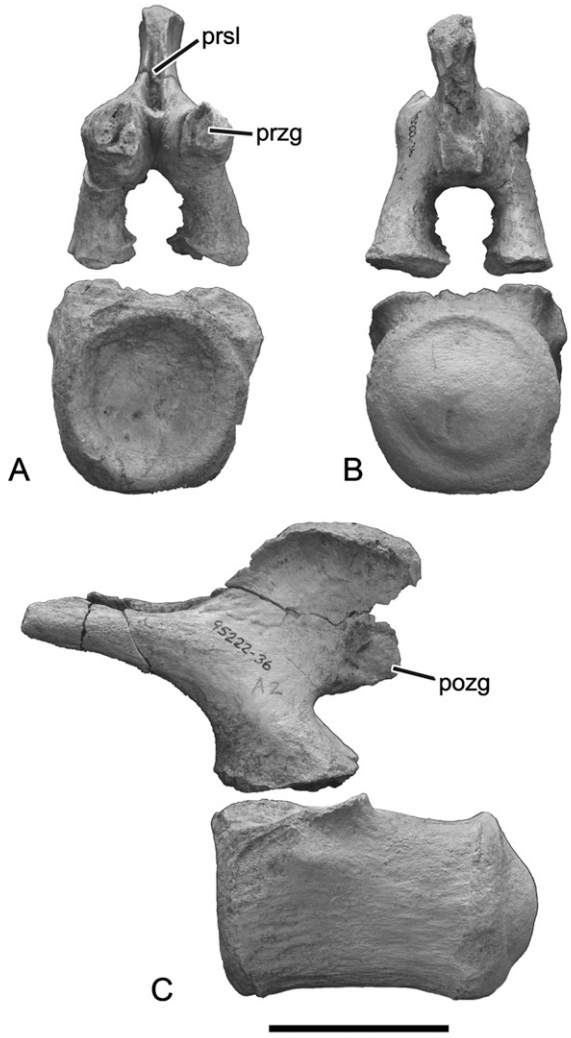


FIGURE 29. Distal caudal vertebra (FMNH PR 2209) of *Rapetosaurus krausei* in **A**, anterior view; **B**, posterior view; **C**, left lateral view. **Abbreviations**: **pozg**, postzygapophysis; **prsl**, prespinal lamina; **przg**, prezygapophysis. Scale bar equals 3 cm.

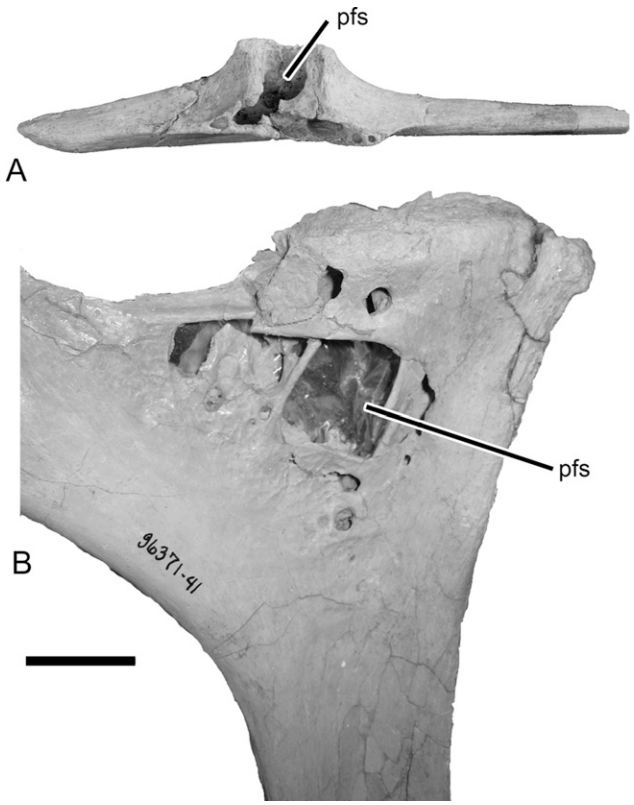


FIGURE 30. Ribs of *Rapetosaurus krausei*. **A**, Detail of proximal end of cervical rib (FMNH PR 2209). **B**, Detail of proximal end of dorsal rib (SMM P2007.4.1). **Abbreviations**: **pfs**, pneumatic fossa. Scale bar equals 3 cm.

The prdl extends horizontally toward the diapophysis, forming the dorsal boundary of the large anterolateral fossa. The anterolateral fossa of the second dorsal vertebra is expanded relative to the small, ventrally positioned anterolateral fossa of dorsal vertebra 1. An additional, rounded fossa occurs in the second dorsal vertebra between the acdl and pcdl. The cpol, pcdl, and spdl form the boundaries of the triangular posterolateral fossa. In dorsal vertebra 2 and all successive dorsal vertebrae, the posterolateral fossa has its broadest exposure posteriorly and is consistently larger than the anterolateral fossa.

**Dorsal 3 and 4**—Dorsal vertebrae 3 (Fig. 16) and 4 (Fig. 17) each include a disarticulated centrum and neural arch that rearticulate perfectly along the neurocentral facets. The centra are relatively short and have deep lateral pneumatic fossae. The neural arch facets extend the full length of the centrum. They are slightly medially constricted, and embody the transition to the more elongate, straight neural arch facets typical of more posterior dorsal vertebrae.

The diapophyses extend from the neural arch via steeply angled, straight, transverse processes. The parapophyses in dorsal vertebrae 1 and 2 are located on the centrum, but by the fourth dorsal vertebra they are positioned more dorsally on the neural arch. The pre- and postzygapophyses are slightly more anteroposteriorly compressed and transversely expanded than in more the first two dorsal vertebrae. The neural spine is triangular in anterior view. As in the more anterior dorsal vertebrae, a well-developed prsl extends dorsal to the tip of the neural spine along the midline of the concave anterior face. A broad, triangular

TABLE 1. Vertebral measurements (cm) in *Rapetosaurus krausei* (FMNH PR 2209).

| | | Centrum | | | | |
|---|---|---|---|---|---|---|
| | | Anterior | | Posterior | | Neural Spine |
| Element | Maximum Length | Height | Width | Height | Width | Height |
| C3 | 12.0 | 2.9 | 3.1 | 3.3 | 3.6 | *5.7 |
| C4 | 15.0 | 3.1 | 3.4 | 3.2 | 4.4 | *8.6 |
| C5 | 19.5 | 3.1 | 4.4 | 3.9 | 5.4 | — |
| C6 | 22.1 | 5.1 | 3.2 | 4.3 | 6.6 | — |
| C7 | 22.5 | 3.3* | 5.4 | 3.5 | 6.9 | — |
| C8 | 24.8 | 3.3 | 5.4 | 5.4 | 7.1 | — |
| C9 | 27.3 | 4.3 | 5.9 | 5.1 | 6.3 | *14.1 |
| C10 | 28.9 | 6.1 | 5.5 | 6.5 | 7.2 | 20.1 |
| C11 | 28.2 | 3.9 | 5.1 | 5.7 | 7.1 | 20.1 |
| C12 | 28.9 | 6.1 | 5.5 | 6.5 | 7.2 | *10.9 |
| C13 | 26.2 | 4.6 | 7.9 | 7.7 | 9.5 | — |
| C14 | 26.2 | 6.5 | 7.4 | 7.8 | 8.9 | — |
| C15 | 27.9 | 5.9 | 6.8 | 6.5 | 8.8 | — |
| C16 | 10.6 | 5.7 | 9.8 | 8.1 | 10.4 | — |
| C17 | — | — | — | — | — | 10.2 |
| D1 | — | — | — | — | — | — |
| D2 | — | — | — | — | — | 15.6 |
| D3 | 11.1 | 5.9 | 8.9 | 6.3 | 9.6 | 16.7 |
| D4 | 10.2 | 5.8 | 10.3 | 7.1 | 10.1 | 17.2 |
| D5 | 10.0 | 6.3 | 10.2 | 7.3 | 10.7 | 18.4 |
| D6 | 10.2 | 6.3 | 9.5 | 5.7 | 9.4 | 16.5 |
| D7 | 10.8 | 7.3 | 8.3 | 6.9 | 8.5 | 16.0 |
| D8 | 10.5 | 7.1 | 9.4 | — | — | 16.0 |
| D9 | 9.3 | — | — | 6.8 | 9.0 | 15.1 |
| D10 | 9.4 | 6.7 | 7.2 | 7.3 | 8.5 | 15.2 |
| S1 | — | — | — | — | — | — |
| S2 | 8.0 | 7.6 | 8.2 | 6.8 | 7.0 | 15.2 |
| S3 | 7.2 | 7.6 | 7.8 | 7.0 | 9.5 | — |
| S4 | 7.4 | 7.1 | 7.0 | 8.0 | 8.2 | — |
| S5 | — | — | — | — | — | 18.5 |
| S6 | 6.3 | 8.0 | 12.0 | 8.5 | 8.0 | — |
| Ca1 | 6.9 | 6.5 | 6.3 | 7.0 | 7.3 | — |
| Ca2* | 6.4 | 7.6 | 6.4 | 7.8 | 8.0 | 8.4 |
| Ca3* | 6.8 | 6.8 | 6.8 | 5.8 | 5.9 | 8.3* |
| Ca4 | 6.3 | 5.5 | 5.5 | 4.8 | 4.9 | 5.2 |
| Ca5 | — | — | — | — | — | 5.1 |
| Ca6 | 5.9 | 4.1 | 4.2 | 3.9 | 4.1 | 4.5 |
| Ca7 | 5.3 | 4.2 | 4.6 | — | — | 4.0 |
| Ca8 | 6.2 | — | — | 3.8 | 4.9 | — |
| Ca9 | 5.7 | 3.6 | 3.7 | 3.1 | 3.4 | 2.5* |
| Ca10 | 5.4 | 3.5 | 3.2 | 3.2 | 3.4 | 3.5 |
| Ca11 | 4.9 | 3.0 | 2.7 | 3.0 | 3.0 | 2.1 |
| Ca12 | 4.7 | 2.8 | 2.5 | 2.4 | 2.7 | 2.1 |
| Ca13 | 4.7 | 2.8 | 2.6 | 2.8 | 2.8 | 1.9 |
| Ca14 | 4.6 | 2.4 | 2.4 | 2.4 | 2.2 | 1.6 |
| Ca15 | 4.2 | 2.2 | 2.1 | 2.0 | 2.1 | — |
| Ca16 | 3.3 | 2.0 | 1.8 | 1.8 | 1.8 | — |
| Ca17 | 3.3 | 1.5 | 1.3 | 1.2 | 1.3 | — |

FMNH PR 2209 consists of 47 articulated or associated vertebrae. Numbers below for the cervical, dorsal, and sacral regions reflect true anatomical position in the vertebral column. Numbers for caudal vertebrae are not accurate and only reflect relative position in the caudal series. Caudal vertebrae that articulate precisely with preceding or subsequent elements are marked with *. Dashes indicate where measurements could not be taken because of breakage or because element wasn't preserved.

prespinal fossa surrounds the prsl. A robust tprl extends between the prezygapophyses and forms the dorsal boundary to bilateral shallow concavities that abut the neural canal. The sprl are absent in the third dorsal vertebra, whereas the short prdl extends lateral to the prezygapophsyes at an angle of ~35°. The spdl is planar with a flattened anterolateral surface. As it approaches the neural spine, an ovoid foramen divides the spdl into dorsal and ventral branches for a short distance. The posl extends to the tip of the neural spine's flattened posterior face. The angle between the left and right halves of the tpol becomes progressively more acute from dorsal vertebrae 1–3. In dorsal vertebra 3 it maintains a steep 'V' shape at the midline and extends dorsally to the postzygapophyses to form the lateral boundaries of a shallow posterior excavation. A short, vertical extension of the tpol reaches ventrally to the neural canal, and lies at the center of an elevated region formed by the bilateral cpol. Lateral to the cpol, the posterolateral fossa retains its laminar boundaries ventrally, laterally, and medially, but not dorsally. In the third dorsal vertebra, the cpol is perforated by several foramina.

The migration of the parapophysis onto the neural arch interrupts the acdl, and breaks it into the acpl, paradiapophysdeal lamina (ppdl), and the prezygoparapophyseal lamina (prpl). This interruption thus divides the anterolateral fossa into three distinct fossae that persist until the parapophysis becomes conjoined with the diapophysis in more posterior dorsal vertebrae. In dorsal vertebrae 3 and 4, the anterolateral fossa is now small and restricted to a position just anterior and ventral to the diapophysis. It is bounded posteriorly by the prpl, ventrally by the parapophysis, and anteriorly by the cprl. A second fossa lies behind this one and is bounded posteriorly by the pcdl,

anteriorly by the ppdl, dorsally by the diapophysis, and ventrally by the posterior centroparapophyseal lamina (pcpl). A third, ventral fossa is bounded dorsally by the pcpl anteriorly by the acpl, and ventrally by the neurocentral facet. The posterior surface of the parapophysis, the cpol, and the pcdl were highly vascularized and/or pneumatized, as evidenced by the well-developed foramina.

**Dorsal vertebrae 5 and 6**—Centra do not vary dramatically in these dorsal vertebrae, but neural arches continue to change as the parapophysis migrates dorsally (Fig. 18–19). By the sixth dorsal vertebra, the parapophysis is at the level of the diapophysis, but still distinct from it. The transverse processes are incompletely preserved for each, but are much narrower than in the more anterior dorsal vertebrae and extend outward at a lower angle, with diapophyseal and prezygapophyseal facets at about the same level in dorsal vertebra six.

In anterior view, the tprl is much broader anteroposteriorly than in preceding vertebrae and overhangs the pedicles of the neural arch. This anterior extension results in a deep trough ventral to the tprl, between it and the neural canal. This trough is divided by a sharp, midline lamina similar to the ventral extension of the tpol observed on the posterior surfaces of more anterior dorsal neural arches. On either side of this lamina, small oval concavities occur dorsolateral to the neural canal. Dorsal to the tprl, a prsl arises on the midline and continues to the distalmost part of the neural spine. In dorsal vertebrae 5–6 the broad, triangular prespinal fossa is divided into medial and lateral portions by a well-developed sprl, and is bounded dorsally by a broad, flat spdl that extends ventrolaterally at a steep angle. In posterior view, the tpol of dorsal vertebrae 5–6 is broad. Dorsal to the tpol and between the postzygapophyses the posterior excavation of the neural spine is flat and broad, rather than the troughlike excavation of more anterior dorsal vertebrae. Ventral to the highly angled postzygapophyses, elongate, narrow cpol extend to the neurocentral junction and form the lateral boundaries of a deep median sulcus. This sulcus is bounded dorsally by the tpol and also occurs as a shallow excavation of the elevated cpol in the fifth dorsal vertebra. The posterolateral fossa persists lateral to the cpol. Lateral lamination is simpler than in the cervicodorsal and anterior dorsal vertebrae, concomitant with the merging of parapophysis and diapophysis in a conjoined facet. In lateral view, three fossae are noteworthy: (1) the anterolateral fossa, bounded by the acdl, pcdl, and transverse process; (2) the posterolateral fossa, bounded by the cpol, pcdl, and the spdl; and (3) the spinodiapophyseal fossa. The pre- and postzygapophyses and confluent diapophysis/parapophysis all occur at the same level in the sixth dorsal vertebra, and the neural spine extends posterior to the elongated, rectangular neural arch facets.

**Dorsal vertebrae 7 and 8**—Neural arches for dorsal vertebrae 7 (Fig. 20) and 8 (Fig. 21A, B, E) are far more robust than those of more anterior dorsal vertebrae, with more substantive lamination and deeper fossae. Neural spines are relatively shorter, blockier, and posteriorly angled. In anterior view, the prezygapophyses are set at a level distinct from that of the anterior face of the neural spine, resulting in a deepening of the prespinal fossa. The prespinal fossa is bounded ventrally by the tprl, and contains a prsl that extends for the length of the neural spine. The division of the prespinal fossa into medial and lateral portions persists in dorsal vertebrae 7 and 8. The ventral extension of the tprl extends on the midline toward the neural canal, and is surrounded by an elliptical cavity on each side. The prdl extends laterally from the transversely expanded prezygapophysis, to contact the dorsally facing diapophysis at an angle of $\sim 45^\circ$ to the horizontal. In posterior view the neural spine is robust with a rounded apex and a broad, posteroventrally directed face. The posl extends to the distal neural spine, and is robust in dorsal vertebrae 7 and 8. Ventral to the tpol, a shallow concavity is formed between the columnar, robust cpol.

The posterolateral fossa has a wide posterior exposure and is bounded dorsally by the podl. It contains a number of unnamed accessory laminae. In lateral view, the antero- and posterolateral fossae are ventrally constricted, but are subequal in size. The spinodiapophyseal fossa is greatly expanded, and the ventral branch of the spdl originates, in part, from the postzygapophysis. The neural spine is posteroventrally tipped at an angle of $\sim 45^\circ$ to the horizontal, and extends posterior to the neurocentral facets. The neural canal is short in these three vertebrae, with the neural canal roof only half of the length of the neural arch facets. Although the neural arch facets maintain a length consistent with that of preceding dorsal vertebrae, they are narrower in dorsal vertebrae 7 and 8.

**Dorsal vertebrae 9 and 10**—Dorsal vertebrae 9 (Fig. 21C–E) and 10 (Fig. 22) mark the beginning of the dorsosacral transition. The centra are shorter and slightly stouter than in preceding dorsal vertebrae, and they retain well-defined pleurocoels. The centrum of dorsal vertebra 9 is cemented to the centrum of dorsal vertebra 8 (Fig. 21). The centrum of dorsal vertebra 10 bears neural arch facets that are narrower than in all preceding dorsal vertebrae. The ninth and tenth dorsal neural spines continue the trend toward a transversely narrow and more erect morphology, and are similar enough to be described together, below.

The prezygapophyses are narrow and short transversely. The tprl is shortened anteroposteriorly relative to those of preceding dorsal vertebrae. The prsl extends the full length of the anterior face of the neural spine and lies at the center of the prespinal fossa. The prdl is short due to the close proximity of the prezygapophysis and diapophysis. In posterior view, the neural spine is expanded, and broadly excavated between the postzygapophyses. It bears a posl that extends to the distal tip of the neural spine. The spinodiapophyseal fossa is expanded, whereas the antero- and posterolateral fossae are slightly constricted.

**Dorsal vertebrae, Comparisons**—The opisthocoelous dorsal centra exhibited by *Rapetosaurus* and most other derived titanosaurs differ from the amphiplatyan dorsal centra of *Andesaurus* (MUCPv-132, Calvo and Bonaparte, 1991) and *Argentinosaurus* (MCF-PVPH-1, Bonaparte and Coria, 1993). *Rapetosaurus* dorsal centra lack ventral concavities observed in some other derived titanosaurs including *Opisthocoelicaudia* (ZPAL MgD-I/48, Borsuk-Bialynicka, 1977) and *Neuquensaurus* (MCS-5/18-19, Salgado et al., 2005). In most titanosaurs, including *Rapetosaurus*, the pneumatic fossae are well-developed, deep, simple pits, bounded by sharp borders. *Rapetosaurus* shares the presence of a straight, narrow neurocentral junction with other titanosaurs, and shares a neural canal that is wider than high with *Malawisaurus* (SMU-Mal 238, Gomani, 2005), *Isisaurus* (ISI R335, Jain and Bandyopadhyay, 1997), *Saltasaurus* (PVL 4017-10, 136, Powell, 1992), and *Lirainosaurus* (MCNA 7445, Sanz et al., 1999).

In *Rapetosaurus* and *Opisthocoelicaudia* the diapophysis lies dorsal to the prezygapophyses in the dorsal series. Diapophyses of dorsal vertebrae in *Rapetosaurus, Malawisaurus, Isisaurus, Opisthocoelicaudia, Argentinosaurus*, and *Lirainosaurus*, are flattened dorsally and the spdl meets the neural spine at 90°. In *Rinconsaurus* posterior dorsal vertebrae, diapophyses are directed laterally and upward (MRS-Pv 17, Calvo and González Riga, 2003), whereas in *Tendaguria* (HMN MB.R2092.1-2, Bonaparte et al., 2000) the diapophyses are posteroventrally directed, dorsally convex, and meet the neural spine at an obtuse angle. Neural spines and diapophyses are nearly perpendicular to one another in the posterior dorsal vertebrae of *Rapetosaurus, Opisthocoelicaudia*, and *Argentinosaurus*. In *Rapetosaurus, Saltasaurus*, and *Neuquensaurus* a fossa exists beneath the postzygapophyses and above the neural canal. In *Rapetosaurus* this fossa persists throughout the dorsal series.

Neural spines in *Rapetosaurus* dorsal vertebrae are relatively tall, distally undivided and bluntly triangular with a web-like

spdl, and exhibit well-defined anterior, lateral, and posterior fossae and laminae. Neural spine height varies among titanosaurs, with *Argentinosaurus* bearing the lowest spine:centrum height ratio, and *Phuwiangosaurus* (PW 1-4, Martin et al., 1999) at the opposite end of this spectrum with neural spines over two times as high as the centrum. *Rapetosaurus* is also at the high end of this spectrum, with spine:centrum height ratios ranging from 2.2 to 2.9. *Rapetosaurus* neural spines account for ~40% of the total vertebral height in posterior dorsal vertebrae, whereas in *Andesaurus* and *Isisaurus* the neural spines constitute ~75% of the total height of the vertebra. *Rapetosaurus* anterior dorsal neural spines are posteriorly-tipped as much as 60°, whereas more posterior dorsal neural spines are more erect. This pattern is shared with that observed in other derived titanosaurs including *Malawisaurus, Saltasaurus*, and *Rocasaurus* (MPCA-Pv46, Salgado and Azpilicueta, 2000). The blunt, triangular distal neural spine of *Rapetosaurus* differs from the square distal spine in *Malawisaurus* and *Saltasaurus*.

*Rapetosaurus* dorsal neural arches exhibit strongly developed spinal fossae and laminae that contrast with the simpler neural arches of more basal titanosaurs. Anteriorly, the prezygapophyses in *Rapetosaurus* are separated by a shallow fossa that bears the prsl, extends ventrally, and is confluent with the dorsal boundary of the neural canal. Although *Saltasaurus* bears a similar fossa, it is not as ventrally extensive as in *Rapetosaurus*, and the neural canal in *Saltasaurus* is instead bound by the tprl. The tprl is absent in several titanosaurs including *Argentinosaurus* and *Rocasaurus*.

Accessory intervertebral articulations occur in *Rapetosaurus*, but are not homologous with the hyposphene-hypantrum articulations observed in basal titanosaurs like *Andesaurus, Argentinosaurus, and Epachthosaurus* (UNPSJB-PV 920, Martínez et al., 2004). Instead, *Rapetosaurus* and *Malawisaurus* are unique among titanosaurs in exhibiting a median prominence within a shallow fossa that lies between the cpol of anterior dorsal vertebrae. This prominence is a distinctive ventral extension of the tpol, which may serve to reduce neck flexibility in these taxa. The ventral extension of the tpol persists throughout the dorsal vertebral series in *Rapetosaurus*, and in middle and posterior dorsal vertebrae, a median, ventral extension of the tprl also forms. Other titanosaurs, including *Ampelosaurus* (MD-E C3 247, Le Loueff, 1995) bear well-developed tpol but do not share the ventral extension with *Rapetosaurus*.

*Rapetosaurus* shares the presence of a single, dorsoventrally extensive prsl that extends to the distal end of the neural spine with *Isisaurus, Malawisaurus, Saltasaurus*, and *Rinconsaurus*. This extensive prsl differs from the short, dorsoventrally restricted prsl of *Opisthocoelicaudia, Argentinosaurus*, and *Magyarosaurus* (BMNH R4896, pers. observ.), and from the proximally bifid prsl observed in *Andesaurus* and *Pellegrinisaurus*. The posl of *Rapetosaurus* is also dorsoventrally extensive and persists at the tip of the neural spine. This morphology contrasts with the very short posl of *Isisaurus, Opisthocoelicaudia*, and *Ampelosaurus*. The acdl in *Andesaurus* is nearly vertical, whereas in *Rapetosaurus*, *Saltasaurus*, and *Epachthosaurus* it slants strongly anteriorly. In contrast with *Rapetosaurus, Isisaurus* and *Opisthocoelicaudia* lack a sprl.

### Sacral Vertebrae

Like other titanosaurs, *Rapetosaurus* had six sacral vertebrae. The series is incomplete in FMNH PR 2209, but representative elements from all six sacral vertebrae are preserved in varying combinations: two sacral vertebrae include centra, neural arch, and right and left sacral ribs; two sacral vertebrae are represented only by centra; one is represented by the centrum and both sacral ribs; and one is represented by the neural arch and one sacral rib (Figs. 23–27). The elements that can be rearticulated perfectly along sutural surfaces are described as units below. These preserved elements form a natural series, and their order as it appears below is based on morphology and articulation with preceding or subsequent elements.

In general, the sacral centra retain the general spool-like shape observed in dorsal vertebrae, and three of the sacral centra bear pneumatic foramina/fossae. Neural spines were presumably completely co-ossified in an adult *Rapetosaurus*, as indicated by the sutural articulations between pre- and postzygapophyses in all preserved neural arches. The preserved neural spines are low relative to those of other titanosaurs, and are only slightly more than twice the height of the centra. The anterior sacral ribs are short, broad wings that bear a small proximal crest on the anterior face. In more caudal sacral ribs, this crest is elaborated into a gracile and extensive, sheet-like posterodorsally directed flange.

**Sacral Vertebra 1**—The first preserved sacral vertebra consists of a well-preserved, short and opisthocoelous centrum, with a well-developed sutural contact on the posterior surface that articulates perfectly with the centrum of sacral vertebra 2. As for the other sacral centra, the ventral margin is convex, and the centrum is punctuated by a deep lateral pneumatic foramen.

**Sacral Vertebra 2**—Sacral vertebra 2 consists of a well-preserved centrum, right and left sacral ribs, and a neural arch (Fig. 23) The centrum is short and slightly opisthocoelous, with a convex ventral margin and clearly demarcated sutural surfaces on its anterior and posterior articular faces, both of which articulate perfectly with preceding and following centra. Though the centrum lacks a pleurocoel, two small pneumatic foramina with sharp boundaries perforate the lateral surface of the centrum and lie directly posterior to the large sacral rib facet. The facet extends over half of the length of the centrum, splays posterolaterally away from the body of the centrum, and results in a widening of the centrum's anterior margin in dorsal view. The neural arch facets are subrectangular in dorsal view and taper posteriorly into narrower facets. They are contiguous with the sacral rib facets on the anterodorsal part of the centrum, but extend dorsally to a more elevated position. The posterodorsal margin of the centrum is rugose, and it articulates with the subsequent sacral centrum and neural arch.

Right and left sacral ribs each bear a dorsal flange that is short and gently rounded, restricted to the medial third of the rib, and excavated by a shallow trough along its posterior surface. When articulated, this flange extends posterodorsally. The medial articular surface of the sacral rib bears two distinct regions: a dorsal subtriangular region that articulates with the neural arch, and a ventral subrectangular portion that articulates with the centrum. The lateral margin of the sacral rib is dorsoventrally expanded and compressed anteroposteriorly to form a long, slender flange of bone for articulation with the other sacral ribs and the ilium.

The overall morphology of the neural arch is similar to that of the most posterior dorsal vertebrae in bearing laterally directed diapophyses, and a nearly erect neural spine. Anteriorly, the cprl medially bounds a small facet that occupies the anterolateral portion of the diapophysis. The prezygapophyses are modified into rugose sutural contacts. The prsl extends dorsal to this rugose region for the full length of the neural spine. Right and left sprl extend dorsomedially from the prezygapophyses to border the shallow excavation on the anterior surface of the neural spine. The aliform diapophysis extends in an oblique line dorsolaterally to ventromedially. It articulates with the sacral rib via an elongate, anteroposteriorly compressed surface. Anteriorly, the neural canal is subrectangular with a flat dorsal boundary formed by the confluent prezygapophyses. Both the pre- and postzygapophyses lie below the level of the diapophysis. Wide, rugose pre- and postzygapophyseal facets are broad sutural surfaces that dominate the anterior and posterior faces of the neural

arch above the neural canal. The posterolateral fossa persists and is divided by several unnamed bony laminae. A well-developed pre-spinous fossa is ventrally positioned and is bounded ventrally by the podl, and dorsally by the spdl. Dorsal to the postzygapophyseal facets, a high, sharp, posl arises and extends to the distal end of the neural spine. The neural canal is greatly dorsoventrally expanded relative to that in presacral vertebral series. It is triangular dorsally, and widened transversely to expose the neural canal beneath the postzygapophyses. In lateral view, the diapophysis is anteroventrally tipped and lies anterior to the apex of the erect neural spine. The posterolateral, anterolateral, and spinodiapophyseal fossae are all subtriangular.

**Sacral Vertebra 3**—Sacral vertebra 3 consists of only a centrum that articulates perfectly along the sutural scars with the second sacral centrum, with the fourth sacral centrum, and with the right rib of the fourth sacral vertebra. The anterior and posterior articular faces for the sacral centrum are flattened and rugose. Sutural surfaces on the anterior and posterior surfaces of this centrum match the sutural facets for sacral vertebrae 2 and 4. The lateral pneumatic fossa is expanded relative to that of sacral vertebra 2, but maintains its position just posterior to the sacral rib facet and is anteroposteriorly expanded. A second, more ventrally positioned pneumatic fossa occurs on the right side, and lies ventral to the sacral rib facet. The subrectangular articular facet for the sacral rib lies on the anterolateral surface of the centrum. Once again, this facet may be divided into components for the rib (most of the lateral surface of the facet) and the neural arch (an elongated, rod-like, dorsally directed facet). The posteriormost surface of the centrum bears a small facet that houses an anteroventral portion of the fourth right sacral rib and centrum of the fourth sacral vertebra.

**Sacral Vertebra 4**—A well-preserved centrum and right and left sacral ribs represent the fourth sacral vertebra (Fig. 24). The sacral ribs articulate with the sacral 3 and 4 centra along their respective facets. The centrum is slightly opisthocoelous with clearly demarcated anterior and posterior sutural facets for articulation with the preceding and subsequent sacral centra. The sacral rib facets are anteriorly positioned and extend onto the dorsal surface of the centrum. In lateral view, they are subrectangular and extend farther anteroventrally than in the other sacral vertebrae. Pneumatic fossae are present, and the lateral surface of the centrum and the posterior portion of the sacral rib facet are perforated by several foramina.

The dorsomedial convexity of the fourth sacral rib is greatly expanded and arises well above the body of the rib. It is angled slightly laterally toward the facet for articulation with the ilium. The rib is flattened anteroposteriorly, with a bulbous lateral articular surface for the sacricostal yoke and ilium. This surface contacts the centra of both sacral vertebrae 3 and 4. The facet for the diapopohysis of the neural arch extends dorsally along the rib's expanded convexity, and is marked ventrally by a small notch. A well-demarcated neurovascular canal and groove extend across the posterior margin of the rib, and course toward this laterally placed notch.

**Sacral Vertebra 5**—Sacral vertebra 5 includes a partial neural arch and left sacral rib that may be rearticulated along their common sutures (Fig. 25). The neural arch also articulates perfectly along sutural contacts with the neural arch of the sixth sacral vertebra.

The neural arch bears a nearly erect neural spine that is slightly tipped anteriorly. The transverse processes extend nearly perpendicular to the spinous process, but are gently curved anteroventrally toward the neurocentral junction. In a mature *Rapetosaurus*, the prezygapophyseal facets would have been fully fused to the preceding vertebrae, and the tprl eliminated by sutural articulations. The prsl extends to the distal end of the neural spine and is strongly developed with numerous branches. There are small fossae between lateral and medial cpol, and the neural canal opening is constricted, with a triangular dorsal outline. The postzygapophyseal facets are broad and subcircular, with a slight ventral extension onto the cpol. They lie dorsal to the prezygapophyses and ventral to the diapophysis. The tpol is narrow and restricted, and forms the dorsomedian border of the broad, U-shaped neural canal. The posterolateral fossa is shallow. All other fossae are absent. The diapophyseal articulation angles anteroventrally but no longer extends anterior to the apex of the spinous process. The neural arch facets are subcircular at their posterior margin, but narrow anteriorly to form elongate rectangles.

The sacral rib is much thinner anteroposteriorly than preceding sacral ribs, and it has coplanar centrum and neural arch articular surfaces. The proximal articular surface for the centrum is reduced and circular. Dorsal to it a notch formed at the base of the posterodorsal process is expanded relative to the homologous notch in more anterior sacral vertebrae. The neural arch articular surface is reduced, and occupies only a small portion of the posterodorsal process. The anterior surface of the posterodorsal process is marked by two vascular foramina. One perforates the body of the rib, whereas the other, positionally similar to the fossae in other sacral ribs, is positioned on the dorsomedial edge of the rib. The posterodorsal process is also shortened (although broken distally), such that it does not overhang the sacricostal yoke and iliac articular surface.

**Sacral Vertebra 6**—The sixth sacral vertebra includes a centrum, neural arch, and both sacral ribs (Fig. 26). The centrum departs from the morphology of preceding centra. It is slightly procoelous, with posteriorly positioned neural arch facets, and anteriorly positioned sacral rib facets. Two small pneumatic fossae perforate the posterior surface of the sacral rib facets. The anterior surface of this centrum is slightly concave and bears rugosities for articulation with the preceding sacral. The posterior face of the centrum is weathered, but slightly convex. Sacral rib facets are anterodorsally directed and subcircular.

Only the anterior face of the neural arch is preserved well enough to warrant description. It articulates perfectly with the posterior surface of the preceding sacral neural arch. The prezygapophyseal facets are broad and oval, and the tprl extends between them as a simple, narrow tongue roofing a portion of the neural canal. The diapophysis remains aliform with a broad anteroposteriorly compressed articular surface for the sacral rib. Ventral to the diapophyseal surface a small notch matches the similarly positioned excavation on the sacral rib and, when articulated, these notches completely enclose an intervertebral foramen for the passage of sacral nerves. The spdl and fossae persist, although a rugose elaboration of the prezygapophyses precludes the presence of the anterolateral fossa.

The posterodorsal wings of the left and right sacral ribs are strongly compressed anteroposteriorly to result in a thin, narrow process that is quite distinct from the body of the rib. This process arises from the medial portion of the element and extends laterally well above the iliac articulation. The medial face of this process is rugose and elongate for articulation with the transverse process of the neural arch. Ventrally, interposed between this process and the body of the rib is a transversely expanded excavation. Together with a similar notch on the neural arch, an intervertebral vertebral foramen for the passage of sacral nerves and blood vessels would have been formed between the rib and the neural arch. The body of the rib is somewhat laterally flattened at the iliac articulation. Anteriorly and posteriorly, fossae develop along the base of the posterodorsal process at the lateral intersection between the process and the body of the rib. These fossae may be homologous to the neurovascular foramina noted above in the other sacral ribs.

**Sacral Vertebrae, Comparisons**—*Rapetosaurus* sacral vertebrae are rounded or ventrally convex in cross-section and maintain a relatively consistent size; only the sixth sacral centrum is

slightly broader than preceding centra. The sacral centra of *Opisthocoelicaudia* (ZPAL MgD-I/48, Borsuk-Bialynicka, 1977) are instead ventrally concave, whereas in *Neuquensaurus* (MCS-5/16, Salgado et al., 2005) the third to fifth sacral centra are significantly narrower than other vertebrae in the series. *Rapetosaurus* is unique among known titanosaurs in that all sacral vertebrae have laterally positioned pneumatic fossae. A few other titanosaurs including *Opisthocoelicaudia*, *Isisaurus, Epachthosaurus* (UNPSJB-PV 920, Martínez et al., 2004), and *Gondwanatitan faustoi* (MN 4111-V, Kellner and Azevedo, 1999) exhibit more limited sacral vertebral pneumaticity.

Sacral neural spines in *Rapetosaurus* are long, undivided, and characterized by retention of most of the spinal laminae noted in the presacral series. The sacral neural arches of *Rapetosaurus* are vertically oriented and relatively low compared to those in other titanosaurs: they only account for half of the total height of the vertebra. In constrast with *Epachthosaurus*, there is no evidence of accessory vertebral articulations in the sacral series of *Rapetosaurus*, and *Rapetosaurus* and *Opisthocoelicaudia* share sacral diapophyses that meet the neural spine at a 90° angle. *Rapetosaurus, Saltasaurus* (PVL 4017-19, Powell, 1992), and *Neuquensaurus* share the presence of a proximal excavation of the sacral ribs.

### Caudal Vertebrae

Elements from a total of 17 caudal vertebrae were recovered with the juvenile *Rapetosaurus* skeleton collected at MAD 93-18 (Table 1, Figs. 27–29). The sample includes 16 centra, 11 of which can be rearticulated with their respective neural arches. Five caudal vertebrae are represented only by their centra, and one is represented only by an unfused neural arch. Chevrons were found closely associated with four of the specimens described here. The 17 preserved caudal vertebrae are nearly sequential with one another, ranging from the mid-proximal to distal regions of the tail. Few, if any caudal vertebrae are missing from the tip of the tail. The most proximal caudal vertebrae were not preserved with the juvenile skeleton, and size and shape criteria indicate that an additional 7–11 caudal vertebrae are required to fill morphological gaps in the preserved series. In Table 1, preserved caudal vertebrae are numbered sequentially. This number merely reflects relative position within the caudal series and does not indicate exact caudal number.

All caudal vertebral centra are procoelous with anteriorly positioned neural arches. There is no evidence of pneumaticity in any preserved caudal vertebra. Caudal ribs were not found in association with any centrum or neural arch, though clear facets for their articulation are preserved on many middle caudal vertebrae. Similarly, chevrons were found in association with FMNH PR 2209, but only one specimen preserves chevrons in articulation with their respective vertebrae (Fig. 28). All preserved caudal neural arches have anteriorly projecting prezygapophyses, laterally broad, posteriorly swept neural spines, and exhibit prsl and posl in shallow pre- and postspinal fossae. More posterior caudal centra are slightly elongate, but, like the middle caudal vertebrae, retain equal centrum width:centrum height. Centra remain procoelous, though the degree of procoely decreases in posterior caudal vertebrae. In posterior caudal vertebrae, the neural arch is transversely compressed into a thin blade, but is broad anteroposteriorly in lateral view. The prezygapophyses project beyond the anterior margin of the centrum, whereas the postzygapophyses are small and restricted to the base of the neural spine.

**Proximal and Middle Caudal Vertebrae**—The proximal and middle caudal vertebrae of *Rapetosaurus* are strongly procoelous, and they exhibit anteroposteriorly short, high centra with slightly concave lateral sides, broadly convex ventral surfaces (Fig. 27). The anterior articular face is canted such that the dorsal boundary surface extends anteriorly beyond the ventral boundary. The posterior articular face is strongly convex, with a dorsally offset apex of the posterior 'ball.' The anterior and posterior chevron facets impart a longitudinal groove that runs the length of the centrum's ventral surface. The neural arch facets on all proximal caudal vertebrae are anteriorly positioned and subrectangular in dorsal view. They are continuous with the anterolaterally positioned caudal rib facet. When the neural arch and centrum are articulated, the rib facet takes the shape of a broad triangle (Fig. 27C, D). The apex of the triangle is formed by the arch's contribution to the rib facet, whereas the base of the triangle is broad, subrectangular, and positioned on the centrum. Throughout the caudal series rib facets gain a more restricted lateral exposure, and neural arch facets narrow slightly. The neural arch is high, with an elongated neural spine. The neural spine is relatively broad both antero-posteriorly and transversely, and the presence of strongly developed spinal laminae increases its anteroposterior breadth. The prezygapophyses are elongate, anteriorly directed, and extend well beyond the anterior margin of the centrum, arising anterior to the cotyle. Prezygapophyseal facets face dorsomedially and are separated by a well-developed tprl. As in dorsal vertebrae, the tprl forms the ventral boundary of a prespinal fossa that houses a strongly developed prsl. The prsl extends to the distal tip of the neural spine. The postzygapophsyes lie just dorsal to the opening of the neural canal, on the ventral one-third of the neural spine, and are divided by a "V" shaped tpol and a median trough containing the posl. The posterior articular face in mid-caudal vertebrae is distinct from the body of the centrum.

**Distal Caudal Vertebrae**—Progressing more posteriorly, mid-caudal centra are relatively elongated, and soon attain a height to length ratio that is retained for the remainder of the series (Table 1; Figs. 28, 29). Most of the centra and neural arches described in this section were found in close proximity in MAD 93-18, and most can be rearticulated perfectly. Chevron facets extend ventrally well below the ventral border of the centrum in most caudal vertebrae, and occur on both anterior and posterior regions of the centra. A slight midline ridge bisects the space between chevron facets on the ventral surface of the centra. The lateral portions of the centra are saddle-shaped. Throughout this region of the caudal series neural arches are tall and maintain their anteroventrally straight pedicles, and distally expanded, bladelike neural spines. The elongate prezygapophyses project even further anteriorly over the centrum, and extend over half of the preceding centrum. The prezygapophyseal facets are small ovals that face dorsolaterally. The prsl and posl persist, as does a well-developed tprl and tpol.

Centra of consecutive distal caudal vertebrae gradually shorten. They are procoelous, although their anterior faces are shallower than those of more anterior centra (Fig. 29C). The posterior articular face in posterior caudal vertebrae merges smoothly with the body of the centrum. Neural arch facets are narrow and elongate, but still anteriorly positioned, even in the most distal caudal vertebrae. Neural arches thin transversely in more caudal parts of the series, although they maintain elongate prezygapophyses that extend well beyond the anterior margin of the centra. Distalmost caudal vertebrae have poorly developed pre- and postzygapophyseal facets, and the neural spines are low and bladelike. The most posterior centrum preserved with this juvenile *Rapetosaurus* specimen is only slightly procoelous, with extremely narrow neural arch facets. No chevron facets occur on the cylindrical centrum. It retains the width to height ratio (1:1) of the other preserved caudal vertebrae.

**Caudal Vertebrae, Comparisons**—Procoelous caudal vertebrae with subequal centrum width:height ratios characterize *Rapetosaurus* and most other titanosaurs. Exceptions include the amphiplatyan centra of *Andesaurus* (MUCPv 132, Calvo and Bonaparte, 1991) and the opisthocoelous centra of *Opisthocoelicaudia* (ZPAL

MgD-I/48, Borsuk-Bialynicka, 1977). A few titanosaurs including *Rinconsaurus* (MRS-Pv 26, Calvo and González Riga, 2003) exhibit series of posterior caudal vertebrae that include procoelous, amphiplatyan, and biconvex caudal centra. A subgroup of titanosaurs including *Saltasaurus* (PVL 4017-28, 38, Powell, 1992), *Lirainosaurus* (MCNA 7471, Sanz et al., 1999), Malagasy Taxon B (FMNH PR 2240, Curry Rogers 2002), *Rocasaurus*, and *Rinconsaurus* exhibit caudal centra that are dorsoventrally compressed and transversely broad with centrum width:height $\geq$ 2:1. In *Rapetosaurus*, the anterior and posterior chevron facets impart a longitudinal groove that runs the length of the centrum's ventral surface, as in the syntype specimen of "*Titanosaurus" madagascariensis* (UCB 92829 Déperet, 1896a, b). In contrast to *Rapetosaurus, Rocasaurus* (MPCA Pv46, Salgado and Azpilicueta, 2000) centra are marked by a deep ventral cavity divided into two parts by a sagitally oriented midline ridge.

All titanosaurs are characterized by anteriorly positioned neural arches on all caudal vertebrae. In *Rapetosaurus* the mid-caudal neural spines are transversely expanded and anteroposteriorly reduced with slightly rounded distal margins in lateral view. They are taller than the height of the centrum in mid-caudals, and in more posterior caudals, *Rapetosaurus* neural spines shorten dorsoventrally and elongate anteroposteriorly and gain a low, rounded, blade-like morphology. This general neural spine morphology is shared with *Alamosaurus* (USNM 10486, Gilmore 1922a), *Saltasaurus, Adamantisaurus mezzalirai* (MUGEO 1282, Santucci and Bertini, 2006), and *Ampelosaurus* (MD C3 893, 208, pers. observ.). It contrasts with the dorsally directed, rectangular neural spine of *Epachthosaurus* (UNPSJB-PV 920, Martínez et al., 2004), with the posterorly inclined, rectangular neural spine of *Isisaurus* (ISI R335, Jain and Bandyopadhyay, 1997), and with the posteriorly inclined, rounded neural spine of *Neuquensaurus* (MCS-5/1-8, Salgado et al., 2005). *Saltasaurus* and *Neuquensaurus* are unique among titanosaurs in the concave anterior pedicles of the neural arch, and differ specifically from *Rapetosaurus* in the dorsal orientation of their prezygapophyses. The prsl and posl of *Rapetosaurus* and most other titanosaurs extend to the tip of the neural spine in anterior caudal vertebrae. Exceptions include *Isisaurus*, which exhibits shorter and more restricted spinal laminae, and *Rinconsaurus* and *Phuwiangosaurus* (PW 1-4, Martin et al., 1999), which lack a prsl or a posl in the proximal and middle caudal vertebrae. *Rapetosaurus* and *Adamantisaurus* share robust prsl and posl, but the latter has much larger and better-developed postzygapophyses and a more robust distal neural spine, and lacks a robust sprl. Hyposphene-hypantrum articulations do not occur in the caudal series of *Rapetosaurus*, in contrast to *Epachthosaurus*.

### Ribs and Chevrons

**Cervical Ribs**—Isolated, partial cervical ribs were found disarticulated, but closely associated with their respective vertebrae in FMNH PR 2209. The ribs are delicately tapered, with a rounded anterior projection that extends well beyond the anterior margin of the centrum. All preserved cervical ribs exhibit shallow excavations of their dorsomedial surfaces, each containing multiple, irregular pneumatic foramina (Fig. 30A). The posterior prong of each cervical rib extends posteriorly beneath at least three succeeding vertebrae. The cervical ribs of successive vertebrae lie above those of preceding vertebrae so that at any point in the series the cervical ribs form a vertically stacked bundle three to four ribs thick.

**Dorsal Ribs**—A number of disarticulated partial dorsal ribs were recovered with FMNH PR 2209 but none is directly associated with any particular dorsal vertebra (Fig. 4C, E). Dorsal ribs of *Rapetosaurus* are similar in most regards to those of other titanosauriforms. The capitulum and tuberculum are separated, and the capitulum of each rib is perforated with proximal pneumatic foraminae. In other, larger specimens of *Rapetosaurus* (e.g., Fig. 30B), the pneumatic features are elaborated, with pneumatic features (e.g., hollowing of the rib) extending into the body of the rib.

**Chevrons**—Six chevrons were found in direct association with caudal vertebrae at MAD 93-18 (Figs. 28, 31). The proximal chevron rami are deeply divided, without a proximal "crus" joining the articular regions. The division between rami extends for one-half to three-fifths the full length of the chevron and forms a narrow "V" at its ventral apex. In the distal part of the tail, chevrons are transversely compressed, anteroposteriorly expanded and bladelike, and somewhat posteriorly directed. Articular facets are well differentiated in all preserved chevrons.

**Ribs and Chevrons, Comparisons**—The extreme elongation and distal tapering of pneumatized cervical ribs into thin rods is shared by derived titanosaurs including *Rapetosaurus, Saltasaurus* (PVL 4017, Powell, 1992), and *Erketu (*IGM100/1803, Ksepka and Norell, 2006), as well as with more basal Titanosauriformes (e.g., *Sauropoisedon*, Wedel et al., 2000a, 2000b; *Brachiosaurus*, Wilson and Sereno, 1998). When compared with the dorsal ribs of *Epachthosaurus* (UNSPSJB-PV 920, Martínez et al., 2004) and other known titanosaurs, *Rapetosaurus* dorsal ribs are more slender with a more rounded distal cross-section.

*Rapetosaurus* chevrons are comparable to those of *Isisaurus* (ISI R 335, Jain and Bandyopadhyay, 1997), *Adamantisaurus* (MUGEO 1282, Santucci and Bertini, 2006), *Epachthosaurus* (UNPSJB-PV 920, Martínez et al., 2004), and *Saltasaurus* (PVL 4017-55, Powell, 1992). They differ slightly from the chevrons with broad, U-shaped haemal canals that characterize *Andesaurus* (MUCPv132, Calvo and Bonaparte, 1991) and *Malawisaurus* (SMU Mal-194. Gomani, 2005). The well-developed articular facets of *Rapetosaurus* chevrons also differ from the poorly differentiated facets of *Rinconsaurus* (MRS-Pv 20, Calvo and González Riga, 2003).

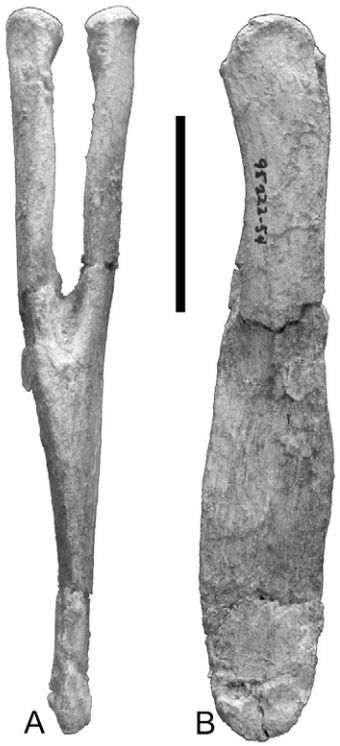


FIGURE 31. Chevron from mid-caudal series (FMNH PR 2209) of *Rapetosaurus krausei* in **A**, anterior view; **B**, right lateral view. Scale bar equals 1 cm.

TABLE 2. Measurements (in cm) of pelvic and pectoral girdle elements of *Rapetosaurus krausei* (FMNH PR 2209).

| | | | | | Articular Surfaces | | | |
|---|---|---|---|---|---|---|---|---|
| | | Maximum Breadth | | | Contribution to glenoid | | Facet for corresponding element | |
| Element | Maximum Length | Proximal | Midshaft | Distal | A-P | M-L | A-P | M-L |
| Scapula | 54.2 | 29.3 | 12.3 | 15.0 | — | — | ~11.0 | 4.1 |
| Coracoid | 18.6 | — | — | — | 4.0 | 3.2 | 11.0 | 4.6 |
| Sternal Plate | 34.1 | — | 16.8 | — | — | — | — | — |
| Ilium | | | | | — | — | — | — |
| Pubis | 48.1 | 21.0 | 12.0 | 14.2 | — | — | — | — |
| Ischium | 26.2 | 12.2 | 11.7 | 8.5 | — | — | — | — |

**Abbreviations: A-P**, anteroposterior breadth of surface; **M-L**, mediolateral breadth of surface.
Dashes indicate measurements that could not be taken. Contralateral elements with similar measurements are preserved for each of the elements.

## Pectoral Girdle

Right and left scapulae, coracoids, and sternal plates were recovered from site MAD 93-18 (Table 2, Figs. 32–34). In FMNH PR 2209, a juvenile specimen, the scapula and coracoid remain unfused. The glenoid has equal contributions from the coracoid and scapula.

**Scapula**—The scapula is gently curved medially, and bears a small rugosity on the lateral surface just dorsal to the intersection between scapular blade and body (Fig. 32). The margin of the acromion is damaged in both specimens, but it would have extended anterior to the coracoid articulation. The acromion is slightly concave on its lateral surface and is bounded posteriorly by a strong ridge. The scapular spine does not extend to the anterior border of the scapula and is not aligned at a right angle to the long axis of the element. Instead, it gently curves posteroventrally and reaches the border of the scapular body. Although not perfectly preserved, the scapular glenoid faces anteriorly and merges anterodorsally with the narrow region of coracoid articulation. The scapular contribution to the glenoid is subrectangular in cross-section, with a tapered anterodorsal boundary. It is slightly medially deflected as in other somphospondylans (Wilson and Sereno, 1998). The scapular blade is continuous with the anterodorsal edge of the scapula and extends posterodorsally without any marked expansion of its distal extremity. The proximal portion of the blade intersects the scapular body via an acute angle bounded ventrally by the scapular spine.

**Coracoid**—The right and left coracoids articulate with the scapulae described above. The coracoid has a rounded, subrectangular outline (Fig. 33). In *Rapetosaurus* the lateral surface of the coracoid is irregularly convex, and the medial surface is slightly concave. The anterodorsal border is thickened and exhibits an oblique ridge that originates near the midpoint of the anterodorsal border. This ridge radiates posteroventrally, extends for one-third the width of the element, and ends below to the coracoid foramen. The coracoid foramen perforates the element along its border with the scapula, and passes obliquely through to emerge on the medial surface at the scapulocoracoid

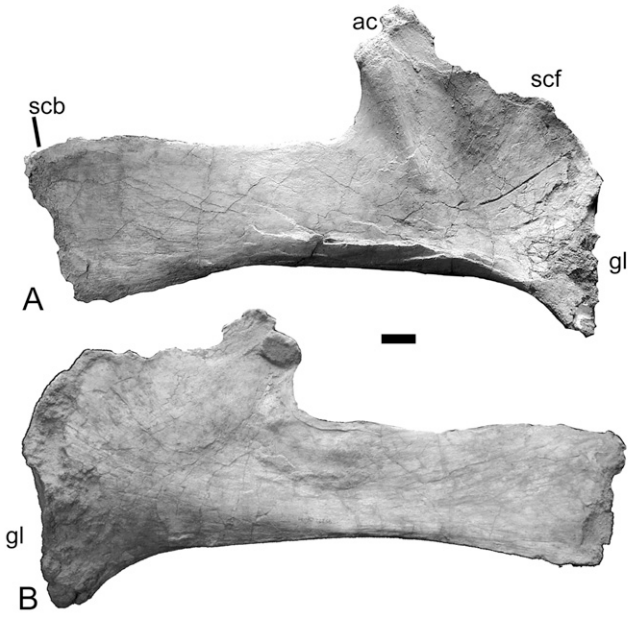


FIGURE 32. Right scapula (FMNH PR 2209) of *Rapetosaurus krausei* in **A**, lateral view; **B**, medial view. **Abbreviations**: **ac**, acromion process; **c**, coracoid articular facet; **gl**, glenoid fossa; **scb**, scapular blade; **scf**, supracoracoideus fossa. Scale bar equals 3 cm.

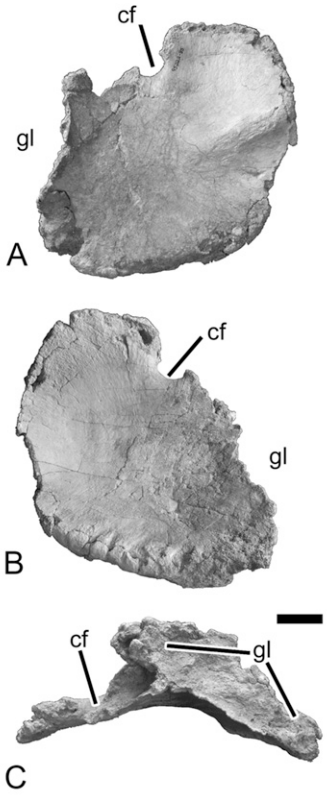


FIGURE 33. Right coracoid (FMNH PR 2209) of *Rapetosaurus krausei* in **A**, lateral view; **B**, medial view; **C**, posteroventral (glenoid) view. **Abbreviations**: **cf**, coracoid foramen; **gl**, glenoid fossa; **sc**, scapular articular facet. Scale bar equals 3 cm.

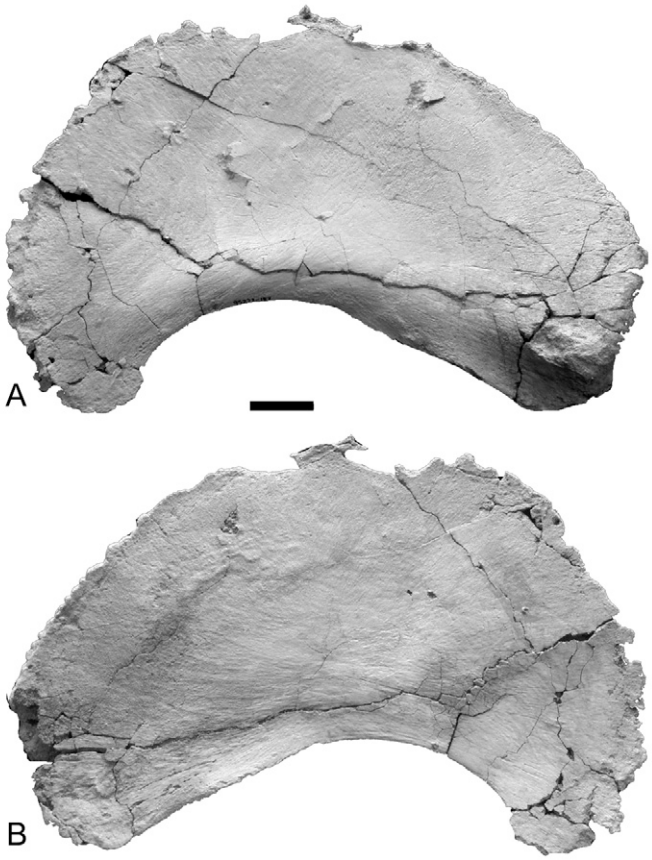


FIGURE 34. Right sternal plate (FMNH PR 2209) of *Rapetosaurus krausei* in **A**, ventral view, articular surface towards top right; **B**, dorsal view, articular surface towards top left. Scale bar equals 3 cm.

suture. The coracoid foramen is open in this juvenile specimen. In posteroventral view, the proximal expansion of the glenoid surface precludes exposure of the coracoid foramen. The glenoid surface is medially angled, elongated proximodistally, and mediolaterally compressed. There is no infraglenoid lip, and the glenoid surface is smaller than the scapular facet.

**Sternal Plate**—The sternal plates are semilunate, laminar, and only expanded at their anterior extremes (Fig. 34). As in all other titanosaurs, the sternal plate has strongly concave lateral borders and an elongate, highly convex medial border. The posterior end of the sternal plate is slightly thickened and squared off for articulation with the cartilaginous sternal ribs. The inner borders of the plates are slightly thickened and rugose for articulation with the contralateral sternal plate. When the posteromedial borders of the sternal plates are articulated, they are widely separated posteriorly.

**Pectoral Girdle, Comparisons**—The uniform width of the *Rapetosaurus* scapular blade is most consistent with that observed in other derived titanosaurs including *Alamosaurus* (USNM 10486, Gilmore, 1922a), *Opisthocoelicaudia* (ZPAL MgD-I/48, Borsuk-Bialynicka, 1977), *Saltasaurus* (PVL 4017-106, Powell, 1992), and *Neuquensaurus* (MLP CS 1096, Powell, 1986), and quite distinct from the anteriorly expanded scapulae of *Phuwiangosaurus* (PW 1-7, Martin et al., 1999) and *Isisaurus* (ISI R335, Jain and Bandyopadhyay, 1997; Wilson and Upchurch, 2003) and the constricted scapular blade of *Rinconsaurus* (MRS-Pv 43, Calvo and González Riga, 2003). The acute angle of the *Rapetosaurus* scapular blade-body intersection is similar to that of *Ligabuesaurus* (MCF-PVPH-233, Bonaparte et al., 2006), but differs from the obtuse angle observed in *Isisaurus* and *Opisthocoelicaudia*, and the more acute angle in *Phuwiangosaurus* and *Saltasaurus*.

The general rounded outline of the *Rapetosaurus* coracoid is similar to that observed in *Malawisaurus*, SMU-Mal 235, Gomani, 2005), but differs from *Alamosaurus* and *Rinconsaurus*, which have a smooth, quadrangular outline and sharp anterodorsal border. The rounded coracoid of *Rapetosaurus* differs substantially from the coracoids of *Saltasaurus* (PVL 4017-38, Powell, 1992, 2003), *Neuquensaurus*, and Malagasy Taxon B. In these taxa coracoids are rectangular with a distinctive "infraglenoid lip" and the scapular articularly facet is expanded and subrectangular instead of mediolaterally compressed and linear. The coracoid foramen is positioned in close proximity to or on the scapulocoracoid articulation in *Saltasaurus, Neuquensaurus*, and *Rapetosaurus*. In Malagasy Taxon B and *Opisthocoelicaudia*, the coracoid foramen is larger and occupies a more central position.

Overall, the sternal plates of *Rapetosaurus* do not differ significantly from those of other titanosaurs (e.g., *Malawisaurus*, SMU-Mal 188-1, Gomani, 2005; *Erketu*, IGM 100/1803, Ksepka and Norell, 2006).

## Forelimb

Representative elements of the forelimb include right and left humeri and radii, a left ulna, and a complete right and partial left metacarpus (Table 3, Figs. 37–39). The disarticulated nature of FMNH PR 2209 makes it impossible to determine whether carpals simply are not preserved, or whether they were unossified. The deltopectoral crest of the right humerus is markedly pathologic, bearing a prominent exostosis and an abnormally protruding posterior surface.

**Humerus**—The humerus is typical for that of most neosauropods in having a long shaft that is flattened anteroposteriorly, strongly expanded proximal and distal ends, a small degree of distal torsion, as well as poorly developed epicondyles (Fig. 35). The humeral head of *Rapetosaurus* lies level with the proximal end of the deltopectoral crest, and is positioned medial to the midline. The proximal end of the humerus is broad and anteriorly concave, accentuated by a well-developed, subrectangular deltopectoral crest that curves anteriorly and extends for just less than half the total length of the humerus. The humeral diaphysis is straight. The proximal end is thickened below the head towards the diaphysis. A rounded rugosity occurs just proximal to the midshaft on the posterior surface for insertion of brachial musculature. At mid-diaphysis the humerus is quite gracile and tapers to a narrow elliptical cross-section. The distal condyles project anteriorly with the radial condyle extending only slightly onto the posterior surface of the humerus whereas the ulnar condyle has a wider posterior extent. The ulnar condyle is slightly larger in transverse and anteroposterior dimensions than the radial condyle, and is slightly laterally flared. The positioning of these condyles indicates that the ulna occupied a position both posterior and lateral to the radius.

**Radius**—The gracile radius (midshaft width:length $< 0.25$) takes the form of an anteriorly bowed pillar with subequally expanded proximal and distal ends (Fig. 36). The entire element appears slightly twisted medially in its distal half. In dorsal view, the posterior margin of the proximal end is accordingly convex. The convex ulnar articular surface tapers to a narrow crest, extending distally and outward, and is one of the most diagnostic features of the antebrachium in *Rapetosaurus*. This crest is formed by the 'interosseus ridge' for the attachment of an interosseus membrane between radius and ulna. The ridge extends nearly the full length of the radius, terminating near the distal condyle on the lateral surface of the element. The oblique extension of this crest along the radius corresponds to a longitudinal crest along the anteromedial face of the ulna, confirming that the radius extended obliquely, from proximolateral to distomedial

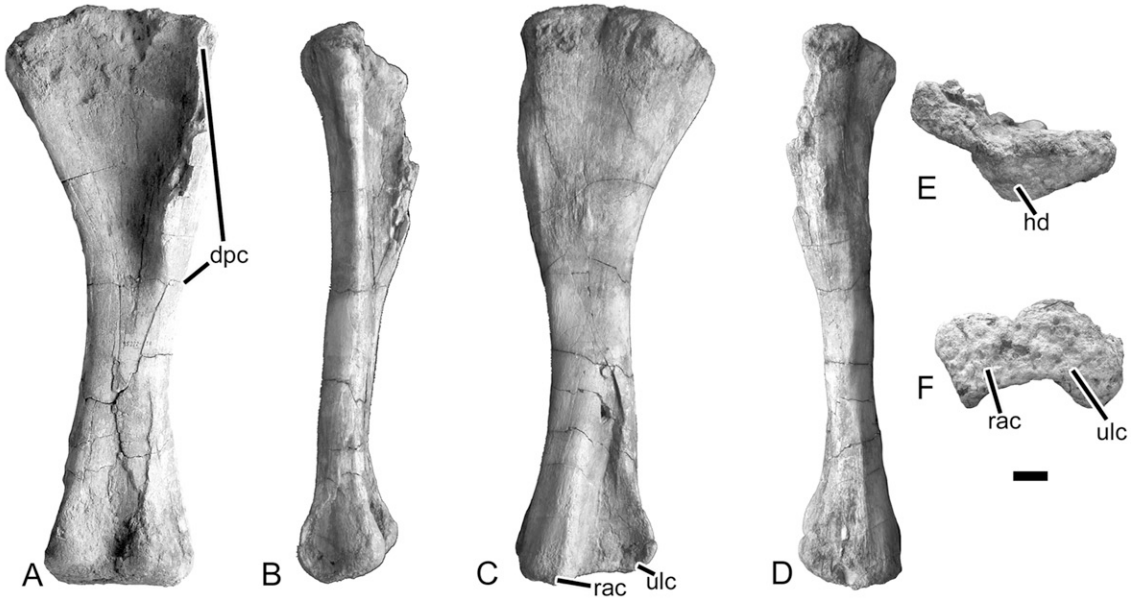


FIGURE 35. Left humerus (FMNH PR 2209) of *Rapetosaurus krausei* in **A**, anterior view; **B**, medial view; **C**, posterior view; **D**, lateral view; **E**, proximal view (anterior towards top); and **F**, distal view (anterior towards top). **Abbreviations**: **dpc**, deltopectoral crest; **hd**, humeral head; **rac**, radial condyle; **ulc**, ulnar condyle. Scale bar equals 3 cm.

across the anterior surface of the ulna. There is no additional ridge for pronator teres along the posteromedial surface of the *Rapetosaurus* radius. Instead, in *Rapetosaurus* the entire medial surface of the radius tapers to a thin, anteriorly bowed ridge. A broad subrectangular muscle scar marks the posteromedial surface at the distal end of the radius. The distal articular surface is a transversely expanded oval in distal view. Its surface is slightly convex as a whole, but is almost flat medially to form the articular surface for the carpus.

**Ulna**—The robust ulna has a broad and stout proximal end, and narrows toward its distal end (Fig. 37). The proximal articular surface is convex and features a low and rounded olecranon process that articulates with the posterior part of the medial surface of the humeral condyle. The proximal half of the ulna is triangular in cross-section, with the apex of the triangle directed anteriorly. The proximal ulna is dominated by a long, narrow anteromedial process and a well-developed lateral radial articulation. The anterolateral process of the ulna is shorter than the anteromedial process and both slope gently away from the olecranon. The lateral face of the ulnar shaft is broadly concave for reception of the radius. It bears a low ridge that extends distally from the proximal end of the ulna and cups the lateral surface of the radius. More medially, a sharp, oblique ridge for attachment of the interosseus muscle or membrane bounds the medial surface of the lateral concavity. Along the distal portion of the ulna a small rounded concavity indicates the articulation of the distal radius. This facet corresponds exactly to the posterior tuberosity on the radius' distal surface. This medially placed facet corroborates the oblique placement of the radius. Proximally, the radius occupies the anterior surface of the ulna, whereas more distally it twists toward the medial surface. The distal articular surface of the ulna is a rounded triangle, with an anteromedial apex and a posterior base.

**Manus**—The metacarpals fit closely together at their proximal ends (Fig. 38E). When articulated, they are oriented almost vertically and form a semilunate arch with a flat proximal surface, for articulation with the carpals, which were either ossified or cartilaginous. Metacarpals I, II, and III are nearly parallel to each other, but metacarpals IV and V diverge distally and attain a position slightly posterior to the other metacarpals. The length of the metacarpals increases slightly through metacarpal III, but decreases through metacarpals IV and V. Metacarpal V is the shortest and is even more robust than metacarpal I. All metacarpals are somewhat triangular in cross-section, although the directions of their apices and bases vary throughout the series. Their proximal ends widen dorsally and taper in a posterior direction (metacarpal I), are triangular with dorsal bases and posterior apices (metacarpals II and III), or take the shape of elongate ovals with transversely oriented long axes (metacarpals IV and V). Posterior expansions of the proximal ends are most likely associated with the insertion of flexor palmaris profundus and the plantar aponeurosis (Borsuk-Bialynicka, 1977). In the articulated manus, the posterior crests converge toward one another. In distal view, all metacarpal articular surfaces are slightly saddle shaped with subrectangular outlines. Though manual phalanges have not yet been definitively identified for any titanosaur, the presence of articular surfaces at the distal ends of metacarpals implies the presence of phalanges (see below).

Metacarpal I is only slightly shorter than metacarpals II–IV. The proximal end of metacarpal I in *Rapetosaurus* is characterized by an ovate articular surface, which narrows posterolaterally into a sharp, elongate posterior process. This process is slightly concave laterally where it wraps around the posteromedial surface of metacarpal II and forms the posterior and medial boundaries of the semilunate manus. The shaft is straight for most of its length, and slightly expanded distally in dorsal view. In lateral view, the shaft narrows in its distal half and twists so that the medial condyle is visible. The lateral surface of the proximal shaft is dominated by a broad, triangular concavity for articulation with metacarpal II. The medial surface of metacarpal I is broad proximally, tapering slightly below midshaft. Also slightly below midshaft, a thin oblique ridge extends in a proximodorsal-distoventral direction. In posterior view this elongate ridge extends toward the distolateral surface of the element, and likely indicates the insertion of extensor carpi radialis (Borsuk-Bialynicka, 1977). The distal end of metacarpal I is subrectangular in outline and characterized by an anterior convexity and a posterior trochlea. This articular surface is asymmetrical and beveled medially.

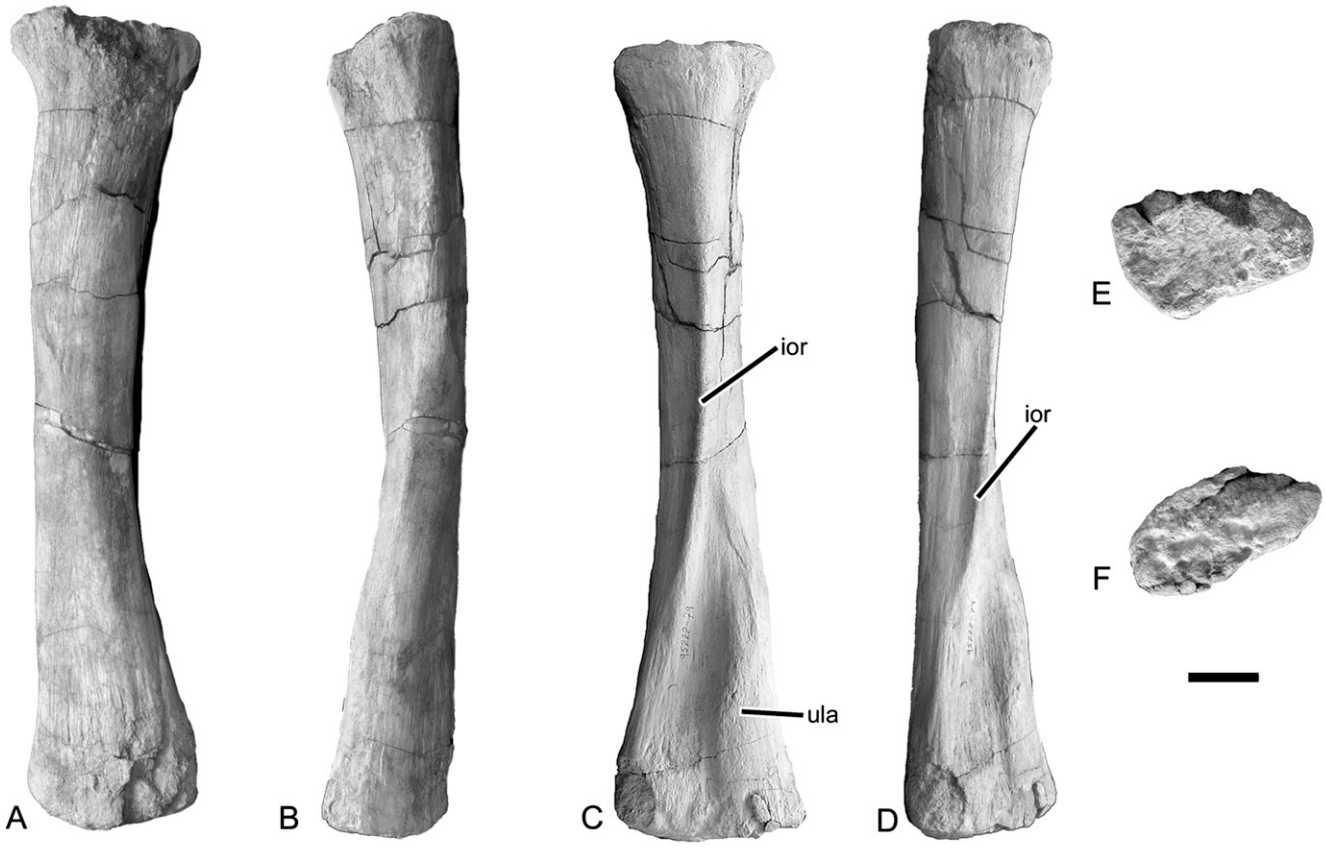


FIGURE 36. Left radius (FMNH PR 2209) of *Rapetosaurus krausei* in **A**, anterior view; **B**, medial view; **C**, posterior view; **D**, lateral view; **E**, proximal view (anterior surface towards top); **F**, distal view (anterior towards top). **Abbreviations**: **ior**, interosseous ridge for attachment of interosseous membrane; **ula**, ulnar articular facet. Scale bar equals 3 cm.

Metacarpal II is the most gracile of all manual elements. Its shaft is triangular in cross-section, with medial and lateral articular areas for metacarpals I and III, respectively. As in other titanosaurs, the proximal end of the element is a rounded triangle in proximal view, with an anterior base and posterior apex. The shaft is vertically oriented and marked by a single midshaft rugosity. The posterior surface of the shaft is divided into medial and lateral portions by a sharp ridge extending from the apex of the proximal articular surface. In distal view, the end of the element is oval and has a slight notch for articulation with the distal end of metacarpal III that extends toward the anterolateral surface of the element. The distal end is beveled slightly laterally.

Metacarpal III is the longest and most vertically oriented of the manual elements. In *Rapetosaurus*, metacarpal III maintains a triangular cross-section that is most pronounced proximally. The proximal end has a broad dorsal base and a posterior apex with equilateral medial and lateral sides. From the posterior apex an elongate ridge extends distally, turns laterally at midshaft, and divides metacarpal III into three distinct surfaces. The dorsal surface of the element is broad, flat, and tapers distally. This surface is unmarred by muscle scars or indicators of vascularity. The posteromedial surface of metacarpal III is distinctive in its 'V'-shaped articular facet for metacarpal II. This proximal facet is bounded ventrally at the midshaft by a well-defined neurovascular foramen. This foramen forms a bony prominence that is also visible in dorsal view of the element. Posterolaterally, metacarpal III bears a triangular articular facet for metacarpal IV and a faint ridge in its distal one-third that may have served as an insertion point for extensor digitorum communis (Borsuk-Bialynicka, 1977). The articular facets for metacarpals II and IV are both slightly concave. The distal end of metacarpal III is subrectangular in distal view with a long axis oriented anteroposteriorly. A small excavation along the medial boundary marks an abutment with the distal end of metacarpal II, whereas the lateral surface is slightly convex.

Metacarpal IV is slightly shorter than metacarpal III, and is equivalent in length to metacarpal II. It differs from metacarpals II and III in its more strongly expanded proximal end. In proximal view, metacarpal IV departs from the triangular morphology of metacarpals II and III, and instead takes the shape of an elongate oval that narrows dorsally. Elongate ridges extend from the dorsal and posterior margins of this proximal surface. The posterior ridge extends the full length of the element, but veers laterodistally toward its termination at the distal condyle. This ridge divides the metacarpal into medial and lateral halves, which bear the articular surfaces for metacarpals III and V, respectively. In distal view, the articular surface of metacarpal IV is broad and subrectangular with a medially oriented base and lateral apex.

Metacarpal V is the shortest and most robust of all metacarpals. The proximal end of metacarpal V is strongly compressed mediolaterally, flat medially, and slightly convex laterally. The shaft is relatively straight in dorsal view, but in lateral view, the proximal end is notably flared anteroposteriorly. The shaft is also anteroposteriorly expanded in its distal extreme. The medially

TABLE 3. Appendicular measurements (cm) in *Rapetosaurus krausei* (FMNH PR 2209).

| | | Maximum Breadth | | | | |
|---|---|---|---|---|---|---|
| | | Proximal | | | Distal | |
| Element | Maximum Length | Transverse | Ant-post | Shaft | Transverse | Ant-post |
| Humerus | 52.4 | 20.3 | 6.6 | 8.6 | 14.3 | 5.7 |
| Ulna | 37.2 | 12.6 | 4.5 | 7.1 | 6.4 | 6.4 |
| Radius | 36.5 | 8.2 | 5.9 | 4.6 | 8.8 | 3.8 |
| MTC I | 17.3 | 1.4 | 6.0 | 2.1 | 3.9 | 3.4 |
| MTC II | 17.7 | 2.9 | 3.9 | 2.4 | 3.4 | 4.0 |
| MTC III | 18.4 | 3.8 | 3.6 | 2.5 | 4.0 | 3.3 |
| MTC IV | 18.3 | 2.8 | 6.6 | 3.4 | 5.9 | 3.7 |
| MTC V | 16.8 | 1.9 | 5.0 | 2.3 | 3.3 | 3.9 |
| Femur | 65.7 | 17.7 | 13.0 | 11.1 | 17.3 | 15.4 |
| Tibia | 50.0 | 6.3 | 14.8 | 4.0 | — | — |
| Fibula | 46.6 | 4.3 | 8.8 | 5.1 | 4.9 | 7.2 |
| MTT I | 6.3 | 2.6 | 5.7 | 1.9 | 4.0 | 3.4 |
| MTT II | 8.2 | 3.3 | 5.8 | 1.8 | 4.1 | 3.0 |
| MTT III | 8.9 | 3.0 | 4.8 | 1.7 | 3.8 | 2.3 |
| MTT IV | 8.8 | 2.2 | 4.8 | 1.4 | 3.6 | 1.7 |
| MTT V | 5.9 | ~2.0 | 4.0 | 1.1 | 0.6 | 1.0 |

Contralateral elements with similar measurements are preserved for humerus, radius, and metacarpals I–IV. "Ant-post" refers to breadth measured from anterior to posterior surfaces of proximal and distal ends of each element.

placed articular surface for metacarpal IV is strongly flared anteroposteriorly, and ends abruptly at the mid-diaphysis where a neurovascular canal interrupts the lateral surface. In distal view the surface of metacarpal V is subcircular with a slightly concave medial border. It is notably wider and more rounded than the flattened proximal condyle.

**Forelimb, Comparisons**—The humeral heads of *Opisthocoelicaudia* (ZPAL MgD-I/48, Borsuk-Bialynicka, 1977), *Neuquensaurus*

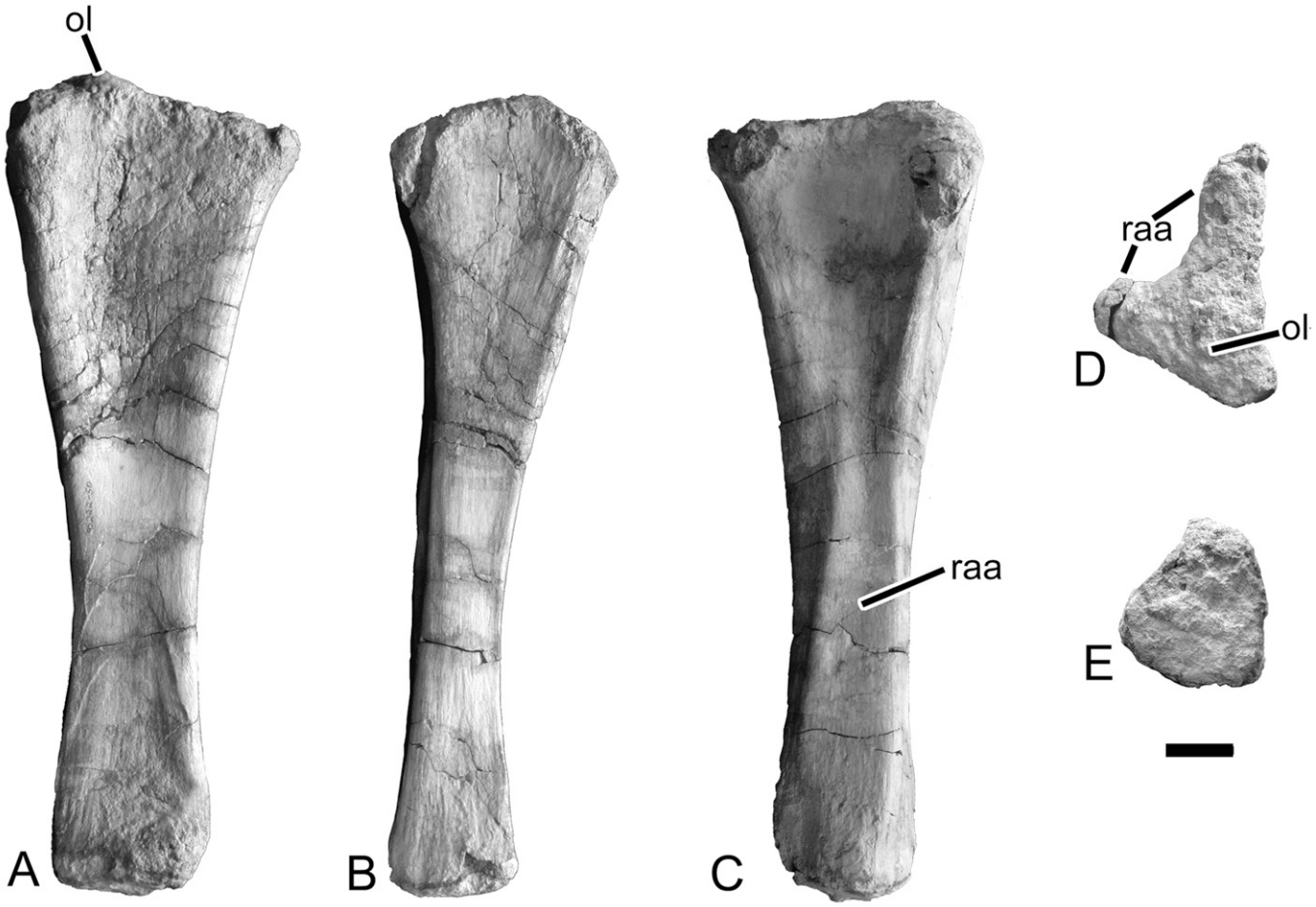


FIGURE 37. Left ulna (FMNH PR 2209) of *Rapetosaurus krausei* in **A**, medial view; **B**, posterior view; **C**, lateral view; **D**, proximal view (anterior towards top); and **E**, distal view (anterior towards top). **Abbreviations**: **ol**, olecranon process; **raa**, radial articulation. Scale bar equals 3 cm.

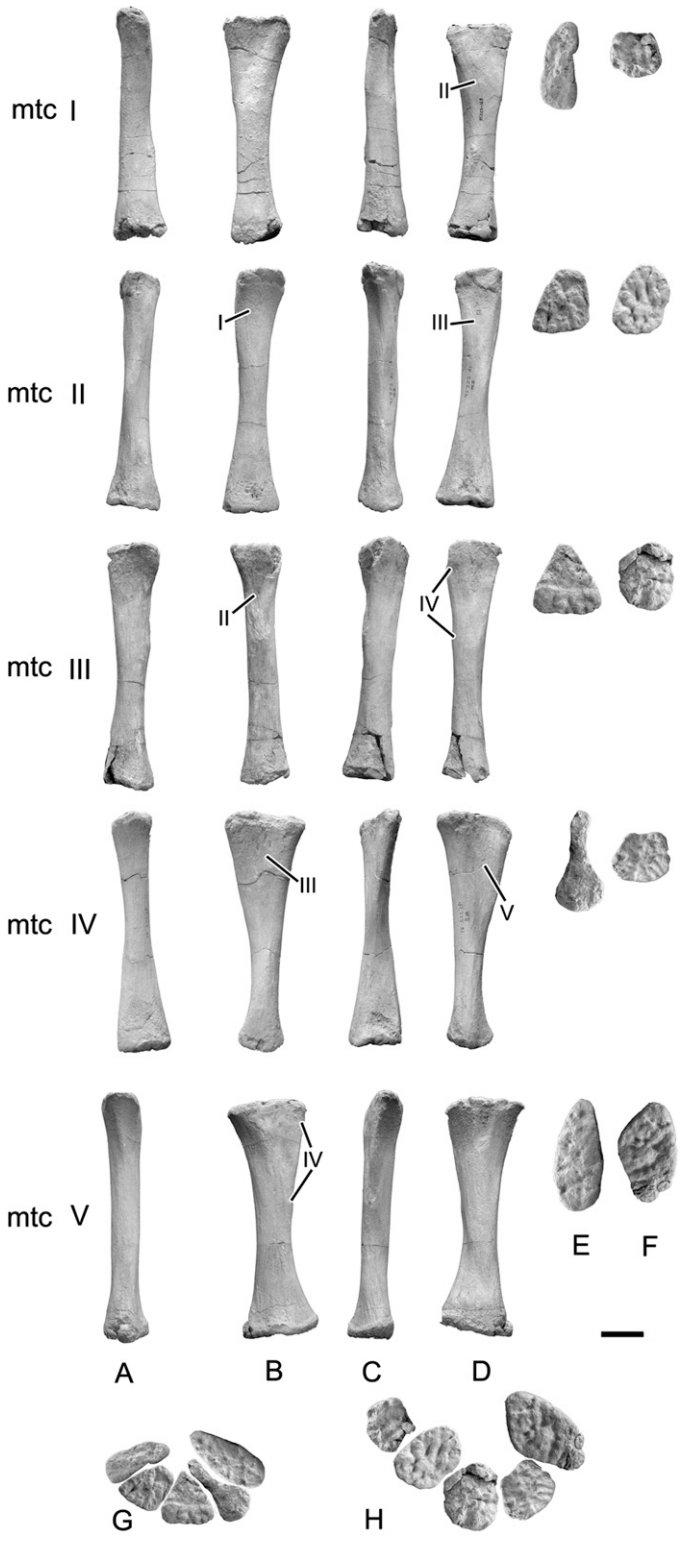


FIGURE 38. Manus (FMNH PR 2209) of *Rapetosaurus* krausei including left metacarpals I-III, and V, and right metacarpal IV (reversed) in **A**, dorsal view; **B**, posterior view; **C**, medial view; **D**, lateral view; **E**, proximal view; **F**, distal view. **G**, articulated metacarpus in proximal view; **H**, articulated metacarpus in distal view. External towards bottom in **E–G**. **Abbreviations**: **I–V**, articular surfaces for corresponding metacarpals; **mtc**, metacarpal. Scale bar equals 3 cm.

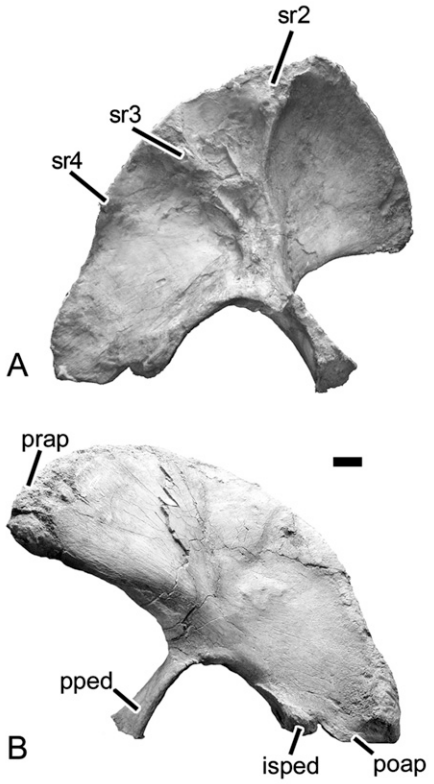


FIGURE 39. Left ilium (FMNH PR 2209) of *Rapetosaurus krausei* in **A**, medial view; **B**, lateral view. **Abbreviations**: **isped**, ischial peduncle; **poap**, postacetabular process; **pped**, pubic peduncle; **prap**, preacetabular process; **sr**, sacral rib facet. Scale bar equals 3 cm.

(MLP CS 1099, Powell, 1986, 2005), and *Argyrosaurus* (PVL 4628, Powell, 1986) lie proximal to the deltopectoral crest. This morphology contrasts with *Rapetosaurus* in which the humeral head is level with the proximal end of the deltopectoral crest. A medially concave shaft characterizes the humerus of *Saltasaurus* (PVL 4017-67, Powell, 1992) and differs from the distally straight shaft in *Rapetosaurus*. The humeri of *Saltasaurus* and *Malawisaurus* (SMU Mal-221, Gomani, 2005) are slightly more gracile than *Rapetosaurus*. In most titanosaurs the deltopectoral crest extends for only one-third of the length of the humerus (e.g., *Ligabuesaurus*, MCF-PVPH-233, Bonaparte et al., 2006), whereas in *Rapetosaurus* and other derived titanosaurs the deltopectoral crest extends at least one-half the length of the humerus.

Radial shafts are similarly gracile and bear a rounded proximal end in *Rapetosaurus* and *Magyarosaurus* (UB R1060, pers. observ.), in contrast to the more robust radii of *Saltasaurus* (PVL 4017-73, Powell, 1992, 2003) and *Ampelosaurus* (MD-E C3 236, pers. observ.). *Saltasaurus, Neuquensaurus*, and *Rapetosaurus* share the presence of a clearly defined interosseus crest. *Rapetosaurus* lacks the elongated, posteromedial ridge for *pronator teres* common to the radii of most other titanosaurs (e.g., *Opisthocoelicaudia*).

The low but well-defined olecranon process of the *Rapetosaurus* ulna also characterizes *Saltasaurus* (PVL 4017-74, Powell, 1992), *Neuquensaurus*, *Magyarosaurus* (UB R1514, pers. observ.), and *Phuwiangosaurus* (PW 1-9, Martin et al., 1999). This morphology contrasts with that of the elevated, distinct olecranon in *Malawisaurus* (SMU Mal-190, Gomani, 2005) and *Ampelosaurus* (MD-E C3 300, pers. observ.). The narrow proximal ulna in *Rapetosaurus* also contrasts with the expanded proximal ulna in *Alamosaurus* (TMM 43621-1, Lehman and Coulson, 2002).

Metacarpals are poorly known for other titanosaurs, but the complete right metacarpus of *Epachthosaurus* generally compares well with that of *Rapetosaurus*. Metacarpal I is the shortest metacarapal, and metacarpal III is the longest metacarpal in *Rapetosaurus* and most other titanosaurs. In *Pellegrinisaurus* (MPCA 1500, Powell, 1986; Salgado, 1996) and *Opisthocoelicaudia* metacarpal I is the longest, whereas in *Alamosaurus* (USNM 15560, Gilmore, 1946) metacarpal II is the longest. The distal ends of metacarpal I in *Opisthocoelicaudia* and *Antarctosaurus* are flat, rather than medially beveled as in *Rapetosaurus*. *Rapetosaurus* and *Malawisaurus* (SMU Mal-208, Gomani, 2005) share the presence of an oval distal end with a lateral notch on metacarpal III as well as the twisting of the shaft of metacarpal IV. The rounded distal morphology observed in *Saltasaurus* metacarpal IV differs from the subrectangular morphology observed in *Rapetosaurus* and most other titanosaurs. In contrast with the proximal expansion of metacarpal V in *Rapetosaurus*, in *Alamosaurus, Opisthocoelicaudia*, and *Janenschia* the proximal and distal ends of metacarpal V are subequally expanded.

### Pelvic Girdle

The pelvic girdle is represented by right and left ilia, pubes, and ischia (Table 2, Figs. 39–42). The preacetabular process of the ilium is strongly flared anterolaterally as in other titanosaurs, and the ischium is only 54% the length of the pubis. The acetabulum is composed primarily of the ilium, with smaller ischial and pubic contributions. The left ilium and left pubis were found in close association in the southwest corner of the quarry. The rest of the elements were more broadly distributed in MAD 93-18 (Fig. 4E).

**Ilium**—The ilium has a high, anterolaterally flared iliac blade that reaches its greatest height anterior to the pubic peduncle (Figs. 39, 42). The entire anterodorsal surface of the iliac blade forms a semicircular, broadly curved surface. The iliac blade is massive anteriorly, but tapers posteriorly, thickening only at the posteriormost tip of the ilium. The ventral margin of the preacetabular process is slightly concave in lateral view. The massive postacetabular process of the ilium is transversely expanded and rugose along its dorsal margin for the origin of the iliocaudalis muscle (Borsuk-Bialynicka, 1977). The postacetabular portion of the ilium extends slightly ventral to the short ischial peduncle where it thickens and bears rugosities for ligamentous insertions. It is separated from the ischial peduncle by a small notch. The pubic peduncle is elongate (about four times as long as the ischiadic peduncle), gracile, and anteroventrally oriented, as in all other known titanosaurs. It comprises over half of the acetabulum. In contrast, the ischiadic peduncle is very low, consisting of little more than a rounded sutural surface. In *Rapetosaurus*, the ischial peduncle does not extend ventrally beyond the postacetabular process. Directly above the ischial sutural surface a large tuberosity indicates the insertion of hip extensors and rotators.

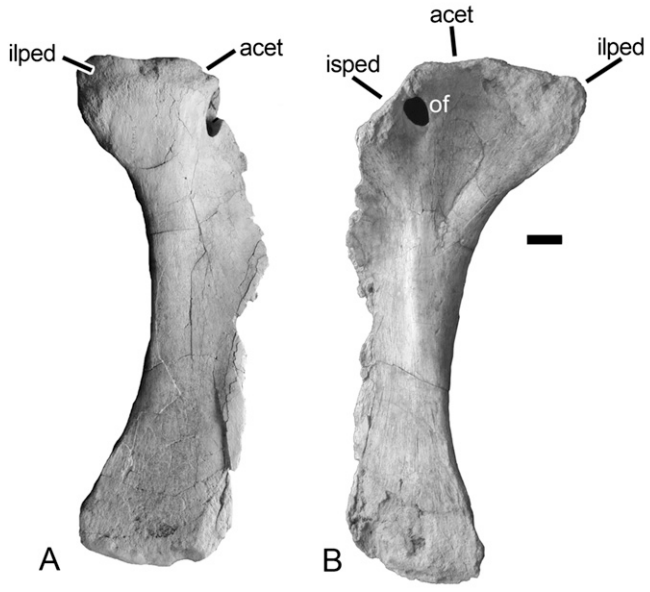


FIGURE 40. Left pubis (FMNH PR 2209) of *Rapetosaurus krausei* in **A**, anterolateral view; **B**, medial view. **Abbreviations**: **acet**, acetabulum; **ilped**, iliac peduncle; **isped**, ischial peduncle; **of**, obturator foramen. Scale bar equals 3 cm.

The medial surface of the ilium is characterized by the lateral sweep of the iliac blade, and by the distinctive facets for articulation with the sacral ribs. Three sacral rib facets are visible, and indicate that the sacral ribs did not extend beyond the dorsal margin of the iliac blade. The two most prominent sacral rib facets occur dorsal to the acetabulum as elongate, dorsally radiating ridges. The iliac blades are laterally splayed, and the ilia did not contact one another along their dorsal margins.

**Pubis**—Both preserved pubes are missing the medial pubic articular wing (Fig. 40, 42). The left pubis articulates with the left ilium and ischium described here. The most unusual feature of the *Rapetosaurus* pubis is a twisting of the proximal end to result in a clear view of the obturator foramen in anterior, medial, and lateral views. The pubis of *Rapetosaurus* is elongate and gracile with a long and laterally compressed blade. The proximal end of the pubis is a narrow plate that passes distally into the shaft, and medially into a symphyseal portion. The proximal part of the pubis is exposed in lateral view, and a slight lateral curvature toward the posteriorly directed ischial contact allows the obturator foramen to be seen in most views. A broad, flat, shelf marks the pubis-ilium contact anteriorly. This shelf grades posteriorly into a slightly lower, angled area that constitutes the pubic contribution to the acetabulum. The wide obturator foramen marks the beginning of the ischial articular surface in *Rapetosaurus*, and extends posteroventrally at a sharp angle away from the proximal pubis. The posteromedial portion of the pubic shaft is paper-thin where it articulates with the contralateral element. Distally, the shaft of the pubis is straight and thin, with little transverse expansion. It maintains its dorsoventral height, and is not flared. The ischial articular surface is laterally curved and merges with the thin pubic articulation more distally.

**Ischium**—The right ischium is more complete than the left, preserving its entire pubic and ischial articular surfaces, as well as its contribution to the acetabulum (Figs. 41, 42). In general, the ischium takes the shape of a broad, nearly semilunar plate. The proximal region of the ischium is gently concave and thin where it contributes to the acetabulum, but then curves sharply posterodorsally to form a distinct, rounded iliac peduncle. The iliac peduncle lies at a level well above the pubic articulation and the acetabulum and constitutes part of the posterior border of the acetabulum. A well-defined muscle scar is developed anterior to the posterolateral concavity, near the middle of the element. This muscle scar may be for the origin of the ischial head of the flexor tibialis (Borsuk-Bialynicka, 1977). The anteromedial portion of the ischium is rugose and, in an adult animal, would have been firmly co-ossified with the pubis. The ischium's ventrally expanded articular surface for the contralateral ischium is elongate and thin, occupying approximately half the length of the blade. It is angled posteriorly ventral to the pubic peduncle. Ventral to the pubic articulation, the ischial articular surface angles steeply posterolaterally toward the distal extremity of the element. The *Rapetosaurus* ischium is slightly rectangular along its ischial articular surface. The two ischia would have contacted one another in a broad, flat, sutural surface.

**Pelvic Girdle, Comparisons**—The ilium displays the generalized morphology known for other titanosaurs (e.g., *Isisaurus*, ISI R335, Jain and Bandyopadhyay, 1997; *Saltasaurus*, PVL 4017-93, Powell,

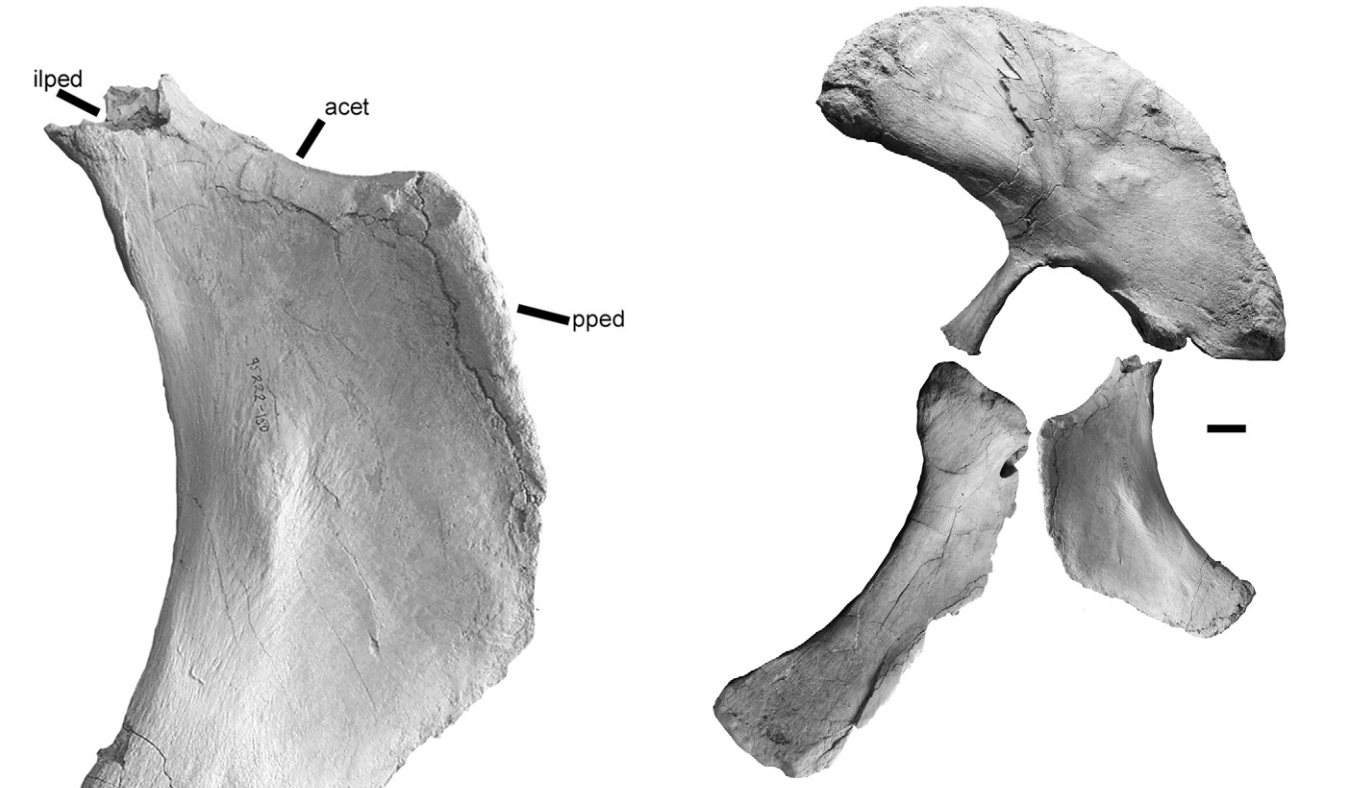

FIGURE 42. Articulated pelvic girdle of *Rapetosaurus krausei* in left lateral view. Left ilium, left pubis, right ischium (reversed). Scale bar equals 3 cm.

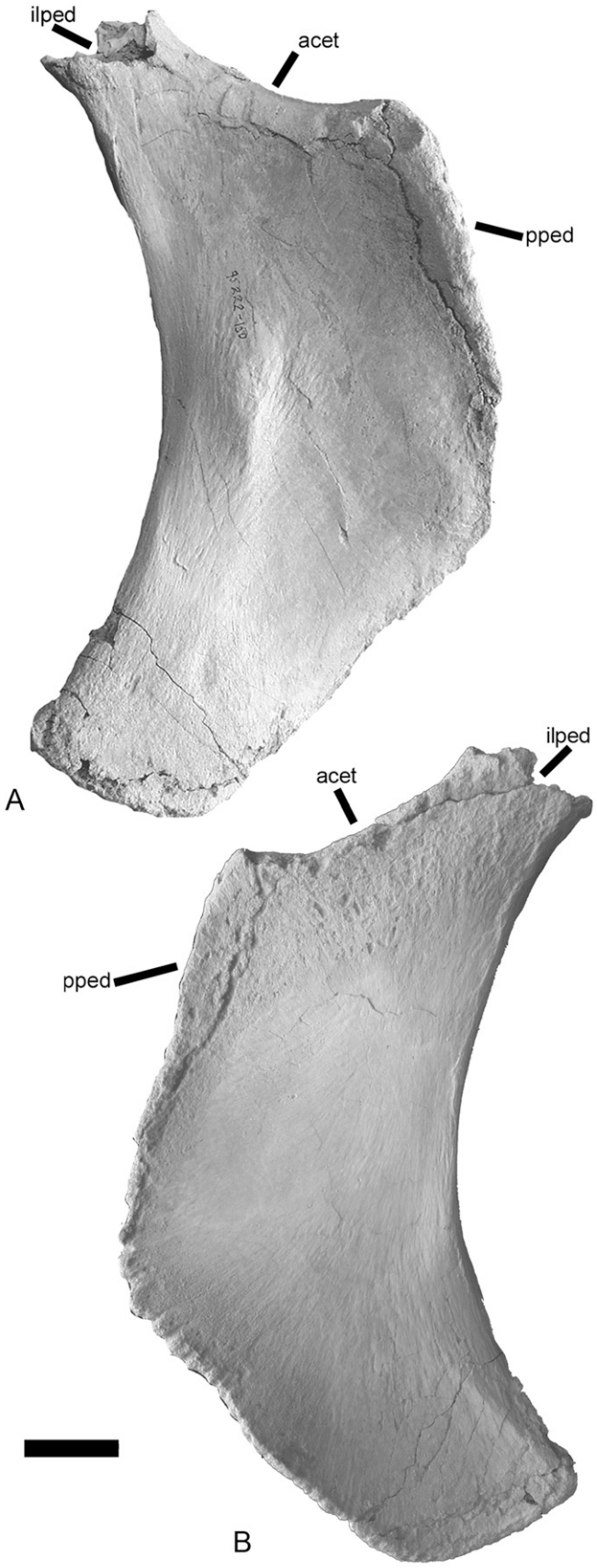


1992, 2003; *Rocasaurus*, MPCA Pv46, Salgado and Azpilicueta, 2000). *Opisthocoelicaudia* (ZPAL MgD-I/48, Borsuk-Bialynicka, 1977), *Phuwiangosaurus* (PW 1-10, Martin et al., 1999), and *Epachthosaurus* (UNPSJB-PV 920, Martínez et al., 2004) are characterized by relatively low preacetabular processes that are not dorsoventrally expanded to the extreme observed in *Rapetosaurus*. In *Isisaurus* the ischial peduncle is longer and better defined than in *Rapetosaurus* and most other titanosaurs.

Overall, the pubis of *Rapetosaurus* is extremely compressed transversely, with little to no expansion of its proximal or distal ends, as in *Isisaurus, Alamosaurus* (TMM-43621-1, Lehman and Coulson, 2002), *Saltasaurus* (PVL 4017-95, Powell, 1992), and *Magyarosaurus* (BMNH R3851, pers. observ.). This unexpanded morphology greatly contrasts with that of *Opisthocoelicaudia* and *Epachthosaurus*, each characterized by robust pubes marked by well-developed muscle scars. *Rapetosaurus* exhibits a shelf-like morphology of the iliac peduncle, which contrasts with the perpendicular articulation between the acetabular and iliac articular surfaces in *Andesaurus* (MUCPv132, Calvo and Bonaparte, 1991) and *Ampelosaurus* (MD-E C3 57, pers. observ.). The ischial articular surface of *Rapetosaurus* is much longer than that of *Alamosaurus*, and the acetabular portion is longer than in *Opisthocoelicaudia*. In both *Rapetosaurus* and *Opisthocoelicaudia* this shelf grades posteriorly into lower, angled acetabular area. The anterior margin of the *Rapetosaurus* pubic shaft is thin and not expanded as in other neosauropods (Wilson and Sereno, 1998; Upchurch, et al., 2004) and some titanosaurs (e.g., *Andesaurus, Ampelosaurus)*.

← FIGURE 41. Right ischium (FMNH PR 2209) of *Rapetosaurus krausei* in **A**, lateral view; **B**, medial view. **Abbreviations**: **acet**, acetabulum; **ilped**, iliac peduncle; **pped**, pubic peduncle. Scale bar equals 3 cm.

The broad, flat *Rapetosaurus* ischium is similar to that of *Malawisaurus* (SMU Mal-42, Jacobs et al., 1993; Gomani, 2005) and *Saltasaurus* (PVL 4017-99, Powell, 1992). It contrasts dramatically with the ischia of *Andesaurus* (MUCPv132, Calvo and Bonaparte, 1991), *Isisaurus, Opisthocoelicaudia, Ampelosaurus* (MD-E C3 593, pers. observ.), and *Phuwiangosaurus* (PW 1-14, Martin et al, 1999), in which the posterior portion of the ischial blade is extremely narrow relative to the body. *Rapetosaurus* and *Rinconsaurus* (MRS-Pv 101, Calvo and González Riga, 2003) both exhibit rectangular pubic peduncles, but in *Rapetosaurus* the iliac peduncle is much narrower and less distinct from the acetabulum. A relatively large iliac peduncle is observed in most titanosaurs, including *Rapetosaurus*, but in *Malawisaurus* and *Saltasaurus* it is square rather than rounded. *Rapetosaurus* exhibits an ischium that is rectangular along its long pubic articular regions as in *Malawisaurus, Alamosaurus* (USNM 10487, Gilmore, 1922a), and *Saltasaurus*.

### Hind Limb

A left femur, partial left tibia, right fibula, and partial left and right pes represent the known elements from the hind limb of *Rapetosaurus* (Table 3, Figs. 45–47). No tarsal elements were recovered from MAD 93-18. Because sauropods are known to have ossified astragali, the absence of this element is likely an artifact of preservation. It is impossible to determine whether the absence of calcaneum in FMNH PR 2209 is an artifact of taphonomy, or whether it is absent or unossified as hypothesized for some other sauropods (e.g. McIntosh, 1990).

**Femur**—The femur is typical of graviportal animals in having a broad shaft that is somewhat flattened anteroposteriorly. It bears several features characteristic of other titanosaurs, including the presence of a medial deflection of the head of the femur along with a low, laterally oriented flange (Fig. 43). These derived femoral characteristics are possibly related to the development of a unique "wide-gauge" gait, and the ability to utilize bipedal postures in feeding (Borsuk-Bialynicka, 1977; Wilson and Carrano, 1999). The head of the femur is distinctively convex. As in other titanosaurs, it is situated dorsal to the level of the greater trochanter and faces dorsally, rather than medially as in other neosauropods. The greater trochanter is an elongate ridge extending distally below the femoral head. An elongate lateral flange is developed slightly distal to the greater trochanter. The posterior surface of the lateral flange is rugose for the attachment of the m. iliofemoralis (Borsuk-Bialynicka, 1977). Distal to the lateral flange, a slight concavity on the anterolateral surface of the femur indicates the insertion of thigh flexors. The fourth trochanter is low, long, poorly developed ridge, and is restricted to the posterior surface of the femoral midshaft. It serves as the insertion for the caudifemoralis complex (Borsuk-Bialynicka, 1977). At mid-diaphysis the femur is anteroposteriorly compressed with an elliptical cross-section. On the posterior side of the femur a long, thickened ridge extends distal to the medial side of the greater trochanter. This ridge continues distally

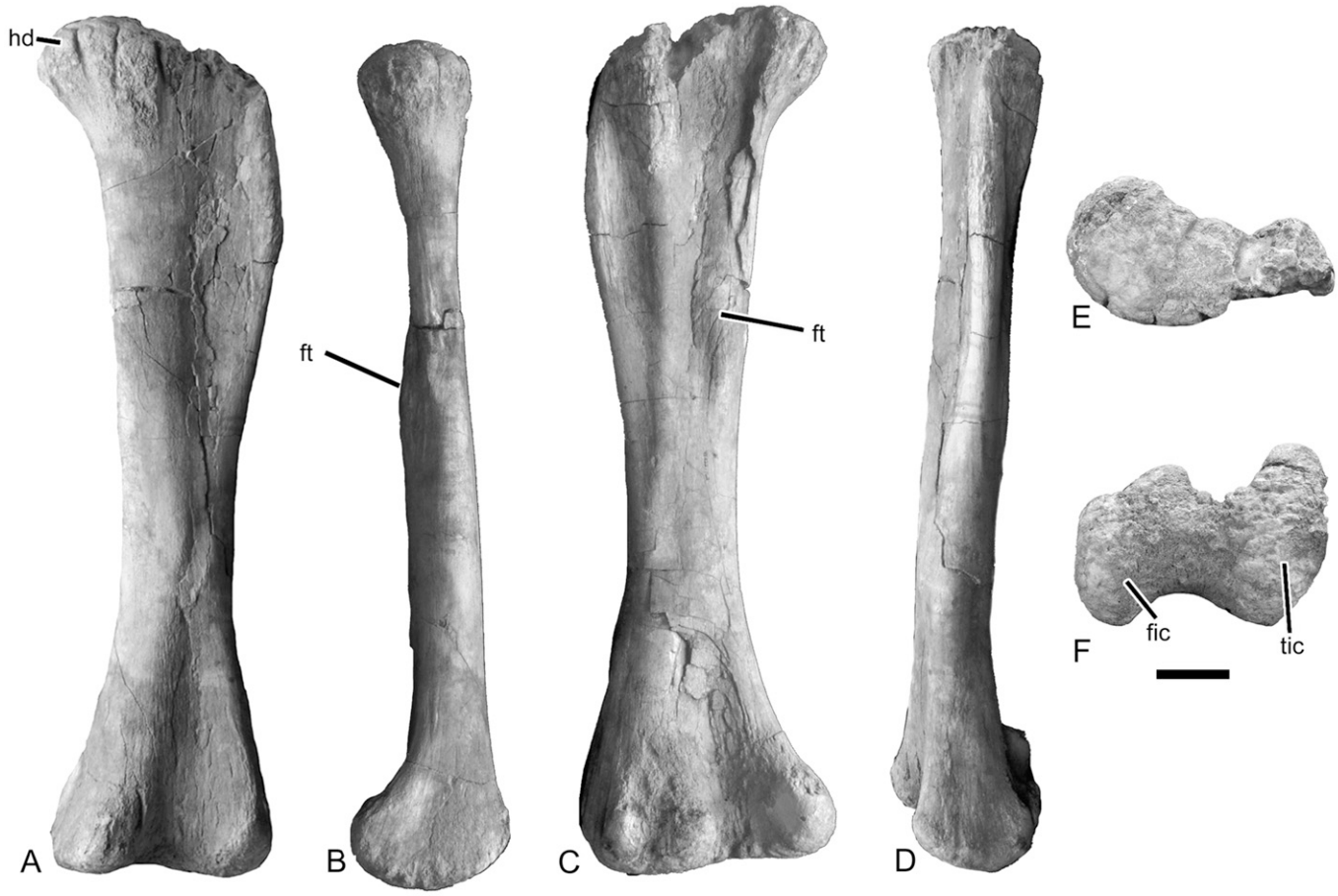


FIGURE 43. Left femur (FMNH PR 2209) of *Rapetosaurus krausei* in **A**, anterior view; **B**, medial view; **C**, posterior view; **D**, lateral view; **E**, proximal view (anterior towards bottom); **F**, distal view (anterior towards bottom). **Abbreviations**: **fic**, fibular condyle; **ft**, fourth trochanter; **hd**, head; **tic**, tibial condyle. Scale bar equals 5 cm.

and is bounded medially and laterally by slight concavities. The tibial condyle is expanded anteroposteriorly to form a broad articular surface. The fibular condyle is more anteroposteriorly compressed.

**Tibia**—The tibia is missing its distal third (Fig. 44). It is flattened mediolaterally and broader anteroposteriorly than transversely in its preserved portion. The proximal articular surface is an anteroposteriorly directed, concave oval as in most other titanosaurs. The short cnemial crest of *Rapetosaurus* projects anterolaterally as a sharp, elongate ridge and forms the anterior boundary of a shallow groove for reception of the fibula. Distal to the cnemial crest the tibial shaft widens to form a broad, smooth anterior surface. A fibular process that forms the posterior boundary of the fibular fossa marks the lateral surface of the tibia. It is broadly convex and extends well beyond the lateral extent of the cnemial crest. The medial surface of the tibia is anteroposteriorly broad proximally, and tapers distally into a narrow, subrectangular, anterolaterally flared end. The preserved portion of the distal end of the tibia is marked by a shallow concavity posteriorly.

**Fibula**—The fibula is much more slender than the proximal tibia, although it is roughly equivalent in breadth to that of the tibia at midlength (Fig. 45). Its extremities are slightly expanded and subequal in size. The anterior border of the fibula is concave proximally but straightens distally, whereas the posterior border is convex proximally and concave distally. Thus the fibula exhibits a slightly sigmoidal outline in lateral view. The proximal articular surface of the fibula is slightly convex, whereas its medial margin is concave and cups the tibia. An elongate, narrow crest extends along the medial surface of the fibula and separates anterior and posterior excavations. The shaft of the fibula expands only slightly in its distal third. Fibular muscle scars include an oval, rough concavity directly distal to the proximal articular surface on the posterior wall of the element. This scar may be for the insertion of m. iliofibularis as in *Opisthocoelicaudia* (Borsuk-Bialynicka, 1977). It is elongate and extends onto the lateral surface of the bone more distally. Anteriorly, an elongate sharp crest extends toward the distal surface of the fibula from the iliofibularis scar. This crest may represent an extension of this articular surface along the anterior border of the fibula. The lateral surface of the fibula is marked by an extensive rugosity on the midshaft, representing the origin of one or more heads of flexor digitorum longus (Borsuk-Bialynicka, 1977). The distal end of the fibula forms a rounded triangle in distal view with an anterior apex and a flat, posterior base.

**Pes**—Left metatarsals I–IV and a right metatarsal V were collected from MAD 93-18 (Table 3, Fig. 46). All but metatarsal V are pristinely preserved, allowing an unequivocal assessment of their articular surfaces and contacts, as well as the overall morphology of the metatarsus. When articulated, the metatarsals form a broad, slightly arched pes that is strikingly different from the more tightly curved manus (Figs. 38G, 40G). The length of the metatarsals increases from I to III, with metatarsal IV slightly shorter than that of metatarsal III. Metatarsal V is the shortest metatarsal. All metatarsals are subquadrangular in transverse section. Their proximal ends widen plantarly (metatarsal I), are subrectangular (metatarsal II), or taper plantarly (metatarsals III–IV). The proximal articular surfaces of metatarsals I to III have convex medial borders and slightly concave lateral borders. The proximal borders of metatarsal IV are nearly straight.

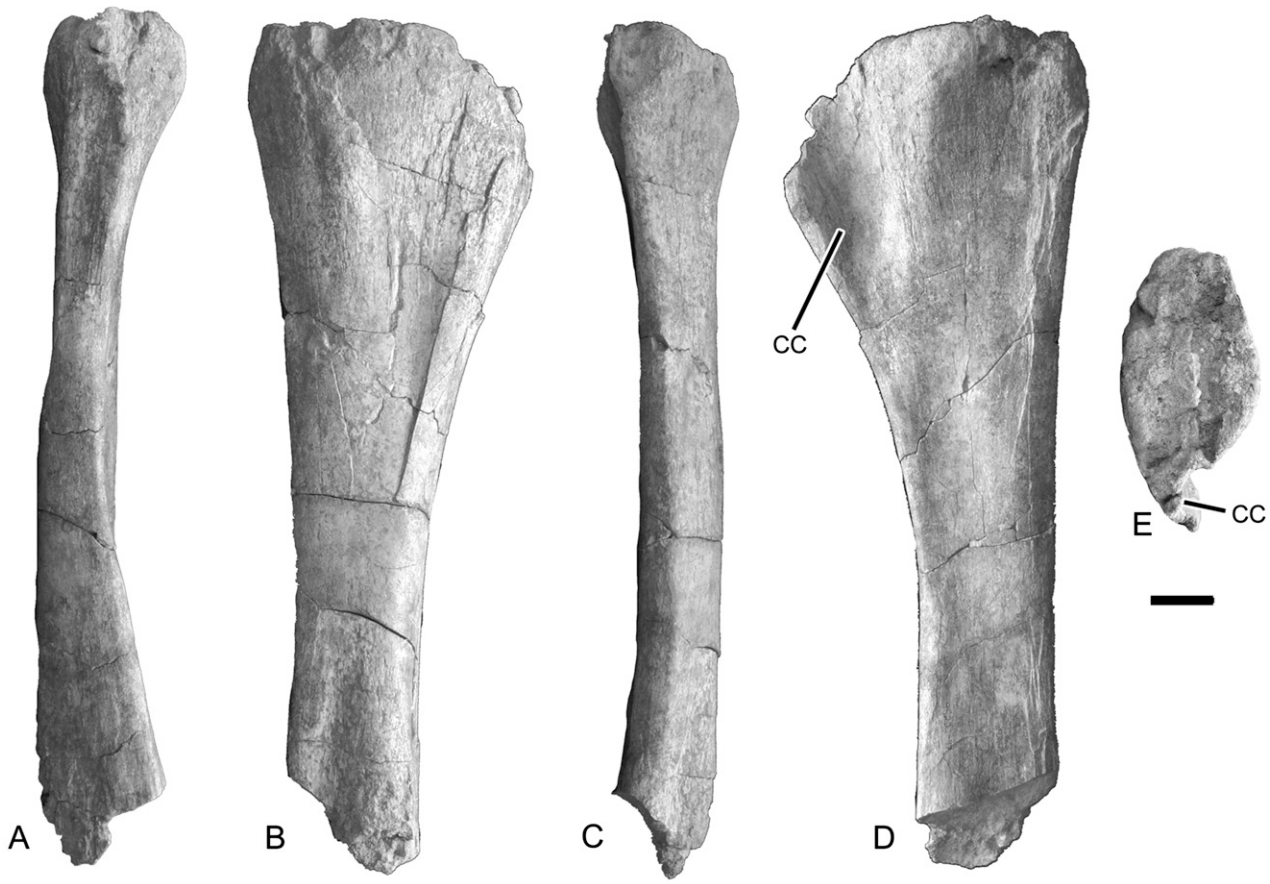


FIGURE 44. Left tibia (FMNH PR 2209) of *Rapetosaurus krausei* in **A**, anterior view; **B**, medial view; **C**, posterior view; **D**, lateral view; **E**, proximal view. Distal end is broken. **Abbreviation**: **cc**, cnemial crest. Scale bar equals 3 cm.


FIGURE 45. Right fibula (FMNH PR 2209) of *Rapetosaurus krausei* in **A**, anterior view; **B**, medial view; **C**, posterior view; **D**, lateral view; **E**, proximal view (anterior toward bottom); **F**, distal view (anterior towards top). **Abbreviation**: **lt**, lateral trochanter. Scale bar equals 3 cm.

The distal articular surfaces of metatarsals I to III have plantar concavities and dorsal convexities. These articular surfaces have dorsal and plantar extensions, giving some indication of flexion and extension possibilities, and are medially displaced. In contrast, the distal surface of metatarsal IV is flattened and reduced anteroposteriorly, without a prominent posterior concavity. Metatarsals are not well documented in other titanosaurs, thus restricting the comparative discussion below.

Metatarsal I is the most robust metatarsal, with a proximal end that is broadened dorsoplantarly and tapered to an elongated lateral point dorsally. Metatarsal I articulates with metatarsal II via a broad, flat surface, and meets a medial extension of the proximal articular surface of metatarsal II dorsally. The shaft is slender at mid-diaphysis relative to that of other titanosaurs. Laterally, a long, sharp ridge extends obliquely from the plantolateral corner of the element to its distal extreme. This ridge results in a slightly twisted lateral surface, with a wide dorsal region for articulation with metatarsal II, and a narrowed ventral portion. The distal end of the element is transversely expanded and dominated by well-developed condyles for articulation with the first phalanx. The medial condyle is larger and deeper than the lateral condyle. The medial and lateral articular surfaces are separated on the plantar surface by a shallow flexor indentation.

Metatarsal II is slightly longer and more gracile than metatarsal I. In proximal view, it is subrectangular. The diaphysis is transversely compressed. Medial and lateral triangular articular regions for metatarsals I and II, respectively, mark the proximal shaft. A short dorsomedial extension marks the articular region for metatarsal I, and helps lock that element in place. A proximal, ovoid muscle scar and two small excavations (possibly neurovascular)

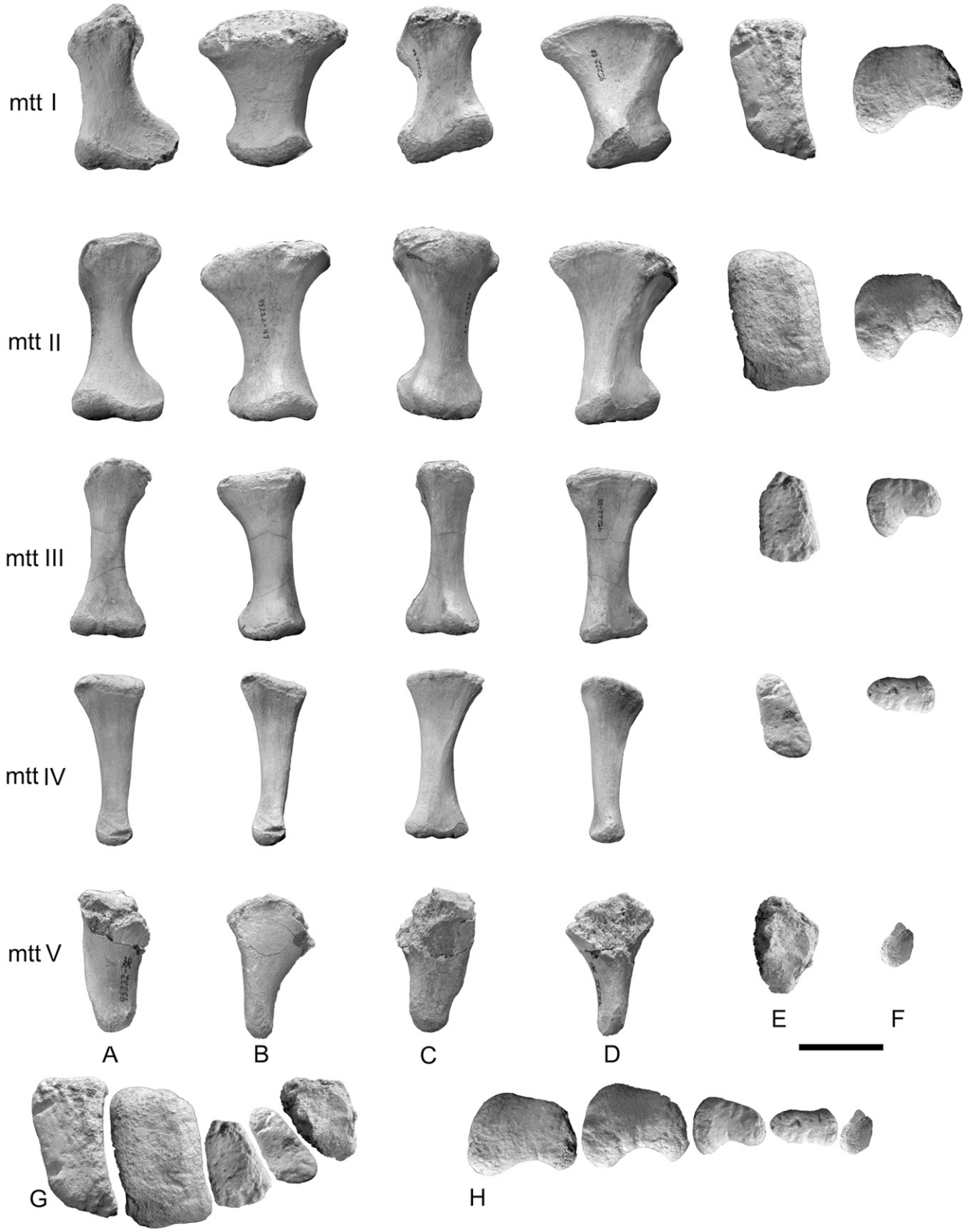


FIGURE 46. Pes (FMNH PR 2209) of *Rapetosaurus krausei* including left metatarsals I–IV, and right metatarsal V (reversed) in **A**, dorsal view; **B**, medial view; **C**, plantar view; **D**, lateral view; **E**, proximal view (dorsal toward bottom); **F**, distal view, dorsal towards top. **G**, articulated metatarsus in proximal view; **H**, articulated metatarsus in distal view. **Abbreviation**: **mtt**, metatarsal. Scale bar equals 3 cm.

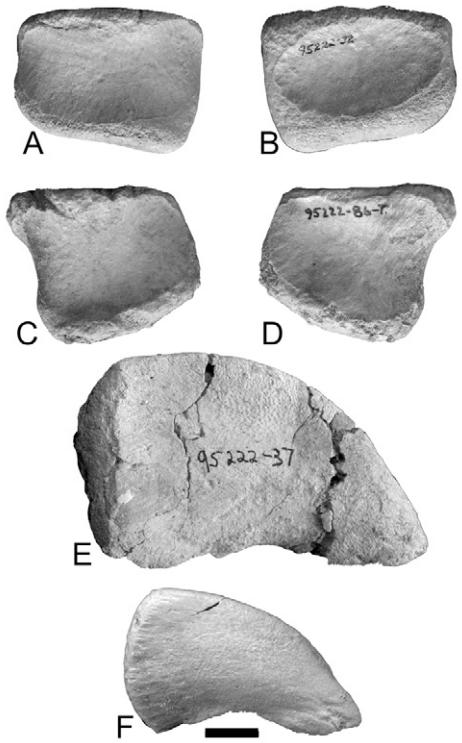


FIGURE 47. *Rapetosaurus* pedal and ungual phalanges (FMNH PR 2209). **A**, phalanx III-1 in dorsal view; **B**, phalanx III-1 in plantar view; **C**, Phalanx I-1 in dorsal view; **D**, phalanx I-1 in plantar view; **E**, ungual phalanx in lateral view; **F**, ungual phalanx in lateral view. Scale bar equals 1 cm.

mark the plantar surface. The distal condyle is similar to that of metatarsal I; it is medially displaced so that the medial condyle is substantially larger than the lateral one.

Metatarsal III is the longest and most gracile of the metatarsals. Its proximal end is rectangular and narrower than that of metatarsal II. The dorsal margin of the proximal end is slightly wider than that of metatarsal II, with a more pronounced tapering to the plantar margin. Triangular areas of articulation for metatarsals II and IV mark its medial and lateral surfaces. The plantolateral edge of the element is slightly expanded and concave to cradle metatarsal IV. Unlike the condition in metatarsals I and II, the proximal and distal ends of metatarsal III are less broadly expanded and fan-shaped. The distal articular surface is saddle-shaped, with medially displaced condyles. This displacement is particularly obvious in lateral view of the element, where the medial condyle is easily observed in lateral view.

Metatarsal IV is only slightly shorter than metatarsal III. Its proximal articulation is a more gracile version of the same feature in metatarsal III, with tapered posterior and broad dorsal surfaces. It departs from the morphology of metatarsals I–III in its transversely expanded and posterodorsally flattened distal condyles. The medial distal condyle retains a slightly broader morphology in line with the medial displacement of metatarsals I–III. A small, elongate muscle scar extends along the posteromedial surface of the element, presumably for flexor musculature.

Right metatarsal V tapers distally from a broadened proximal portion. The proximal end of the element is comprised of two articular regions. A dorsal articular surface angles sharply anterodorsally to a pinnacle, then merges with the second, more posteroventrally positioned surface. It is subequal to metatarsal I in length, but is significantly more gracile, ending distally in a narrow point. The distal surface is small and rounded and lacks a well-demarcated articular surface. There is no clear separation of medial and lateral condyles.

The phalangeal formula for *Rapetosaurus* is indeterminate at present. Phalanges I-1 (Fig. 47A–B) and ungual phalanx I-2 (Fig. 47C–D) are preserved, as is the proximal phalanx for metatarsal III (Fig. 47E), and an indeterminately positioned ungual phalanx (Fig. 47F). The poorly developed distal articular surface of metatarsal V indicates that the fifth digit may have been rudimentary or completely lacking. It appears that the first phalanges are characterized by some degree of asymmetry, with shortened medial walls relative to the lateral surfaces of each element. This asymmetry apparently decreases from digits I to III. Phalanx I-1 is subrectangular with a pronounced lengthening of the medial surface relative to the extremely shortened lateral surface. The distal and proximal articular surfaces join one another along the acute lateral border. Medially, the proximal articular surface veers toward the midline and is more extensive than the dorsoventrally compressed distal surface. The distal articular region does not extend significantly onto the ventral surface of the element. In contrast, phalanx III-1 is more robust, less dorsoventrally compressed, and less laterally tapered. It is subrectangular with a broad, suboval proximal articular surface. Phalanx III-1 has a medially displaced distal articular surface that extends onto the ventral side of the element. As in phalanx I-1, the proximal and distal articular surfaces merge on the lateral surface of the element. This is also true of the medial surface in phalanx III-1. Unguals are crescent shaped and strongly flattened laterally. The proximal articular surface is anteroposteriorly elongate and transversely flattened.

**Hind limb, Comparisons**—Femoral morphology is nearly identical in most titanosaurs, though variations occur in the degree of lateral bulge, shape of the femoral head, and development of distal condyles. When compared to other titanosaur taxa, the *Rapetosaurus* femur is very gracile at mid-diaphysis and equally expanded proximally and distally. Other titanosaurs do not exhibit the degree of mid-diaphyseal constriction observed in *Rapetosaurus*. Instead the femur exhibits a straighter shaft in *Alamosaurus* (TMM 41541-1, Lehman and Coulson, 2002), *Opisthocoelicaudia* (ZPAL MgD-I/48, Borsuk-Bialynicka, 1977), *Saltasaurus* (PVL 4017-79, Powell, 1992, 2003), *Ligabuesaurus* (MCF-PVPH-233, Bonaparte et al., 2006), and *Rinconsaurus* (MRS-Pv 49, Calvo and González Riga, 2003). In contrast with *Rapetosaurus*, the head of the femur of *Neuquensaurus* (MCS-9, Salgado et al., 2005) is not elevated much beyond the level of the lateral bulge. The distal femora of *Rapetosaurus, Opisthocoelicaudia*, *Saltasaurus*, and *Neuquensaurus* are characterized by a medial condyle that is higher than the lateral one. The two distal condyles are shifted mediolaterally and are broadly visible in anterior view in these taxa. This shift is similar to that observed in other macronarians (e.g., *Camarasaurus, Brachiosaurus*: Wilson and Sereno, 1998).

In contrast with the rounded proximal tibia of *Rapetosaurus*, the proximal articular surfaces of the tibiae of *Alamosaurus* (TMM 43621-1, Lehman and Coulson, 2002) and *Lirainosaurus* (MCNA 7471, Sanz et al., 1999) are square and robust. *Rapetosaurus, Opisthocoelicaudia*, and *Magyarosaurus* (BMNH R3853, pers. observ.), share the presence of an anterolaterally projecting, short cnemial crest, but differ from *Saltasaurus* (PVL 4017-88, Powell, 1992, 2003), in which the cnemial crest curves laterally. Unlike *Saltasaurus, Neuquensaurus*, and *Gondwanatitan* (Kellner and Azevedo, 1999:fig. 21), the lateral surface of the tibia behind the cnemial crest in *Rapetosaurus* is not concave.

*Rapetosaurus* fibulae are generally similar to those of *Saltasaurus* (PVL 4017-89, Powell, 1992) *Malawisaurus* (SMU Mal-189, Gomani, 2005), *Magyarosaurus* (BMNH R122, pers. observ.), and *Neuquensaurus* (MCS-5/26, Salgado et al., 2005). The fibula of *Ligabuesaurus* is straighter and less expanded proximally than in

*Rapetosaurus*. Both proximal and distal ends are strongly expanded in *Ampelosaurus* and *Phuwiangosaurus* (PW 1-18, Martin et al., 1999) instead of the subequal morphology of fibular extremities in *Rapetosaurus*. *Alamosaurus* (TMM 43621-1, Lehman and Coulson, 2002) exhibits a slightly twisted morphology not observed in *Rapetosaurus*.

Metatarsal I in *Rapetosaurus* is distinguishable from that of other sauropods, but it maintains some similarity in relative size and shape with *Opisthocoelicaudia*, and shares a proximodorsal bony extension with *Saltasaurus*, *Epachthosaurus*, and *Euhelopus* (PMU 233-234, Wiman, 1929). In general, the pes of *Rapetosaurus* is more gracile than that of *Epachthosaurus*, as exemplified by metatarsal II. In *Epachthosaurus* and *Janenschia* (HMN MB.R 2093.1-12, Bonaparte et al., 2000) metatarsal III is more robust than in *Rapetosaurus*. In *Rapetosaurus* the third metatarsal is the longest, whereas in *Epachthosaurus*, the fourth metatarsal is the longest. The fifth metatarsal of *Janenschia* and *Rapetosaurus* each bear a single proximal condyle, in contrast with the divided proximal condyle of *Opisthocoelicaudia*. In *Janenschia* this condyle is flat and in *Rapetosaurus* it is dorsally convex.

### Osteoderms

Osteoderms were not preserved with FMNH PR 2209 at MAD 93-18. The depositional setting of the site lends itself to the preservation of small, fragile elements (including disarticulated small cranial elements, caudal vertebrae, and phalanges), so the absence of osteoderms with this juvenile skeleton is particularly interesting; perhaps titanosaur osteoderms occur only at later ontogenetic stages. That said, osteoderms are also clearly associated with other, adult *Rapetosaurus* specimens (Curry, 2001; Curry Rogers and D'Emic, unpubl. data), and confirm the lithostrotian status of *Rapetosaurus* (Wilson and Upchurch, 2003; Curry Rogers, 2005). They may be absent in FMNH PR 2209 simply due to the juvenile developmental stage of this specimen (Hutton, 1986; Vickaryous and Hall, 2006). Osteoderms, although not abundant components of the Maevarano Formation fossil record, are present and exhibit a variety of morphologies (Depéret, 1896 a,b; Dodson et al., 1998, Curry Rogers and D'Emic, unpubl. data). They are most commonly recovered from the Maevarano Formation as isolated, surface-collected specimens. See Dodson et al. (1998) for a discussion of osteoderm morphology and a comparison of these specimens (some of which may not be referable to *Rapetosaurus)* with others from South American, Spanish, and African titanosaurs.

## SUMMARY AND CONCLUSION

*Rapetosaurus* is characterized by a relatively gracile skeleton. A detailed ontogenetic record of *Rapetosaurus* skeletal material exists, with a number of individuals including very small juveniles (femur length $\leq$13 cm; n=3) and large adults (femur length $\geq$ 150 cm; n=5), and many specimens of intermediate size (n=10). The neck is elongated, probably as the result of an increase in cervical vertebra count and individual vertebral elongation, as well as duplication and/or incorporation (Upchurch, 1994; Wilson and Sereno, 1998). Elongation indices (sensu Upchurch, 1998) for cervical vertebrae range from $\sim$3.3 to 4.3. Extremely elongated cervical ribs characterize *Rapetosaurus*. The vertebral column is pneumatized as far posteriorly as the sixth sacral centrum. None of the preserved middle and posterior caudal vertebrae exhibit pneumatic foramina. Caudal centra are persistently procoelous, though the degree of procoely decreases toward the tip of the tail. The anterior and posterior articular surfaces of caudal centra retain a consistent width to height ratio of 1:1. The dorsal ribs are pneumatic, and impart a wide, barrel-shaped morphology to the trunk of *Rapetosaurus*. The pelvic girdle is characterized by a lateral deflection of the preacetabular process, and ischia that are significantly shorter and broader than the pubes (only about 54% the length of the pubis). The forelimb is about 87% the length of the hind limb (including the longest metacarpal and metatarsal, but not including phalanges or tarsal and carpal elements). The ratio of sternal plate to humerus length is 0.65. It is clear that at least as juveniles, *Rapetosaurus* individuals were not heavily armored with osteoderms, although it is clear that they did exhibit osteoderms at later ontogenetic stages. Inclusion of *Rapetosaurus* in future cladistic analyses will have important further implications for resolving titanosaur phylogeny. The associated cranial and postcranial material of FMNH PR 2209 clearly demonstrate the anatomy of a titanosaur skull and provide evidence that corroborates hypotheses that the Mongolian genera *Nemegtosaurus* and *Quaesitosaurus* are titanosaurs (Calvo, 1994; Salgado et al., 1997; Wilson and Sereno, 1998; Curry Rogers and Forster, 2001, 2004; Curry Rogers, 2005; Wilson 2005a), and provide a suite of characters that may be ascribed to a broader array of titanosaurs (Wilson, 2005b). Nine key analyses of titanosaur relationships (Salgado et al., 1997; Upchurch, 1998; Sanz et al., 1999; Curry Rogers and Forster, 2001; Wilson, 2002; Calvo and González Riga, 2003; Upchurch et al., 2004; Curry Rogers 2005) suggest some general agreement on titanosaur phylogeny, which may be related to data recycling (most analyses build upon and modify characters from Upchurch, 1998 and Wilson, 2002). Curry Rogers (2005) included nearly 50% new data, primarily derived from the skeleton of *Rapetosaurus krausei* described herein, and *Rapetosaurus*, is, by far, the most completely scored taxon included in that study. Of the 29 titanosaurs included in the analysis, 14 genera were scoreable for less than 15% of their data. *Rapetosaurus* was scored for 82% of cranial characters, and 92% of postcranial characters (Curry Rogers, 2005). More than 30 valid titanosaur species still need to be accommodated by detailed phylogenetic resolution, and the well-preserved skeleton of *Rapetosaurus* described in this paper will assist in spanning the gap between titanosaurs known only from skulls, those known solely from postcranial remains, and those with more poorly known combinations of these data.

## ACKNOWLEDGMENTS

I thank D. W. Krause, C. Forster, and the members of the Mahajanga Basin Project from 1993-2007 for the invitation to work on Madagascar's sauropods, and for their careful recovery of these materials. A. Rasoamiaramanana, G. Ravololonarivo, and the late B. Bakotosamimanana of the Université d'Antananarivo, P. Wright, B. Andriamihaja, and the staff of the Madagascar Institute pour la Conservation des Environments Tropicaux and the villagers of Berivotra provided indispensable logistical support. I acknowledge the skillful preparation efforts of V. Heisey, as well as those of Field Museum of Natural History paleontology volunteers, and K. Blair, N. Key, R. Newberry, and G. Rector of the Science Museum of Minnesota. I thank T, Ready and C. Theissen of the Science Museum of Minnesota for photographs, M. Hallet for the reconstruction of *Rapetosaurus*, and D. Vital for technical illustrations of vertebrae. Editor J. A. Wilson and reviewers M. D'Emic, L. Salgado, J. Whitlock, and two anonymous reviewers improved the manuscript with thorough, constructive reviews.

I thank the following individuals for providing access to collections in their care, as well as generosity and hospitality while I visited their countries and museums: V. Alifanov, S. Apesteguía, A. Arcucci, S. Bandyopadhyay, J. Blanco, J. Bonaparte, M. Borsuk-Bialynicka, E. Buffetaut, J. Calvo, R. Coria, Z. Csiki, D. Dutheil, T. Fiorillo, J. Flynn, D. Gillette, E. Gomani, J. Gonzalez, Y. Gurovich, L. Jacobs, T. S. Kutty, J. Le Loueff, C. Marsicano, A. Milner, F. Novas, M. Popa, J. Powell, A. Prieur, O., A., I., and L. Rauhut, S. Ray, L. Salgado, D. Sengupta, B. Simpson, P. Taquet,

and D. Unwin. I also thank M. Carrano, P. Curry, M. Gottfried, E. Holt-Werle, P. M. O'Connor, M. O'Leary, R. Rogers, C. Rogers, L. Rogers, and J. A. Wilson for helpful discussions.

I gratefully acknowledge the financial support of the National Science Foundation (DEB-9224396, EAR-9418816, EAR-9706302, DEB-9904045, EAR-0106477, EAR-0116517, EAR-0446488), the National Geographic Society (1999, 2001, 2004), the Jurassic Foundation (1999), The Geological Society of America (1998), the Paleontological Society (1999), and the Stony Brook University Gabor Inke Graduate Research Fellowship (1996-1999).

## LITERATURE CITED

Besairie, H. 1972. Géologie de Madagascar. I. Les terrains sédimentaires. Annales Géologique de Madagascar 35:1–463.

Bonaparte, J. F, and R. Coria. 1993. Un nuevo y gigantesco sauropodo titanosaurio de la Formación Río Limay (Albiano-Cenomanio) del la Provincia del Neuquén, Argentina. Ameghiniana 30:271–282.

Bonaparte, J. F., B. J. González Riga, and S. Apesteguía. 2006. *Ligabuesaurus leanzai* gen. et sp. nov. (Dinosauria, Sauropoda), a new titanosaur from the Lohan Cura Formation (Aptian, Lower Cretaceous) of Neuquén, Patagonia, Argentina. Cretaceous Research 27:364–376.

Borsuk-Bialynicka, M. 1977. A new camarasaurid sauropod, *Opisthocoelicaudia skarzynskii*, gen. n., sp. n. from the Upper Cretaceous of Mongolia. Paleontologica Polonica 37:1–64.

Calvo, J. O. 1994. Jaw mechanics in sauropod dinosaurs. GAIA 10:183–194.

Calvo, J. O., and J. F. Bonaparte. 1991. *Andesaurus delgadoi* gen. et sp. nov. (Saurischia-Sauropoda), dinosaurio Titanosauridae de la Formación Río Limay (Albiano-Cenomanio), Neuquén, Argentina. Ameghiniana 28:303–310.

Calvo, J. O., and B. J. González Riga. 2003. *Rinconsaurus caudamirus* gen. et sp. nov., a new titanosaurid (Dinosauria, Sauropoda) from the Late Cretaceous of Patagonia, Argentina. Revista Geologica de Chile 30:333–353.

Curry Rogers, K. 2001. A new sauropod from Madagascar: implications for lower level titanosaur phylogeny. Journal of Vertebrate Paleontology 21:43A.

Curry Rogers, K. 2002. Titanosaur tails tell two tales: a second Malagasy titanosaur with saltasaurid affinities. Journal of Vertebrate Paleontology 22:47A–48A.

Curry Rogers, K. 2005. Titanosauria: a phylogenetic overview; pp. 50–103 in K. Curry Rogers and J. A. Wilson (eds.), The Sauropods: Evolution and Paleobiology. University of California Press, Berkeley, California.

Curry Rogers, K., and C. A. Forster. 2001. The last of the dinosaur titans: a new sauropod from Madagascar. Nature 412:530–534.

Curry Rogers, K., and C. A. Forster. 2004. The skull of *Rapetosaurus krausei* (Sauropoda:Titanosauria) from the Late Cretaceous of Madagascar. Journal of Vertebrate Paleontology 24:121–144.

Curry Rogers, K., and M. Imker. 2007. New data on 'Malagasy Taxon B,' a titanosaur from the Late Cretaceous of Madagascar. Journal of Vertebrate Paleontology 27:64A.

Depéret, C. 1896a. Note sur les Dinosauriens Sauropodes et Théropodes dans le Crétacé supérieur de Madagascar. Bulletin de la Société Géologique de France 21:176–194.

Depéret, C. 1896b. Sur l'existence de Dinosauriens, Sauropodes et Théropodes dans le Crétacé supérieur de Madagascar. Comptes Rendus Hebdomadiares des Séances de l'Académie des Sciences (Paris) 122:483–485.

Dodson, P., D. W. Krause, C. A. Forster, S. D. Sampson, and F. Ravoavy. 1998. Titanosaurid (Sauropoda) osteoderms from the Late Cretaceous of Madagascar. Journal of Vertebrate Paleontology 18:563–568.

Gilmore, C. W. 1922. Discovery of a sauropod dinosaur from the Ojo Alamo Formation of New Mexico. Smithsonian Miscellaneous Collections 81:1–9.

Gilmore, C. W. 1946. Reptilian fauna of the North Horn Formation of central Utah. United States Geological Survey Professional Paper 210C:1–52.

González Riga, B. J. 2003. A new titanosaur from the Upper Cretaceous of Mendoza Province, Argentina. Ameghiniana 40:155–172.

González Riga, B. J. 2005. Nuevos restos fósiles de *Mendozasaurus neguyelap* (Sauropoda, Titanosauria) del Cretácico Tardío de Mendoza, Argentina. Ameghiniana 42:535–548.

Gomani, E. M. 2005. Sauropod dinosaurs from the Early Cretaceous of Malawi, Africa. Palaeontologia Electronica 8:1–37.

Huene, F. v. 1929. Los Saurisquios y Ornithisquios del Cretáceo Argentino. Anales del Museo La Plata 2:1–196.

Huene, F. v., and C. A. Matley. 1933. The Cretaceous Saurischia and Ornithischia of the central provinces of India. Memoirs of the Geological Survey of India 21:1–74.

Hutton, J. M. 1986. Age determination of living Nile crocodiles from the cortical stratification of bone. Copeia 1986:332–341.

Jacobs, L. L., D. A. Winkler, W. R. Downs, and E. M. Gomani. 1993. New material of an Early Cretaceous titanosaurid sauropod dinosaur from Malawi. Paleontology 36:523–534.

Jain, S. L., and S. Bandyopadhyay. 1997. New titanosaurid (Dinosauria: Sauropoda) from the Late Cretaceous of central India. Journal of Vertebrate Paleontology 17:114–136.

Janensch, W. 1947. Pneumatizität bei Wirbeln von Sauropoden und anderen Saurischiern. Palaeontographica 3:1–25.

Kellner, A. W. A., and S. A. K. Azevedo. 1999. A new sauropod dinosaur (Titanosauria) from the Late Cretaceous of Brazil. National Science Museum monographs 15:111–142.

Ksepka, D. T., and M. A. Norell. 2006. *Erketu ellisoni*, a long-necked sauropod from Bor Guvé (Dornogov Aimag, Mongolia). American Museum Novitates 3508:1–16.

Lavocat, R. 1955. Etude des gisements de Dinosauriens de la region de Majunga (Madagascar). Travaux du Bureau Géologique 69:1–19.

Lehman, T. M., and A. B. Coulson. 2002. A juvenile specimen of the sauropod dinosaur *Alamosaurus sanjuanensis* from the Upper Cretaceous of Big Bend National Park, Texas. Journal of Paleontology 76:156–172.

Le Loeuff, J. 1995. *Ampelosaurus atacis* (nov. gen., nov. sp.), un nouveau Titanosauridae (Dinosauria, Sauropoda) du Crétacé supérieur de la Haute Vallée de l'Aude (France). Comptes Rendus de L'Academie des Sciences de Paris (séries IIa) 321:693–699.

Marsh, O. C. 1878. Principal characters of American Jurassic dinosaurs. Part I. American Journal of Science, Series 3 16:411–416.

Martin, V., E. Buffetaut, and V. Suteethorn. 1994. A new genus of sauropod dinosaur from the Sao Khua Formation (Late Jurassic to Early Cretaceous) of northeastern Thailand. Comptes Rendus de l'Academie des Sciences de Paris 319:1085–1092.

Martin, V., V. Suteethorn, and E. Buffetaut. 1999. Description of the type and referred material of *Phuwiangosaurus sirindhornae* Martin, Buffetaut and Suteethorn, 1994, a sauropod from the Lower Cretaceous of Thailand. Oryctos 2:39–91.

Martínez, R. D., O. Giménez, J. Rodríguez, M. Luna, and M. C. Lamanna. 2004. An articulated specimen of the basal titanosaurian (Dinosauria: Sauropoda) *Epachthosaurus sciuttoi* from the early Late Cretaceous Bajo Barreal Formation of Chubut Province, Argentina. Journal of Vertebrate Paleontology 24:107–120.

McIntosh, J. S. 1990. Sauropoda; pp. 345–401 in D. B. Weishampel, P. Dodson, and H. Osmólska (eds.), The Dinosauria. University of California Press, Berkeley, California.

O'Connor, P. M. 2004. Pulmonary pneumaticity in the postcranial skeleton of extant avians: a case study examining Anseriformes. Journal of Morphology 261:141–161.

O'Connor, P. M. 2006. Pulmonary pneumaticity: an evaluation of soft-tissue influences on the postcranial skeleton and the reconstruction of pulmonary anatomy in archosaurs. Journal of Morphology 267:1199–1266.

Owen, R. 1842. Report on British fossil reptiles, Part II. Reports of the British Association for the Advancement of Science 11:60–204.

Powell, J. E. 1986. Revision de los Titanosauridos de America del Sur. Ph.D. dissertation Universidad Nacional De Tucumán, Tucumán, Argentina, 340 pp.

Powell, J. E. 1992. Osteológia de *Saltasaurus loricatus* (Sauropoda Titanosauridae); pp. 166–230 in J. L. Sanz and A. D. Buscalioni (eds.), Los Dinosaurios y su Entorno Biotico. Instituto "Juan de Valdes", Cuenca.

Powell, J. E. 2003. Revision of South American titanosaurid dinosaurs: palaeobiological palaeobiogeographical, and phylogenetic aspects. Records of the Queen Victoria Museum 111:1–94.

Ravoavy, F. 1991. Identification et mise en catalogue des vertebras fossils récoltes dans le Crétacé supérieur continental de la region de Berivotra (Majunga) fouille 1987. Université d'Antananarivo Mémoire de Recherche 2:55–104.

Rogers, R. R. 2005. Fine-grained debris flows and extraordinary vertebrate burials in the Late Cretaceous of Madagascar. Geology 33:297–300.

Rogers, R. R., J. H. Hartman, and D. W. Krause. 2000. Stratigraphic analysis of Upper Cretaceous rocks in the Mahajanga Basin, northwestern Madagascar: implications for ancient and modern faunas. Journal of Geology 108:275–301.

Russell, D. A., D. Russell, P. Taquet, and H. Thomas. 1976. Nouvelles récoltes de vertébrés dans les terrains continentaux du Crétacé supérieur de la région de Majunga (Madagascar). Comptes Rendus Sommaires de la Société Géologique de France 5:204–207.

Salgado, L. 1996. *Pellegrinisaurus powelli* nov. gen. et sp. (Sauropoda, Titanosauridae) from the Upper Cretaceous of Lago Pellegrini, northwestern Patagonia, Argentina. Ameghiniana 33:355–365.

Salgado, L., S. Apesteguía, and S. Heredia. 2005. A new specimen of *Neuquensaurus australis*, a Late Cretaceous saltasaurine titanosaur from north Patagonia. Journal of Vertebrate Paleontology 25:623–634.

Salgado, L., and C. Azpilicueta. 2000. Un nuevo saltasaurino (Sauropoda, Titanosauridae) de la provincia de Río Negro (Formación Allen, Cretácico Superior), Patagonia, Argentina. Ameghiniana 37:259–264.

Salgado, L., J. O. Calvo, and R. A. Coria. 1997. Evolution of the titanosaurid sauropods. I: phylogenetic analysis based on the postcranial evidence. Ameghiniana 34:3–32.

Santucci, R. M., and R. J. Bertini. 2006. A new titanosaur from western São Paulo State, Upper Cretaceous Bauru Group, South-east Brazil. Palaeontology 49:59–66.

Sanz, J. L., J. E. Powell, J. Le Loeuff, R. Martínez, and X. Pereda-Suberbiola. 1999. Sauropod remains from the Upper Cretaceous of Laño (northcentral Spain). titanosaur phylogenetic relationships. Estudios del Museo de Ciencias Naturales de Alava 14:235–255.

Seeley, H. G. 1888. On the classification of the fossil animals commonly named Dinosauria. Proceedings of the Royal Society of London 43:165–171.

Thévenin, A. 1907. Dinosauriens (Paléontologie de Madagascar IV). Annales de Paléontologie 2:121–136.

Upchurch, P. 1994. Sauropod phylogeny and palaeoecology. Gaia 10:249–260.

Upchurch, P. 1998. The phylogenetic relationships of sauropod dinosaurs. Zoological Journal of the Linnean Society 124:43–103.

Upchurch, P., P. Barrett, and P. Dodson. 2004. Sauropoda; pp. 259–324 in D. B. Weishampel, P. Dodson, and H. Osmólska (eds.), The Dinosauria, 2nd Edition. University of California Press, Berkeley, California.

Vickaryous, M. K., and B. K. Hall. 2006. Osteoderm morphology and development in the nine-banded armadillo, *Dasypus novemcinctus* (Mammalia, Xenarthra, Cingulata). Journal of Morphology 267:1273–1283.

Wedel, M., R. L. Cifelli, and R. K. Sanders. 2000a. Osteology, paleobiology, and relationships of the sauropod dinosaur *Sauroposeidon*. Palaeontologica Polonica 45:343–388.

Wedel, M., R. L. Cifelli, and R. K. Sanders. 2000b. *Sauroposeidon proteles*, a new sauropod from the Early Cretaceous of Oklahoma. Journal of Vertebrate Paleontology 20:109–114.

Wilson, J. A. 1999. A nomenclature for vertebral laminae in sauropods and other saurischian dinosaurs. Journal of Vertebrate Paleontology 19:639–653.

Wilson, J. A. 2002. Sauropod dinosaur phylogeny: critique and cladistic analysis. Zoological Journal of the Linnean Society 136:217–276.

Wilson, J. A. 2005a. Redescription of the skull of *Nemegtosaurus mongliensis* Nowinski (Dinosauria – Saurischia) and comments on Late Cretaceous sauropod diversity. Journal of Systematic Palaeontology 3:283–318.

Wilson, J. A. 2005b. Overview of Sauropod Phylogeny and Evolution; pp. 15–49 in K. Curry Rogers and J. A. Wilson (eds.), The Sauropods: Evolution and Paleobiology. University of California Press, Berkeley, California.

Wilson, J. A. 2006. An introduction to titanosaur phylogeny and evolution; pp. 157–178 in Colectivo Arqueológico-Paleontológico Salense (eds.), Actas de las III Jornadas sobre Dinosaurios y su Entorno. Salas de los Infantes, Burgos, España.

Wilson, J. A., and M. T. Carrano. 1999. Titanosaur locomotion and the origin of "wide-gauge" trackways: a biomechanical and systematic perspective on sauropod locomotion. Paleobiology 25:252–267.

Wilson, J. A., and P. C. Sereno. 1998. Early evolution and higher-level phylogeny of sauropod dinosaurs. Memoirs of the Society of Vertebrate Paleontology 5:1–68.

Wilson, J. A., and P. Upchurch. 2003. A revision of *Titanosaurus* (Dinosauria-Sauropoda), the first 'Gondwanan' dinosaur genus. Journal of Systematic Palaeontology 1:125–160.

Wiman, C. 1929. Die Kriede-Dinosaurier aus Shantung. Paleontologia Sinica (C) 6:1–67.

Submitted October 8, 2008; accepted January 2, 2009.